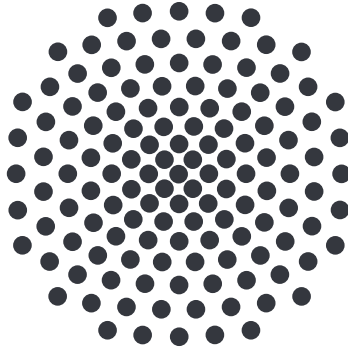


University of Stuttgart



Institute for Theoretical Physics III

Master Thesis:

# Quantum Corrections in Cold Dipolar Gases

November 14, 2017

---

Candidate:

Tobias Ilg

---

Supervisor:

Prof. Dr. H. P. Büchler

Secondary Corrector: Priv.-Doz. Dr. H. Cartarius

---



## **Declaration**

I declare that I have developed and written the enclosed Master Thesis completely by myself, and have not used sources or means without declaration in the text. Any thoughts from others or literal quotations are clearly marked. The Master Thesis was not used in the same or in a similar version to achieve an academic grading or is being published elsewhere. Lastly, I assure that the electronic copy of this Master Thesis is identical in content with the enclosed version.

Stuttgart, 14.11.2017

## Abstract

An ongoing progress in the physics of ultracold atomic gases provides ever deeper insights to many-body physics on a fundamental level. By improved cooling and measurement techniques experimental physicists enter regions, where a perturbation expansion in lowest order is just not enough to describe the physical processes sufficiently. The correct inclusion of higher order corrections is a major challenge to overcome for a better understanding of the mechanisms in quantum many-body physics.

In the course of this work, we will work out the fundamental concepts to treat weakly interacting Bose gases beyond the mean-field level. Not only the treatment of the many-body system is needed, but also the comprehension of the two-body scattering problem is essential to handle the struggles, we will come across in this work. Thus, we will give a short overview of low-energy scattering, before we consider scattering processes in confined systems. The concepts of scattering theory in confined systems will become important later in this work.

We will briefly discuss the most common approach to include beyond-mean-field corrections, namely the Bogoliubov theory. We will notice that the inclusion of scattering processes can lead to divergences in the theoretical description if not treated with care.

The central part of this work focuses on the diagrammatic approach of Hugenholtz and Pines. The field-theoretic treatment of weakly interacting Bose gases will allow us to prevent divergences and thus treat the scattering processes consistently within the theory. We will use the diagrammatic approach to calculate the beyond-mean-field corrections for a dipolar Bose gas. The approach of Hugenholtz and Pines allows for a rigorous treatment of the dipolar interaction without any divergence appearing at all.

In addition, the consistent inclusion of scattering properties will make it possible to describe confined systems. Here, we are interested in the description of a dimensional crossover. We will consider a gas in a box with periodic boundary conditions. As we will see, the system can exhibit three-dimensional as well as quasi-one-dimensional behavior. In contrast to a truly one-dimensional system, the transverse degrees of freedom yield an additional confinement-induced shift to the ground state energy. Using the field-theoretic description, the confinement-induced shift appears naturally, which underlines the beauty of the approach.

## Zusammenfassung

Der ständige Fortschritt im Bereich der tiefkalten Quantengase erlaubt immer tiefere Einblicke in die Physik der Vielteilchensysteme auf einem fundamentalen Niveau. Immer bessere Kühl- und Messverfahren erlauben es Experimentalphysikern in Regionen vorzudringen, in denen eine störungstheoretische Beschreibung in niedrigster Ordnung nicht mehr ausreichend ist, um alle auftretenden physikalischen Prozesse korrekt zu beschreiben. Das fehlerlose Einbeziehen von Korrekturen höherer Ordnung stellt sich dabei als große Hürde auf dem Weg zu einem tieferen Verständnis von quantenmechanischen Vielteilchensystemen heraus.

Im Laufe dieser Arbeit werden wir die Hauptkonzepte ausarbeiten, welche für die Behandlung von Korrekturen, die über die Molekularfeldtheorie hinausgehen, eine entscheidende Rolle spielen. Darin eingeschlossen ist nicht nur die Behandlung von Vielteilchensystemen, sondern auch das Verständnis des Streuproblems zweier Teilchen ist von großer Bedeutung, um später mit den auftretenden Schwierigkeiten umgehen zu können. Aus diesem Grund werden wir einen kurzen Überblick über Tiefenergie-Streuung geben, bevor wir uns mit Streuprozessen in begrenzten Systemen auseinandersetzen.

Wir werden kurz auf Bogoliubovs Theorie eingehen, die den verbreitetsten Ansatz darstellt, um Korrekturen zur Molekularfeldtheorie zu erhalten. Dabei werden wir feststellen, dass das Einbeziehen von Größen aus der Streutheorie zu Divergenzen führen kann, wenn dabei nicht mit ausreichender Vorsicht vorgegangen wird.

Das Hauptaugenmerk dieser Arbeit liegt auf dem diagrammatischen Ansatz von Hugenholtz und Pines. Die feldtheoretische Behandlung von schwach wechselwirkenden Bose Gasen wird Divergenzen verhindern und deshalb zu einer konsistenten Behandlung von Streuprozessen innerhalb der Beschreibung führen. Wir werden den diagrammatischen Ansatz verwenden, um höhere Korrekturen für dipolare Gase zu berechnen. Der Ansatz von Hugenholtz und Pines erlaubt dabei eine rigorose Behandlung der dipolaren Wechselwirkung, ohne das Auftreten von Divergenzen.

Zudem wird das konsistente Einbeziehen von Streugrößen es ermöglichen beschränkte Systeme endlicher Größe zu behandeln. Dabei sind wir insbesondere an der Beschreibung eines dimensionellen Übergangs interessiert. Wir werden ein Gas in einer Box mit periodischen Randbedingungen betrachten. Wie wir sehen werden, kann dieses System sowohl dreidimensionales als auch quasi-eindimensionales Verhalten aufweisen. Im Gegensatz zu einem echt eindimensionalen System führen die transversalen Freiheitsgrade zu einem zusätzlichen physikalischen Effekt. Dieser Effekt erscheint dabei in der feldtheoretischen Beschreibung ganz natürlich, was die Schönheit des Ansatzes unterstreicht.



# Contents

<b>1. Introduction</b>	<b>1</b>
<b>2. Scattering Theory</b>	<b>3</b>
2.1. Formal Scattering Theory . . . . .	3
2.2. Three Dimensions . . . . .	5
2.2.1. The Scattering Amplitude . . . . .	6
2.2.2. Low-Energy Scattering . . . . .	7
2.2.3. Replacement of the Potential . . . . .	8
2.3. One Dimension . . . . .	9
2.3.1. The Scattering Amplitude in One Dimension . . . . .	10
2.3.2. Low-Energy Scattering in one Dimension . . . . .	11
2.4. Confined Systems . . . . .	12
2.4.1. Replacement of the Pseudopotential . . . . .	12
2.4.2. Periodic Boundary Conditions . . . . .	13
<b>3. Bogoliubov Theory</b>	<b>19</b>
3.1. The Hamiltonian . . . . .	19
3.2. Bogoliubov Prescription . . . . .	20
3.3. Bogoliubov Transformation . . . . .	21
3.4. Ground State Energy . . . . .	22
3.5. Reason for Divergence . . . . .	23
3.6. Lee-Huang-Yang Correction . . . . .	27
3.7. One Dimension . . . . .	28
<b>4. Field-Theoretic Approach</b>	<b>31</b>
4.1. The Hamiltonian . . . . .	31
4.2. The Green's Function . . . . .	34
4.3. Perturbation Theory . . . . .	35
4.4. Dyson Equations . . . . .	38
4.5. Lowest Order . . . . .	40
4.6. Beyond Mean-Field . . . . .	42
4.6.1. Dipolar Interaction . . . . .	44
4.7. One Dimension . . . . .	46
<b>5. Confined Systems</b>	<b>49</b>

---

5.1. Limiting Cases . . . . .	49
5.2. Description of the Crossover . . . . .	52
5.3. Confinement-Induced Shift . . . . .	55
5.4. Crossover Behavior . . . . .	58
<b>6. Conclusion</b>	<b>61</b>
<b>A. Scattering Theory</b>	<b>63</b>
A.1. Born Series in Three Dimensions . . . . .	63
A.2. Harmonic Confinement . . . . .	64
<b>B. Ground State Energy</b>	<b>69</b>
<b>Bibliography</b>	<b>71</b>
<b>Aknowledgement</b>	<b>75</b>



# 1. Introduction

The realization of Bose-Einstein condensation in ultracold atom experiments in 1995 [1–3] marked a milestone in the experimental study of quantum mechanical many-body systems and was honored by a Nobel prize for Cornell, Wieman, and Ketterle in 2001. The evidence for Bose-Einstein condensates led to an enormous interest in the field of ultracold atomic gases, which rapidly expanding ever since. The main reason for that is the high level of control, these systems can provide. Using optical lattices, physicists can model systems from scratch, which opens up new opportunities to investigate quantum many-body systems. Besides, the interactions between the particles can be controlled via Feshbach resonances [4, 5]. Thus, the field of ultracold atoms is a playground for both experimental and theoretical physicists to explore the world of many-body quantum mechanics on a macroscopic scale.

Over 20 years after the experimental evidence of Bose-Einstein condensation, the interest in the field is still unbroken. In recent years, the steady progress in cooling, trapping and measurement techniques made it possible for the group around T. Pfau to produce Bose-Einstein condensates, consisting of dipolar atoms for the first time [6]. The condensation of dipolar atoms gathered a lot of interest as the anisotropic and long-range nature of the dipole-dipole interaction provides additional possibilities to explore new quantum phenomena. The most fascinating feature of the dipolar condensates is the formation of patterns of droplets in regions, where a stable solution was not expected [7, 8]. The droplets are a good candidate for a supersolid ground state [9]. These novel quantum liquids are stabilized by the counterplay between the attractive dipolar interaction and quantum fluctuations in the system [10].

Besides the tremendous work experimental physicists had to invest to come to the point at which we are today, the theoretical description of the weakly interacting systems is a huge challenge as well. For a long time, the mean-field Gross-Pitaevskii description [11, 12], in which all particles are assumed to be part of the condensate, was sufficient to describe the experimental observations. However, today it is possible to measure higher order corrections like the depletion of the condensate [13] or beyond-mean-field corrections to the ground state energy [14]. In addition, the mean-field theory fails to describe phenomena like the droplets.

This work focuses on the treatment of beyond-mean-field corrections in weakly interacting Bose gases. As the atomic clouds are kept in traps in experiments, our goal is to build a consistent treatment of beyond-mean-field corrections in confined systems. Before treating the many-body system, we will give a short insight to scattering theory in chapter 2. The objective is to understand the physical processes involved in a scat-

tering event and how to treat scattering in confined systems. In chapter 3, we give an overview of the Bogoliubov theory [15], the most common approach to include beyond-mean-field corrections. As we will see, the correct treatment of scattering processes is involved and can lead to divergences in the theoretical description. Thus, we will introduce the field-theoretic approach of Hugenholtz and Pines [16] in chapter 4, to prevent the problems from the Bogoliubov theory. The field-theoretic approach will allow us to calculate the beyond-mean-field correction for a dipolar Bose gas without the need of curing divergences at all. In addition, the diagrammatic approach is a powerful tool for the description of confined systems. In chapter 5, we will apply it to weakly interacting bosonic particles restricted by periodic boundary conditions, which yields an insight to the peculiarities of confined systems.

## 2. Scattering Theory

In ultracold atomic gases, the particles interact via scattering processes. Hence, a fundamental understanding of low-energy scattering theory is essential for a consistent treatment of weakly interacting Bose gases.

The gases are dilute, and so the densities  $n$  are very low. For such low densities, the range of the interatomic potentials  $r_0$  is much smaller than the mean distance,  $1/n^{1/3}$ , between the particles. Thus, treating binary collisions is sufficient for a theoretical description.

The following sections 2.1-2.3 will give a short insight into scattering theory in one and three dimensions. The aim of these sections is not to provide a complete overview of the topic, but rather to understand the key mechanisms and concepts in low-energy scattering. For a detailed coverage of scattering theory, the reader is referred to standard quantum mechanics textbooks e.g., [17–19]. The last section 2.4 of this chapter will make use of the introduced concepts by applying them to scattering processes in confined systems.

### 2.1. Formal Scattering Theory

In what follows, the elastic scattering of two identical bosons of mass  $m$  is treated in their center-of-mass frame. The interaction potential  $V(r)$  between the particles is assumed to be of short range,

$$rV(r) \rightarrow 0 \quad \text{for} \quad r \rightarrow \infty, \quad (2.1)$$

and isotropic. Thus, it only depends on the distance  $r$  between the particles. The stationary Schrödinger equation of this problem is then given by

$$H |\Psi_{\mathbf{k}}\rangle = E_{\mathbf{k}} |\Psi_{\mathbf{k}}\rangle \quad \text{with} \quad H = H_0 + V, \quad (2.2)$$

where  $H_0$  denotes the Hamiltonian for a free particle  $H_0 = \hat{p}^2/m$ . For energies  $E_{\mathbf{k}} > 0$  the states are unbound and asymptotically free, whereas energies  $E_{\mathbf{k}} < 0$  correspond to bound states. To describe scattering processes, the energy is assumed to be positive, and the Schrödinger equation (2.2) has a solution for every value of  $E_{\mathbf{k}}$ . The remaining task is therefore not to find the eigenenergies as the spectrum is continuous, but to find the scattering states  $|\Psi_{\mathbf{k}}\rangle$ . The eigenstates of  $H_0$  will be denoted by  $|\phi_{\mathbf{k}}\rangle$  and fulfill

$$H_0 |\phi_{\mathbf{k}}\rangle = E_{\mathbf{k}} |\phi_{\mathbf{k}}\rangle \quad \text{with} \quad E_{\mathbf{k}} = \frac{\hbar^2 \mathbf{k}^2}{m}. \quad (2.3)$$

With the use of the states  $|\phi_{\mathbf{k}}\rangle$ , it is now possible to give a formal solution for the scattering states. This solution is known as the Lippmann-Schwinger equation,

$$|\Psi_{\mathbf{k}}\rangle = |\phi_{\mathbf{k}}\rangle + \frac{1}{E_{\mathbf{k}}^+ - H_0} V |\Psi_{\mathbf{k}}\rangle. \quad (2.4)$$

Here, the notation

$$E_{\mathbf{k}}^+ = \lim_{\eta \rightarrow 0^+} E_{\mathbf{k}} + i\eta \quad (2.5)$$

was introduced. For simplicity, the limit  $\eta \rightarrow 0^+$  will be implicit in the following. The Lippmann-Schwinger equation consists of two parts. The first term on the right-hand side of equation (2.4) describes a free incoming state, whereas the second one corresponds to the scattered outgoing state. By choosing a positive sign for the imaginary part in equation (2.5), we can ensure the causality of the Lippmann-Schwinger equation (2.4). This can be seen by introducing the concept of Green's functions.

The Green's function of a free particle is defined by the equation

$$(i\hbar\partial_t - H_0) G_0(t - t') = \delta(t - t'). \quad (2.6)$$

There are two solutions to this equation, namely the retarded Green's function

$$G_0^+(t - t') = -\frac{i}{\hbar} \Theta(t - t') e^{-iH_0(t-t')/\hbar}, \quad (2.7)$$

and the advanced Green's function

$$G_0^-(t - t') = \frac{i}{\hbar} \Theta(t' - t) e^{-iH_0(t-t')/\hbar}. \quad (2.8)$$

The function  $\Theta(t - t')$  denotes the Heaviside step function. Both solutions, (2.7) and (2.8), contain the time-evolution operator of a free particle

$$U(t - t') = e^{-iH_0(t-t')/\hbar} \quad (2.9)$$

and are therefore often called propagators as well.

With the use of these Green's functions, the time-dependent form of the Lippmann-Schwinger equation is

$$|\Psi_{\mathbf{k}}(t)\rangle = |\phi_{\mathbf{k}}(t)\rangle + \int dt' G_0(t - t') V |\Psi_{\mathbf{k}}(t')\rangle. \quad (2.10)$$

The Green's function mediates the impact of a scattering event at a time  $t'$  onto a state at the time  $t$ . As the solution  $|\Psi_{\mathbf{k}}(t)\rangle$  has to obey causality, the correct choice for the Green's function in (2.10) is the retarded one (2.6). Otherwise, the solution  $|\Psi_{\mathbf{k}}(t)\rangle$

would depend on future solutions  $|\Psi_{\mathbf{k}}(t')\rangle$  at times  $t' > t$ . A Fourier transformation of the retarded Green's function yields

$$\begin{aligned} G_0^+(E) &= \lim_{\eta \rightarrow 0^+} \int_{-\infty}^{\infty} dt e^{it(E+i\eta \operatorname{sgn}(t))/\hbar} G_0^+(t) \\ &= \frac{1}{E^+ - H_0}. \end{aligned} \quad (2.11)$$

With the use of the free Green's function, the Lippmann-Schwinger equation is reduced to

$$|\Psi_{\mathbf{k}}\rangle = |\phi_{\mathbf{k}}\rangle + G_0^+(E_{\mathbf{k}})V |\Psi_{\mathbf{k}}\rangle, \quad (2.12)$$

and can be solved iteratively,

$$\begin{aligned} |\Psi_{\mathbf{k}}\rangle &= |\phi_{\mathbf{k}}\rangle + G_0^+(E_{\mathbf{k}})V |\Psi_{\mathbf{k}}\rangle \\ &= |\phi_{\mathbf{k}}\rangle + G_0^+(E_{\mathbf{k}})V |\phi_{\mathbf{k}}\rangle + G_0^+(E_{\mathbf{k}})V |\Psi_{\mathbf{k}}\rangle \\ &= \sum_{n=0}^{\infty} (G_0^+(E_{\mathbf{k}})V)^n |\phi_{\mathbf{k}}\rangle. \end{aligned} \quad (2.13)$$

The series expansion of the solution  $|\Psi_{\mathbf{k}}\rangle$  is known as the Born series. It is equivalent to the standard perturbation theory in quantum mechanics. Hence, we get satisfying approximate solutions for the state  $|\Psi_{\mathbf{k}}\rangle$  by cutting off the series as long as the interactions  $V$  are weak.

Another relevant quantity, which will frequently appear in the following, is the  $T$ -matrix of the system. It is defined by

$$V |\Psi_{\mathbf{k}}\rangle = T |\phi_{\mathbf{k}}\rangle. \quad (2.14)$$

As it connects the incoming state  $|\phi_{\mathbf{k}}\rangle$  with the solution  $|\Psi_{\mathbf{k}}\rangle$ , it contains all information of the scattering event. Therefore, finding the  $T$ -matrix is equivalent to solving the Lippmann-Schwinger equation. The comparison of the definition of the  $T$ -matrix (2.14) and the Lippmann-Schwinger equation (2.13) immediately yields the expression

$$T(E) = \sum_{n=0}^{\infty} V (G_0(E)V)^n = V + VG_0(E)V + VG_0(E)V G_0(E)V \dots \quad (2.15)$$

Hence, the full  $T$ -matrix takes into account an infinite number of interactions. Similar to the Lippmann-Schwinger equation, we obtain approximate solutions for the  $T$ -matrix by cutting off the Born series for the  $T$ -matrix (2.15).

## 2.2. Scattering in Three Dimensions

The previous section has introduced essential concepts of scattering theory like the Lippmann-Schwinger equation, the Born series, or the  $T$ -matrix on a formal level. In the particular case of low-energy scattering in three dimensions, we will now take them under closer consideration.

### 2.2.1. The Scattering Amplitude

In coordinate representation, the Lippmann-Schwinger equation (2.12) reads

$$\Psi_{\mathbf{k}}(\mathbf{r}) = \phi_{\mathbf{k}}(\mathbf{r}) + \int_{\mathbb{R}^3} d^3\mathbf{r}' G_0^+(\mathbf{r}, \mathbf{r}', E_{\mathbf{k}}) V(\mathbf{r}') \Psi_{\mathbf{k}}(\mathbf{r}'). \quad (2.16)$$

The functions  $\phi_{\mathbf{k}}(\mathbf{r})$  are the coordinate representations of the states  $|\phi_{\mathbf{k}}\rangle$ , and for scattering in free space they are given by plane waves,

$$\phi_{\mathbf{k}}(\mathbf{r}) = e^{i\mathbf{k} \cdot \mathbf{r}}. \quad (2.17)$$

The coordinate representation of the Green's function (2.11) is denoted by  $G_0^+(\mathbf{r}, \mathbf{r}', E)$  and takes the form

$$\begin{aligned} G_0^+(\mathbf{r}, \mathbf{r}', E_{\mathbf{k}}) &= \langle \mathbf{r} | G_0^+(E_{\mathbf{k}}) | \mathbf{r}' \rangle \\ &= \frac{m}{\hbar^2} \int \frac{d^3\mathbf{k}'}{(2\pi)^3} \frac{e^{i\mathbf{k}' \cdot (\mathbf{r} - \mathbf{r}')}}{k^2 - k'^2 + i\eta} \\ &= -\frac{m}{\hbar^2} \int \frac{d^3\mathbf{k}'}{(2\pi)^3} \frac{e^{i\mathbf{k}' \cdot (\mathbf{r} - \mathbf{r}')}}{(k' + k + i\eta)(k' - k - i\eta)} \\ &= -\frac{m}{4\pi\hbar^2} \frac{e^{ik|\mathbf{r} - \mathbf{r}'|}}{|\mathbf{r} - \mathbf{r}'|}, \end{aligned} \quad (2.18)$$

where we have introduced  $|\mathbf{k}| = k$ . In the course of this integration, we chose the vector  $\mathbf{r} - \mathbf{r}'$  to coincide with the  $z$ -axis, which allows performing the angular integration. Afterwards, we used the residue theorem to obtain the final result.

Now that we know the form of the Green's function (2.18), we can introduce another important scattering quantity. The exact solution of the Lippmann-Schwinger equation (2.16) for small distances  $r$  between the particles is of minor interest, as for an observer, only the outcome of a scattering event is easily accessible. We can draw the same conclusion for dilute gases. The mean distance between the particles in the gas is large, and so two particles involved in a scattering event will travel a far distance until they interact with other particles. Hence, the relevant region to consider in equation (2.16) is the far field  $r \rightarrow \infty$ . The only quantity that depends on the distance  $r$  between the particles in the integral of the Lippmann-Schwinger equation (2.16) is the Green's function  $G_0^+(\mathbf{r}, \mathbf{r}', E_{\mathbf{k}})$ . Its long-range behavior is determined the expression

$$\begin{aligned} \lim_{r \rightarrow \infty} |\mathbf{r} - \mathbf{r}'| &= \sqrt{(\mathbf{r} - \mathbf{r}')^2} \\ &= r \sqrt{1 - 2\frac{\mathbf{e}_r \cdot \mathbf{r}'}{r} + \frac{r'^2}{r^2}} \\ &\approx r - \mathbf{e}_r \cdot \mathbf{r}', \end{aligned} \quad (2.19)$$

where  $\mathbf{e}_r$  denotes the unit vector in direction of  $\mathbf{r}$ . With the use of the equations (2.18) and (2.19), the far-field behavior of the Lippmann-Schwinger equation reads

$$\begin{aligned} \lim_{r \rightarrow \infty} \Psi_{\mathbf{k}}(\mathbf{r}) &= \phi_{\mathbf{k}}(\mathbf{r}) - \frac{m}{4\pi\hbar^2} \int_{\mathbb{R}^3} d^3\mathbf{r}' e^{-i\mathbf{k}\mathbf{e}_r \cdot \mathbf{r}'} V(\mathbf{r}') \Psi_{\mathbf{k}}(\mathbf{r}') \frac{e^{i\mathbf{k}r}}{r} \\ &= e^{i\mathbf{k} \cdot \mathbf{r}} + f(\mathbf{k}, \mathbf{k}') \frac{e^{i\mathbf{k}r}}{r}. \end{aligned} \quad (2.20)$$

In the far field, the wave function  $\Psi_{\mathbf{k}}(\mathbf{r})$  consists of the incoming part given by a plane wave and the outgoing part proportional to a spherical wave. The function  $f(\mathbf{k}, \mathbf{k}')$  is called scattering amplitude and is given by

$$f(\mathbf{k}, \mathbf{k}') = -\frac{m}{4\pi\hbar^2} \int_{\mathbb{R}^3} d^3\mathbf{r}' e^{-i\mathbf{k}' \cdot \mathbf{r}'} V(\mathbf{r}') \Psi_{\mathbf{k}}(\mathbf{r}') \quad (2.21)$$

where  $\mathbf{k}' = k\mathbf{e}_r$ . In three dimensions, it is connected to the  $T$ -matrix by

$$\begin{aligned} f(\mathbf{k}, \mathbf{k}') &= -\frac{m}{4\pi\hbar^2} \langle \phi_{\mathbf{k}'} | V | \Psi_{\mathbf{k}} \rangle \\ &= -\frac{m}{4\pi\hbar^2} \langle \phi_{\mathbf{k}'} | T(E_{\mathbf{k}}) | \phi_{\mathbf{k}} \rangle. \end{aligned} \quad (2.22)$$

Like the  $T$ -matrix, the scattering amplitude contains the information of an infinite number of interactions between the particles. Note that for the scattering amplitude we require  $|\mathbf{k}| = |\mathbf{k}'|$  as we are interested in elastic scattering processes. Therefore, only matrix elements on the energy shell or short on-shell matrix elements of  $T$  are needed for the scattering amplitude. In general,  $\mathbf{k}'$ ,  $\mathbf{k}$ , and  $E$  can be chosen independently in the matrix elements

$$\langle \phi_{\mathbf{k}'} | T(E) | \phi_{\mathbf{k}} \rangle. \quad (2.23)$$

### 2.2.2. Low-Energy Scattering

In the low-energy regime, the scattering amplitude takes a simple form, and the description of the scattering processes facilitates. The calculation of the scattering amplitude for isotropic potentials at low energies is well-documented in the literature and can be found in every standard quantum mechanics textbook. Therefore, the derivation of the low-energy scattering amplitude will be skipped here, but can, for example, be found in [17]. Expressing all occurring quantities by partial waves, inserting them into the Schrödinger equation (2.2) and expanding for small energies gives the leading order of the scattering amplitude,

$$f(k) = -\frac{1}{\frac{1}{a_s} + ik}. \quad (2.24)$$

It is now important to realize that the low-energy behavior of the scattering amplitude is only determined by the constant  $a_s$ , which is known as the scattering length. As a consequence, the low-energy scattering is universal. The outcome of a scattering event is the same for two different potentials as long as they share the same scattering length. The universal behavior can be understood from a physical point of view. For extremely low energies, the de Broglie wavelength of the particles is much larger than the range  $r_0$  potential  $V$ . As we cannot localize the particles within their de Broglie wavelength, they are spread over a distance much larger than  $r_0$ . Thus, the probability of finding the particles within the range of interaction is small. The spread particles only witness an averaged effect of the potential and cannot resolve the inner structure of the potential. The exact shape of the interaction becomes unimportant. Throughout this work, the three-dimensional scattering length is assumed to be positive,  $a_s > 0$ .

In the limit of vanishing momenta, the wave function (2.20) behaves like

$$\Psi_{\mathbf{k} \rightarrow 0}(\mathbf{r}) = 1 - \frac{a_s}{r} \quad (2.25)$$

and has a node for  $r = a_s$ . We can observe the same behavior in the low-energy scattering on a hard sphere of radius  $a_s$ . For this case, the Schrödinger equation is given by

$$0 = \begin{cases} (\nabla^2 + k^2)\Psi_{\mathbf{k}}(\mathbf{r}) & \text{for } r > a \\ \Psi_{\mathbf{k}}(\mathbf{r}) & \text{for } r \leq a. \end{cases} \quad (2.26)$$

For momenta  $k \rightarrow 0$ , the solution of (2.26) is

$$\Psi_{\mathbf{k} \rightarrow 0}(\mathbf{r}) = \begin{cases} 1 - \frac{a_s}{r} & \text{for } r > a_s \\ 0 & \text{for } r \leq a_s. \end{cases} \quad (2.27)$$

Thus, for positive scattering lengths, a potential with scattering length  $a_s$  governs the same scattering behavior as a hard sphere potential of radius  $a_s$ , which gives an intuitive interpretation of the scattering length.

With the knowledge of the low-energy scattering amplitude  $f(\mathbf{k}, \mathbf{k}')$ , the low-energy on-shell matrix elements of the  $T$ -matrix are given by

$$\langle \phi_{\mathbf{k}'=0} | T(E_{\mathbf{k}}) | \phi_{\mathbf{k}=0} \rangle = \frac{4\pi\hbar^2 a_s}{m}. \quad (2.28)$$

### 2.2.3. Replacement of the Potential

The universal low-energy scattering allows for drastic simplifications in the theoretical description of scattering processes. Instead of performing all calculations with the intricate exact atomic potentials, we can obtain the correct results by much simpler potentials. Hence, we replace the exact potential  $V$  by a pseudopotential,

$$\tilde{V}_{\text{pseudo}}(\mathbf{r}) = g_{3D}\delta(\mathbf{r}), \quad (2.29)$$



that reproduces the correct scattering length if the coupling constant  $g_{3D}$  is chosen correctly. As previously mentioned, the Born series does not have to be evaluated completely, but can be cut off early for weak interactions. The Born series of the scattering amplitude for the pseudopotential reads

$$\begin{aligned} f(\mathbf{k}, \mathbf{k}') &= -a_s \\ &= -\frac{m}{4\pi\hbar^2} \left\langle \phi_{\mathbf{k}'} \left| \tilde{V}_{\text{pseudo}} \right| \phi_{\mathbf{k}} \right\rangle \\ &\quad - \frac{m}{4\pi\hbar^2} \left\langle \phi_{\mathbf{k}'} \left| \tilde{V}_{\text{pseudo}} G_0^+(E_{\mathbf{k}}) \tilde{V}_{\text{pseudo}} \right| \phi_{\mathbf{k}} \right\rangle + \dots \end{aligned} \quad (2.30)$$

In first approximation, which is also known as the first Born approximation, only the leading term of the series in (2.30) is taken into account

$$a_s = \frac{m}{4\pi\hbar^2} V_{\text{pseudo}}(\mathbf{k}' - \mathbf{k}). \quad (2.31)$$

The Fourier transform of the potential (2.29) is denoted by  $V_{\text{pseudo}}(\mathbf{k})$  and we arrive at an expression for the coupling constant

$$g_{3D} = \frac{4\pi\hbar^2 a_s}{m}. \quad (2.32)$$

Thus, the correct pseudopotential in first Born approximation reads

$$V_{\text{pseudo}}(\mathbf{k}) = \frac{4\pi\hbar^2 a_s}{m}. \quad (2.33)$$

Note that in first Born approximation the pseudopotential (2.33) coincides with the exact  $T$ -matrix (2.28). Hence, the usage of the pseudopotential in a theoretical description replaces the interaction  $V$  by the  $T$ -matrix and so by an infinite series of interactions. This is a crucial point to keep in mind while working with pseudopotentials. They can be a powerful tool, as the inclusion of an infinite series of interactions becomes very simple but we must treat them with care. They are no actual physical potentials in a sense that their spectrum is unbound from below [20]. While the first Born approximation of the scattering amplitude for the pseudopotential is still finite, all higher terms diverge, which also reflects its unphysical behavior. An excellent discussion of the renormalization of the delta-potential can be found in [21].

## 2.3. Scattering in One Dimension

The previous section covered the scattering processes in three spacial dimensions. In this section, we will briefly discuss the same concepts for one-dimensional systems. We will need a profound understanding of one-dimensional scattering processes for the treatment of confined systems in section 2.4.

### 2.3.1. The Scattering Amplitude in One Dimension

First, we will introduce the coordinate representations of the Lippmann-Schwinger equation (2.4) and the Green's function (2.7) in one dimension.

The Lippmann-Schwinger equation (2.12) in one spatial dimension is given by

$$\Psi_k(z) = \phi_k(z) + \int_{\mathbb{R}} dz' G_0^+(z, z', E_k) V(z') \psi_k(z'). \quad (2.34)$$

The coordinate representation of the incoming state  $|\phi_k\rangle$  is denoted as  $\phi_k(z)$ . As they are solutions to the free-particle Hamiltonian, they are given by plane waves,

$$\phi_k(z) = \langle z | \phi_k \rangle = e^{ikz}. \quad (2.35)$$

The incoming states might have the same form in three and one dimensions, but the Green's function obeys a different behavior,

$$\begin{aligned} G_0^+(z, z', E_k) &= \langle z | G_0^+(E_k) | z' \rangle \\ &= \frac{m}{\hbar^2} \int_{\mathbb{R}} \frac{dk'}{(2\pi)} \frac{e^{ik'(z-z')}}{k^2 - k'^2 + i\eta} \\ &= -\frac{m}{\hbar^2} \int_{\mathbb{R}} \frac{dk'}{(2\pi)} \frac{e^{ik'(z-z')}}{(k' + k + i\eta)(k' - k - i\eta)} \\ &= \frac{m}{2\hbar^2} \frac{1}{ik} e^{ik|z-z'|}. \end{aligned} \quad (2.36)$$

We performed the integration using the residue theorem. For  $z > z'$ , we close the contour in the upper half plane, whereas the contour is closed in the lower half plane for  $z < z'$ .

For the definition of the scattering amplitude, we need the far-field behavior of the Green's function. Similar to the three-dimensional Green's function, its far-field behavior is determined by

$$\lim_{z \rightarrow \infty} |z - z'| \approx z - z'. \quad (2.37)$$

With the use of the Green's function (2.36) and equation (2.37), the far-field behavior of the Lippmann-Schwinger equation (2.34) is

$$\begin{aligned} \lim_{z \rightarrow \infty} \Psi_k(z) &= e^{ikz} + \frac{m}{2\hbar^2} \int_{\mathbb{R}} dz' \frac{1}{ik} e^{ik|z-z'|} V(z') \Psi_k(z') \\ &\approx e^{ikz} + \frac{m}{2i\hbar^2 k} \int_{\mathbb{R}} dz' e^{-ikz'} V(z') \Psi_k(z') e^{ikz} \\ &= e^{ikz} + f(k) e^{ikz}. \end{aligned} \quad (2.38)$$

The far-field of the one-dimensional Lippmann-Schwinger equation consists of an incoming plane wave and an outgoing plane wave with the scattering amplitude

$$f(k) = \frac{m}{2i\hbar^2 k} \int_{\mathbb{R}} dz' e^{-ikz'} V(z') \Psi_k(z'). \quad (2.39)$$

Analog to the three-dimensional scattering amplitude (2.21), the one-dimensional scattering amplitude (2.39) is connected to the  $T$ -matrix,

$$\begin{aligned} f(k) &= \frac{m}{2i\hbar^2 k} \langle \phi_k | V | \Psi_k \rangle \\ &= \frac{m}{2i\hbar^2 k} \langle \phi_k | T(E_k) | \phi_k \rangle. \end{aligned} \quad (2.40)$$

In this definition of the scattering amplitude, the  $T$ -matrix and the scattering amplitude  $f(k)$  differ in their momentum dependence. In the literature, also other definitions of the scattering amplitude exist, so that it is still proportional to the  $T$ -matrix. Hence, the additional factor  $1/k$  appears in the far-field behavior of the wave function.

### 2.3.2. Low-Energy Scattering in one Dimension

For low-energies, the scattering amplitude  $f(k)$  is universal,

$$f(k) = -\frac{1}{1 + ik a_s^{1D}}. \quad (2.41)$$

Like in three dimensions, it can be fully characterized by the scattering length  $a_s^{1D}$ . The exact form of the potential is irrelevant as long as the potential possesses the correct scattering length.

The one-dimensional the delta-potential,

$$V_{1D}(z) = g_{1D} \delta(z), \quad (2.42)$$

does not face the same problems as the three-dimensional delta-potential. Its spectrum is not unbound from below [18], and the scattering amplitude is exactly solvable,

$$\begin{aligned} f(k) &= \frac{m}{2i\hbar^2 k} \int_{\mathbb{R}} dz' e^{-ikz'} V_{1D}(z') \Psi_k(z') = \left( \frac{mg_{1D}}{2i\hbar^2 k} \right) + \left( \frac{mg_{1D}}{2i\hbar^2 k} \right)^2 + \left( \frac{mg_{1D}}{2i\hbar^2 k} \right)^3 + \dots \\ &= \sum_{n=1}^{\infty} \left( \frac{mg_{1D}}{2i\hbar^2 k} \right)^n = - \left( 1 - ik \frac{2\hbar^2}{mg_{1D}} \right)^{-1}. \end{aligned} \quad (2.43)$$

In the last step we made use of the geometric series. To reproduce the correct scattering behavior, the scattering amplitude (2.43) has to match the low-energy scattering amplitude (2.41). Thus, the coupling constant  $g_{1D}$  has to take the form

$$g_{1D} = -\frac{2\hbar^2}{m a_s^{1D}}. \quad (2.44)$$

We will restrict ourselves to negative scattering lengths,  $a_s^{1D} < 0$ . Thus, the coupling constant  $g_{1D}$  is positive. Note that in one dimension, the delta-potential does not match the  $T$ -matrix. Hence, the delta-potential (2.42) does not take into account an infinite series of interactions, in contrast to the three-dimensional case.

## 2.4. Scattering in Confined Systems

Up to this point, we have discussed the scattering properties of three- and one-dimensional systems. In experimental setups, however, the geometric properties of the trap can complicate a clear distinction of dimensionality. A good example where the boundaries between a three- and a one-dimensional system get blurred is the cigar-shaped trap. These traps are elongated in one direction but tightly confined in the transverse directions. If the energy of a particle in the system is small compared to the energy of a transverse excitation, the transverse excitations are frozen out. Treating the system in only one spacial dimension seems natural. Although the transverse excitations are frozen out, the scattering between the particles is considered in three dimensions as long as the three-dimensional scattering length  $a_s$  is much smaller than the range of the confinement. In this case, the scattering process of two particles is not able to excite one of the particles into a transverse mode. In contrast to truly one-dimensional systems, the virtual processes during the scattering event can occupy transverse modes. Thus, a truly one-dimensional treatment in terms of the one-dimensional scattering length  $a_s^{1D}$  would neglect the virtual processes and influence the validity of the description. The proper way to describe these quasi-one-dimensional systems is to treat them in one spatial dimension but to describe the scattering processes in three dimensions. In other words, a connection between the three-dimensional scattering length  $a_s$  and the one-dimensional coupling constant  $g_{1D}$  is needed. Then, we can describe the quasi-one-dimensional systems, using the one-dimensional delta-potential (2.42) without neglecting the effect of virtual transverse excitations. The aim of this chapter is to derive the coupling constant  $g_{1D}$  for a system confined with periodic boundary conditions.

For a harmonic confinement in the transverse directions, the calculation of  $g_{1D}$  has already been performed by M. Olshanii [22]. In his work, Olshanii solves the three-dimensional Lippmann-Schwinger equation, imposing the correct asymptotic behavior for the wave function. The approach used in this work is different, and we will discuss it in detail for periodic boundary conditions. In appendix A.2 we have applied the approach to a harmonic confinement as well and obtain the same results as Olshanii.

### 2.4.1. Replacement of the Pseudopotential

In section 2.2.3, we discussed the advantages of the pseudopotential but mentioned problems as well. We can determine the coupling constant  $g_{3D}$  only within the first Born approximation, as all higher approximations diverge. To describe the influence of the confinement correctly, we need to take into account the entire Born series. Hence, we must replace the pseudopotential by a ‘true’ potential. The potential

$$V_\Lambda(\mathbf{r})\psi(\mathbf{r}) = g_\Lambda h_\Lambda^*(\mathbf{r}) \int_{\mathbb{R}} d^3\mathbf{u} h_\Lambda(\mathbf{u})\psi(\mathbf{u}) \quad (2.45)$$

allows a simple evaluation of the Born series. The functions  $h_\Lambda$  satisfy

$$\lim_{\Lambda \rightarrow 0} h_\Lambda(\mathbf{r}) = \delta(\mathbf{r}), \quad (2.46)$$

so we recover the delta-potential in the limit  $\Lambda \rightarrow 0$ . An example of  $h_\Lambda$  would be a Gaussian,

$$h_\Lambda(\mathbf{r}) = \frac{e^{-\frac{r^2}{2\Lambda}}}{(2\pi\Lambda)^{3/2}}, \quad (2.47)$$

but the exact form of the function  $h_\Lambda$  is of minor interest.

We can now evaluate the Born series for the scattering amplitude (2.21) with the potential  $V_\Lambda$  and obtain

$$f(\mathbf{k}, \mathbf{k}') = - \left( \frac{4\pi\hbar^2}{mg_\Lambda \tilde{h}_\Lambda^*(\mathbf{k}') \tilde{h}_\Lambda(\mathbf{k})} - \frac{4\pi}{\tilde{h}_\Lambda^*(\mathbf{k}') \tilde{h}_\Lambda(\mathbf{k})} \int_{\mathbb{R}^3} \frac{d^3\mathbf{p}}{(2\pi)^3} \frac{\tilde{h}_\Lambda(-\mathbf{p}) \tilde{h}_\Lambda^*(\mathbf{p})}{k^2 - p^2 + i\eta} \right)^{-1}, \quad (2.48)$$

where  $\tilde{h}_\Lambda(\mathbf{k})$  is the Fourier transform of the function  $h_\Lambda(\mathbf{r})$ . The derivation of this result can be found in appendix A.1.

Next, we need to ensure that the potential  $V_\Lambda$  reproduces the correct scattering length  $a_s$ . Hence, we must solve the equation

$$f(0, 0) = -a_s = - \left( \frac{4\pi\hbar^2}{mg_\Lambda |\tilde{h}_\Lambda(0)|^2} + \frac{4\pi}{|\tilde{h}_\Lambda(0)|^2} \int_{\mathbb{R}^3} \frac{d^3\mathbf{p}}{(2\pi)^3} \frac{\tilde{h}_\Lambda(-\mathbf{p}) \tilde{h}_\Lambda^*(\mathbf{p})}{p^2 - i\eta} \right)^{-1} \quad (2.49)$$

for  $g_\Lambda$ . A short manipulation yields the final result

$$g_\Lambda = \frac{4\pi\hbar^2 a_s}{m |\tilde{h}_\Lambda(0)|^2} \left( 1 - \frac{4\pi a_s}{|\tilde{h}_\Lambda(0)|^2} \int_{\mathbb{R}^3} \frac{d^3\mathbf{p}}{(2\pi)^3} \frac{\tilde{h}_\Lambda(-\mathbf{p}) \tilde{h}_\Lambda^*(\mathbf{p})}{p^2 - i\eta} \right)^{-1}. \quad (2.50)$$

Note that for  $\Lambda \rightarrow 0$  the coupling constant  $g_\Lambda$  vanishes as the integral in equation (2.50) diverges. Thus, the scattering amplitude diverges, which is following the previous considerations in section 2.2.3. For finite values of  $\Lambda$ , the function  $\tilde{h}_\Lambda$  introduces a high momentum cut-off, and the integral remains finite.

The coupling constant  $g_\Lambda$  completes the potential  $V_\Lambda$ . Thus, both the actual interatomic potential  $V$  and the potential  $V_\Lambda$  govern the same low-energy scattering properties. With the use of  $V_\Lambda$ , we can now investigate the scattering properties of confined systems.

### 2.4.2. Periodic Boundary Conditions

In chapter 5 of this work, we want to treat a gas of weakly interacting bosons confined by periodic boundary conditions. Hence, we need to discuss the two-body scattering

problem first, to treat the many-body system correctly. Our goal of this section is to find the correct description of the quasi-one-dimensional limit of the system. Thus, we need to find the connection between the three-dimensional scattering length  $a_s$  and the coupling constant  $g_{\text{pbc}}$  of the one-dimensional potential

$$V_{\text{pbc}}(z) = g_{\text{pbc}}\delta(z). \quad (2.51)$$

If we find this connection, we can use the potential (2.51) for a one-dimensional description of the Bose gas, without neglecting the influence of the transverse modes.

Consider a box that is infinitely elongated along the  $z$ -direction, but of length  $l_{\perp}$  in  $x$ - and  $y$ -direction. We impose periodic boundary conditions, therefore the allowed wave vectors  $\mathbf{k}$  are of the form

$$\mathbf{k} = \begin{pmatrix} k_x \\ k_y \\ k_z \end{pmatrix} \quad \text{with} \quad k_z \in \mathbb{R}, \quad k_x = \frac{2\pi}{l_{\perp}}i, \quad k_y = \frac{2\pi}{l_{\perp}}j, \quad \text{and} \quad i, j \in \mathbb{Z}. \quad (2.52)$$

The background Hamiltonian is that of a free particle and its eigenstates are denoted by  $|\Phi_{\mathbf{k}}\rangle$ . The corresponding eigenenergies  $E_{\mathbf{k}}$  are

$$H_0 |\Phi_{\mathbf{k}}\rangle = E_{\mathbf{k}} |\Phi_{\mathbf{k}}\rangle = \frac{\hbar^2(k_x^2 + k_y^2 + k_z^2)}{m} |\Phi_{\mathbf{k}}\rangle. \quad (2.53)$$

We are interested in the low-energy regime. The particles occupy the transverse ground state  $i = j = 0$ , and we assume that the kinetic energy along the  $z$ -axis is much smaller than the energy to excite a transverse mode,

$$k_z \ll \frac{2\pi}{l_{\perp}}. \quad (2.54)$$

The scattering process itself remains three dimensional as long as the scattering length  $a_s$  is much smaller than the confinement,

$$a_s \ll l_{\perp}. \quad (2.55)$$

The Lippmann-Schwinger equation for the problem reads

$$\Psi_{0,0,k_z}(\mathbf{r}) = e^{ik_z z} + \int_{\mathbb{R}^3} d^3\mathbf{r}' G_0^+(\mathbf{r}, \mathbf{r}', k_z) V(\mathbf{r}') \Psi_{0,0,k_z}(\mathbf{r}'). \quad (2.56)$$

In order to define a scattering amplitude analog to the previous sections, we need to consider the far-field behavior of the Lippmann-Schwinger equation. Thus, we need to

calculate the far-field behavior of the Green's function for the transverse ground state,

$$\begin{aligned}
G_0^+(\mathbf{r}, \mathbf{r}', k_z) &= \frac{m}{\hbar^2} \int_{\mathbb{R}} \frac{dk'_z}{2\pi} \frac{1}{l_{\perp}^2} \sum_{k'_x, k'_y} \frac{e^{i\mathbf{k}' \cdot (\mathbf{r}-\mathbf{r}')}}{k_z^2 - k'^2 + i\eta} \\
&= \frac{m}{2i\hbar^2 l_{\perp}^2 k_z} e^{ik_z|z-z'|} - \frac{m}{2\hbar^2 l_{\perp}^2} \sum'_{k'_x, k'_y} e^{i(k'_x(x-x') + k'_y(y-y'))} \frac{e^{-\sqrt{k_x'^2 + k_y'^2 - k_z^2}|z-z'|}}{\sqrt{k_x'^2 + k_y'^2 - k_z^2}} \\
&\xrightarrow{z \rightarrow \infty} \frac{m}{2i\hbar^2 l_{\perp}^2 k_z} e^{ik_z(z-z')}.
\end{aligned} \tag{2.57}$$

For the second line we evaluated the integration over  $k'_z$  and split off the term  $k'_x = k'_y = 0$  from the sum. The primed sum does not contain this term. In the last line, we performed the limit  $z \rightarrow \infty$ . The result is only valid if

$$k_x'^2 + k_y'^2 - k_z^2 \neq 0,$$

which is guaranteed by the condition (2.54).

With the far-field behavior of the Green's function (2.57), the Lippmann-Schwinger equation becomes

$$\begin{aligned}
\Psi_{k_z}(\mathbf{r}) &= e^{ik_z z} + \int_{\mathbb{R}^3} d^3\mathbf{r}' G_0^+(\mathbf{r}, \mathbf{r}', k_z) V(\mathbf{r}') \Psi_{k_z} \\
&\xrightarrow{z \rightarrow \infty} e^{ik_z z} + f_{\text{pbc}}(k_z) e^{ik_z z}.
\end{aligned}$$

We have introduced the scattering amplitude

$$f_{\text{pbc}}(k_z) = \frac{m}{2i\hbar^2 l_{\perp}^2} \int_{\mathbb{R}^3} d^3\mathbf{r} e^{-ik_z z} V(\mathbf{r}) \Psi_{k_z}(\mathbf{r}) \tag{2.58}$$

of the quasi-one-dimensional system. It describes the scattering processes along the  $z$ -axis of the system. Hence, it does not surprise that the scattering amplitude  $f_{\text{pbc}}$  closely resembles the one-dimensional scattering amplitude (2.39).

The scattering amplitude  $f_{\text{pbc}}$  describes the scattering processes correctly as long as the potential  $V(\mathbf{r})$  possesses the same scattering length  $a_s$  as the interatomic potential. For the potential  $V_{\Lambda}(\mathbf{r})$ , we have ensured this in the previous section. Thus, we will now evaluate the scattering amplitude  $f_{\text{pbc}}$  in complete analogy to the previous section with the potential  $V_{\Lambda}(\mathbf{r})$ ,

$$f_{\text{pbc}}(k_z) = \frac{mg_{\Lambda}}{2i\hbar^2 l_{\perp}^2 k_z} |\tilde{h}_{\Lambda}(0, 0, k_z)|^2 \sum_{n=0}^{\infty} \left[ \frac{mg_{\Lambda}}{\hbar^2 l_{\perp}^2} \sum_{k'_x, k'_y} \int_{\mathbb{R}} \frac{dk'_z}{2\pi} \frac{\tilde{h}_{\Lambda}(-\mathbf{k}') \tilde{h}_{\Lambda}^*(\mathbf{k}')}{k_z^2 - k'^2 + i\eta} \right]^n. \tag{2.59}$$

In contrast to a truly one-dimensional system, the scattering amplitude (2.59) contains the sum over the transverse modes. Making use of the geometric series and splitting off the term involving  $k'_x = k'_y = 0$ , we arrive at

$$f_{\text{pbc}}(k_z) = - \left( 1 - \frac{2ik_z}{|\tilde{h}_\Lambda(0, 0, k_z)|^2} \left( \frac{\hbar^2 l_\perp^2}{mg_\Lambda} + \sum'_{k'_x, k'_y} \int_{\mathbb{R}} \frac{dk'_z}{2\pi} \frac{\tilde{h}_\Lambda(-\mathbf{k}') \tilde{h}_\Lambda^*(\mathbf{k}')}{k'^2 - i\eta} \right) + \mathcal{O}(k_z^3) \right)^{-1}. \quad (2.60)$$

A one-dimensional treatment of the quasi-one-dimensional system must reproduce this scattering amplitude. Otherwise, the transverse degrees of freedom are not taken into account properly.

We have evaluated the one-dimensional scattering amplitude (2.39) for the delta-potential in section 2.3.2. Hence, we can immediately give the scattering amplitude for  $V_{\text{pbc}}$ ,

$$f(k_z) = - \left( 1 - ik_z \frac{2\hbar^2}{mg_{\text{pbc}}} \right)^{-1}. \quad (2.61)$$

In order to describe the interaction between the particles with  $V_{\text{pbc}}$  correctly, we must solve the equation

$$f_{\text{pbc}}(k_z) = f(k_z) \quad (2.62)$$

for  $g_{\text{pbc}}$ . A short calculation yields an expression for the coupling constant

$$g_{\text{pbc}} = \frac{g_{3\text{D}}}{l_\perp^2} \left( 1 - 4\pi a_s \left( \int_{\mathbb{R}^3} \frac{d^3\mathbf{k}'}{(2\pi)^3} \frac{\tilde{h}_\Lambda(-\mathbf{k}') \tilde{h}_\Lambda^*(\mathbf{k}')}{k'^2 - i\eta} - \frac{1}{l_\perp^2} \sum'_{k'_x, k'_y} \int_{\mathbb{R}} \frac{dk'_z}{2\pi} \frac{\tilde{h}_\Lambda(-\mathbf{k}') \tilde{h}_\Lambda^*(\mathbf{k}')}{k'^2 - i\eta} \right) \right)^{-1}. \quad (2.63)$$

The remaining task is to evaluate the sums and integrals that still appear in equation (2.63).

In a one-dimensional description the problems of a delta-potential are absent, as we have seen in section 2.3. Thus, we can take the limit  $\Lambda \rightarrow 0$ . However, we have to keep in mind that the functions  $\tilde{h}_\Lambda(\mathbf{k})$  introduced a high-momentum cut-off for both terms simultaneously. Let us first treat the term involving the sum over the transverse modes,

$$\begin{aligned} \frac{1}{l_\perp^2} \sum'_{k'_x, k'_y} \int_{\mathbb{R}} \frac{dk'_z}{2\pi} \frac{1}{k'^2 - i\eta} &= \frac{1}{2l_\perp^2} \sum'_{k'_x, k'_y} \frac{1}{\sqrt{k_x'^2 + k_y'^2}} = \frac{1}{4\pi l_\perp} \sum'_{i,j} \frac{1}{\sqrt{i^2 + j^2}} \\ &= \frac{1}{4\pi l_\perp} \lim_{R \rightarrow \infty} \sum'_{i^2 + j^2 \leq R} \frac{1}{\sqrt{i^2 + j^2}}. \end{aligned} \quad (2.64)$$



We performed the integration over  $k'_z$  first and then inserted the definition of the wave vectors (2.52). In the last line, we made sure to treat the high-momentum cut-off correctly.

Next, we treat the term involving the integration over the entire  $k$ -space,

$$\begin{aligned} \int_{\mathbb{R}^3} \frac{d^3\mathbf{k}'}{(2\pi)^3} \frac{1}{k'^2 - i\eta} &= \frac{1}{8\pi^2} \int_{\mathbb{R}} \int_{\mathbb{R}} dk'_x dk'_y \frac{1}{\sqrt{k'^2_x + k'^2_y}} = \frac{1}{4\pi l_{\perp}} \int_{\mathbb{R}} \int_{\mathbb{R}} didj \frac{1}{\sqrt{i^2 + j^2}} \\ &= \frac{1}{4\pi l_{\perp}} \lim_{R \rightarrow \infty} 2\pi R. \end{aligned} \quad (2.65)$$

Analog to the expression before, we first evaluated the integration over  $k'_z$ . To treat both expressions equally, we made use of the substitutions  $k'_x = 2\pi i/l_{\perp}$  and  $k'_y = 2\pi j/l_{\perp}$ . The remaining integral is then evaluated in polar coordinates.

With the use of both terms (2.65) and (2.64), we arrive at the final form of the coupling constant

$$g_{\text{pbc}} = \frac{4\pi\hbar^2 a_s}{m} \frac{1}{l_{\perp}^2} \left(1 - \frac{a_s}{l_{\perp}} C_{\text{pbc}}\right)^{-1} \quad \text{with} \quad C_{\text{pbc}} = \lim_{R \rightarrow \infty} \left(2\pi R - \sum'_{i^2+j^2 \leq R} \frac{1}{\sqrt{i^2 + j^2}}\right). \quad (2.66)$$

We determined the constant  $C_{\text{pbc}}$  numerically to  $C_{\text{pbc}} = 3.89\dots$ . The general form of the coupling constant  $g_{\text{pbc}}$  is very similar to the coupling constant for a harmonic confinement obtained by Olshanii [22],

$$g_{\text{ho}} = \frac{4\pi\hbar^2 a_s}{m} \frac{1}{\pi a_{\perp}^2} \left(1 - \frac{a_s}{a_{\perp}} C_{\text{ho}}\right)^{-1} \quad \text{with} \quad C_{\text{ho}} = \lim_{s \rightarrow \infty} \left(\int_0^s ds' \frac{1}{\sqrt{s'}} - \sum_0^s \frac{1}{\sqrt{s'}}\right).$$

The derivation of  $g_{\text{ho}}$  can be found in appendix B.

Like  $g_{\text{ho}}$ , the coupling constant  $g_{\text{pbc}}$  contains the three-dimensional coupling constant  $g_{3\text{D}} = 4\pi\hbar^2 a_s/m$  divided by the area of the confinement. The scattering length is small compared to the confinement, so the correction to the simple prefactor is small,

$$g_{\text{pbc}} \approx \frac{g_{3\text{D}}}{l_{\perp}^2} \left(1 + \frac{a_s}{l_{\perp}} C_{\text{pbc}}\right). \quad (2.67)$$

Note that we can obtain this approximate result also by only using the second Born approximation for all occurring scattering amplitudes. Higher order Born approximations will lead to higher orders in the small parameter  $a_s/l_{\perp}$ .

With the coupling constant  $g_{\text{pbc}}$  we have found a way to treat the scattering processes in quasi-one-dimensional systems confined by periodic boundary conditions consistently. The result of this chapter will play a crucial role for the treatment of the confined weakly interacting Bose gas in chapter 5.



# 3. Bogoliubov Theory

The goal of this work is to understand the physics of weakly interacting Bose gases on a fundamental, diagrammatic level. Before we introduce a field-theoretic method, it is useful to study the most common approach for treating weakly interacting Bose gases, namely the Bogoliubov theory. In his work “On the theory of superfluidity” in 1947 [15], N. Bogoliubov was the first to develop a microscopic theory of superfluidity in a homogeneous system of weakly interacting bosons. His approach is based on simple assumptions that allowed him to treat the ground state of the system. Even 70 years later, his theory is still frequently used in recent theoretical descriptions, e.g., [23]. His approach is straightforward and rather short, compared to field-theoretic descriptions [16, 24, 25]. However, its simplicity can be a curse, since it can veil the physical processes that contribute to the ground state energy if one is not careful enough. Thus, the Bogoliubov theory has to be treated with care. Otherwise, divergences can appear in the description.

The following chapter will give a short insight into the Bogoliubov theory by pointing out the crucial steps and approximations. A more detailed coverage can be found, for example, in [26, 27].

## 3.1. The Hamiltonian

In the following, we will treat a homogeneous system of  $N$  weakly interacting bosons of mass  $m$  at temperature  $T = 0$  in a box of volume  $\Omega$  with periodic boundary conditions. The particles interact via a pairwise interaction potential, which is given by  $V(\mathbf{q})$  in momentum space. In second quantization we describe the system by the Hamiltonian

$$H = H_0 + H_{\text{int}} = \sum_{\mathbf{k}} \varepsilon_0(\mathbf{k}) a_{\mathbf{k}}^\dagger a_{\mathbf{k}} + \frac{1}{2\Omega} \sum_{\mathbf{k}, \mathbf{k}', \mathbf{q}} V(\mathbf{q}) a_{\mathbf{k}+\mathbf{q}}^\dagger a_{\mathbf{k}'-\mathbf{q}}^\dagger a_{\mathbf{k}'} a_{\mathbf{k}}. \quad (3.1)$$

The first term of the Hamiltonian corresponds to the kinetic energy of the particles, where

$$\varepsilon_0(\mathbf{k}) = \frac{\hbar^2 k^2}{2m} \quad (3.2)$$

is the kinetic energy of a free particle with momentum  $\mathbf{k}$ . The operators  $a_{\mathbf{k}}$  and  $a_{\mathbf{k}}^\dagger$  are the annihilation and creation operators of bosonic particles with momentum  $\mathbf{k}$ . They

obey the usual bosonic commutation relations

$$\left[ a_{\mathbf{k}}, a_{\mathbf{k}'}^\dagger \right] = \delta_{\mathbf{k}, \mathbf{k}'}, \quad (3.3)$$

where  $\delta_{\mathbf{k}, \mathbf{k}'}$  is the Kronecker delta. The second term of the Hamiltonian describes the interaction between the particles. The particles are weakly interacting. Thus, the kinetic energy is much larger than the interaction energy.

## 3.2. Bogoliubov Prescription

For low temperatures and weak interactions, the system undergoes a Bose-Einstein condensation. In the absence of any interaction between the particles, the ground state of the system is given by

$$|N_{\mathbf{k}=0}, 0_{\mathbf{k}_1}, 0_{\mathbf{k}_2}, \dots\rangle. \quad (3.4)$$

All  $N$  particles occupy the mode  $\mathbf{k} = 0$  and are part of the condensate. The number of condensate particles is given by  $N_0 = N$ . No other mode  $\mathbf{k}_n$  is excited.

Weak interactions  $V(\mathbf{q})$  act as small perturbation to this ground state. Not all particles are part of the condensate anymore,  $N_0 = N - N'$ , and  $N'$  particles occupy excited states. However, for weak interactions, the fraction  $N_0/N$  stays finite with increasing system size. For large enough systems, the condensate is always macroscopically occupied. For the action of the operators  $a_0$  and  $a_0^\dagger$  this means

$$\begin{aligned} a_0 |N_0, \dots\rangle &= \sqrt{N_0} |N_0 - 1, \dots\rangle \approx \sqrt{N_0} |N_0, \dots\rangle \\ a_0^\dagger |N_0, \dots\rangle &= \sqrt{N_0 + 1} |N_0 + 1, \dots\rangle \approx \sqrt{N_0} |N_0, \dots\rangle. \end{aligned} \quad (3.5)$$

Thus, we can replace the operators  $a_0$  and  $a_0^\dagger$  by the number  $\sqrt{N_0}$ . The replacement of the operators is known as the Bogoliubov prescription.

When we replace all creation and annihilation operators of the condensed state in the Hamiltonian (3.1) by  $N_0$ , we obtain

$$\begin{aligned} H &= \sum_{\mathbf{k}} \varepsilon_0(\mathbf{k}) a_{\mathbf{k}}^\dagger a_{\mathbf{k}} \\ &+ \frac{N_0^2 V(0)}{2\Omega} \\ &+ \sum_{\mathbf{k}}' \left[ \frac{N_0}{\Omega} (V(0) + V(\mathbf{k})) a_{\mathbf{k}}^\dagger a_{\mathbf{k}} + \frac{N_0 V(\mathbf{k})}{2\Omega} (a_{\mathbf{k}}^\dagger a_{-\mathbf{k}}^\dagger + a_{\mathbf{k}} a_{-\mathbf{k}}) \right] \\ &+ \sum_{\mathbf{k}, \mathbf{q}}' \frac{V(\mathbf{q})}{2\Omega} \sqrt{N_0} (a_{\mathbf{k}+\mathbf{q}}^\dagger a_{\mathbf{q}} a_{\mathbf{k}} + a_{\mathbf{k}+\mathbf{q}}^\dagger a_{-\mathbf{q}}^\dagger a_{\mathbf{k}}) \\ &+ \sum_{\mathbf{k}, \mathbf{k}', \mathbf{q}}' \frac{V(\mathbf{q})}{2\Omega} a_{\mathbf{k}+\mathbf{q}}^\dagger a_{\mathbf{k}'-\mathbf{q}}^\dagger a_{\mathbf{k}'} a_{\mathbf{k}}. \end{aligned} \quad (3.6)$$

The Hamiltonian splits into terms of different order in  $N_0$ . The primed sum indicates the absence of the condensate mode. The number of condensate particles is large. Hence, a good approximation is to keep only terms that are at least of order  $N_0$ . This effectively neglects the interaction between excited particles. The only interactions that are taken into account are those between the condensate particles, described by the second line of equation (3.6), and those between a condensate particle and an excited particle, described by the third line of equation (3.6).

Next, we express the number of condensate particles by the total number of particles using particle conservation,

$$N_0 = N - \sum_{\mathbf{k}}' a_{\mathbf{k}}^\dagger a_{\mathbf{k}}. \quad (3.7)$$

We keep only terms of order  $N$ , which yields a quadratic Hamiltonian,

$$H = \sum_{\mathbf{k}} \varepsilon_0(\mathbf{k}) a_{\mathbf{k}}^\dagger a_{\mathbf{k}} + \frac{V(0)N^2}{2\Omega} + \sum_{\mathbf{k}}' \frac{NV(\mathbf{k})}{\Omega} \left[ a_{\mathbf{k}}^\dagger a_{\mathbf{k}} + \frac{1}{2} \left( a_{\mathbf{k}}^\dagger a_{-\mathbf{k}}^\dagger + a_{\mathbf{k}} a_{-\mathbf{k}} \right) \right]. \quad (3.8)$$

### 3.3. Bogoliubov Transformation

The Hamiltonian (3.8) contains off-diagonal elements in the basis spanned by the operators  $a_{\mathbf{k}}$  and  $a_{\mathbf{k}}^\dagger$ . We will diagonalize it by a Bogoliubov transformation. The transformation introduces new operators  $\alpha_{\mathbf{k}}$  and  $\alpha_{\mathbf{k}}^\dagger$  that are linear combinations of the operators  $a_{\mathbf{k}}$  and  $a_{\mathbf{k}}^\dagger$  and fulfill the same commutation relations

$$a_{\mathbf{k}} = u_{\mathbf{k}} \alpha_{\mathbf{k}} - v_{\mathbf{k}} \alpha_{-\mathbf{k}}^\dagger, \quad a_{\mathbf{k}}^\dagger = u_{\mathbf{k}} \alpha_{\mathbf{k}}^\dagger - v_{\mathbf{k}} \alpha_{-\mathbf{k}}, \quad [\alpha_{\mathbf{k}}, \alpha_{\mathbf{k}'}^\dagger] = \delta_{\mathbf{k}, \mathbf{k}'}. \quad (3.9)$$

The new operators couple creation and annihilation operators of opposite momenta. In order to obey the bosonic commutation relations, the amplitudes  $u_{\mathbf{k}}$  and  $v_{\mathbf{k}}$  must satisfy

$$u_{\mathbf{k}}^2 - v_{\mathbf{k}}^2 = 1 \quad (3.10)$$

and can not be chosen independently. We can now express the Hamiltonian (3.8) by the new operators (3.9). The amplitudes  $u_{\mathbf{k}}$  and  $v_{\mathbf{k}}$  are then used to eliminate the off-diagonal elements. A short calculation leads to

$$u_{\mathbf{k}}^2 = \frac{1}{2} \left[ \frac{\varepsilon_0(\mathbf{k}) + NV(\mathbf{k})/\Omega}{E_{\mathbf{k}}} + 1 \right], \quad v_{\mathbf{k}}^2 = \frac{1}{2} \left[ \frac{\varepsilon_0(\mathbf{k}) + NV(\mathbf{k})/\Omega}{E_{\mathbf{k}}} - 1 \right], \quad (3.11)$$

where

$$E_{\mathbf{k}}^2 = \varepsilon_0(\mathbf{k})^2 + \frac{2NV(\mathbf{k})}{\Omega} \varepsilon_0(\mathbf{k}). \quad (3.12)$$

The final Hamiltonian reads

$$H = \frac{V(0)N^2}{2\Omega} - \frac{1}{2} \sum_{\mathbf{k}}' \left[ \varepsilon_0(\mathbf{k}) + \frac{NV(\mathbf{k})}{\Omega} - E_{\mathbf{k}} \right] + \sum_{\mathbf{k}}' E_{\mathbf{k}} \alpha_{\mathbf{k}}^\dagger \alpha_{\mathbf{k}}. \quad (3.13)$$

### 3.4. Ground State Energy and Excitation Spectrum

The Hamiltonian (3.13) is diagonal in the basis spanned by the operators  $\alpha_{\mathbf{k}}$  and  $\alpha_{\mathbf{k}}^\dagger$ . While the operator  $a_{\mathbf{k}}$  and  $a_{\mathbf{k}}^\dagger$  describe the bosonic particles in the gas, the new operators  $\alpha_{\mathbf{k}}$  and  $\alpha_{\mathbf{k}}^\dagger$  describe quasi-particles. The excitation spectrum of the quasi-particles is given by  $E_{\mathbf{k}}$ . If none of these quasi-particles is excited, the system is in its ground state. The energy is then simply given by the first two terms of the Hamiltonian (3.13),

$$E = E_{\text{mf}} - \frac{1}{2} \sum'_{\mathbf{k}} \left[ \varepsilon_0(\mathbf{k}) + \frac{NV(\mathbf{k})}{\Omega} - E_{\mathbf{k}} \right]. \quad (3.14)$$

The first term is called mean-field energy,

$$E_{\text{mf}} = \frac{V(0)N^2}{2\Omega}, \quad (3.15)$$

and corresponds to the interaction energy between condensate particles. The second term describes beyond-mean-field corrections and contains the interactions between condensate and excited particles.

To evaluate the ground state energy (3.14), we have to consider the potential  $V(\mathbf{k})$  first. The particles in the gas interact via scattering processes. If the gas is dilute, scattering events between two particles are rare and processes including more than two particles are very unlikely. Hence, we can restrict ourselves to binary collisions. In chapter 2, we discussed binary collisions in detail. For low energies the scattering between the particles is universal. The outcome of a scattering event is only determined by the scattering length  $a_s$  and does not depend on the exact form of the interaction. For three-dimensional scattering processes, we introduced the pseudopotential (2.29)

$$\tilde{V}_{\text{pseudo}}(\mathbf{r}) = g_{3\text{D}}\delta(\mathbf{r})$$

that reproduces the correct scattering length in first Born approximation. Thus, we chose the potential

$$V(\mathbf{k}) = g_{3\text{D}} = \frac{4\pi\hbar^2 a_s}{m}. \quad (3.16)$$

With the potential (3.16), the excitation spectrum of the quasi-particles (3.12) takes the form

$$E_{\mathbf{k}} = \sqrt{\left(\frac{\hbar^2 \mathbf{k}^2}{2m}\right)^2 + 2ng_{3\text{D}} \left(\frac{\hbar^2 \mathbf{k}^2}{2m}\right)}, \quad (3.17)$$

where we have introduced the density of the particles  $n = N/\Omega$ . The spectrum exhibits the low-momentum behavior

$$E_{\mathbf{k}} \stackrel{|\mathbf{k}| \ll 1}{\approx} \frac{\hbar^2 \sqrt{4\pi n a_s}}{m} |\mathbf{k}|, \quad (3.18)$$

which resembles the dispersion relation of phonons with the sound velocity

$$c = \frac{\hbar^2 \sqrt{4\pi n a_s}}{m}. \quad (3.19)$$

The evaluation of the ground state energy (3.14) is problematic for the potential (3.16). Inserting the potential (3.16) into the energy (3.14) and replacing the sum over momenta by an integral, the energy density takes the form

$$\frac{E}{\Omega} = \frac{1}{2} g_{3D} n^2 - \frac{1}{2} \int_{\mathbb{R}^3} \frac{d^3 \mathbf{k}}{(2\pi)^3} \left[ \varepsilon_0(\mathbf{k}) + n g_{3D} - \sqrt{\varepsilon_0(\mathbf{k})^2 + 2n g_{3D} \varepsilon_0(\mathbf{k})} \right]. \quad (3.20)$$

The integral in the second term behaves like

$$\int_{\mathbb{R}^3} \frac{d^3 \mathbf{k}}{(2\pi)^3} \frac{1}{\mathbf{k}^2} \quad (3.21)$$

for large momenta and diverges. We discuss the reason for this unphysical behavior in the following section.

### 3.5. Reason for Divergence

The divergence appearing in the energy density (3.20) is unphysical. We have to ask ourselves where we were not careful enough in the description of the weakly interacting Bose gas.

A detailed explanation of the occurring divergence in Bogoliubov's theory can be found in the book of David Pines and Philippe Nozières [27]. Here, we will point out the crucial steps to understand the nature of the divergence.

To treat the occurring divergence, we have to understand the Bogoliubov transformation (3.9) on a physical level. In a paper of Brueckner and Sawada [28], the authors are able to obtain the same ground state energy (3.14) without the use of a Bogoliubov transformation. By comparing their approach to the Bogoliubov theory, we can identify the physical concept behind Bogoliubov transformations.

In their paper, Brueckner and Sawada made use of Goldstone's linked cluster expansion [29],

$$E = E_0 + \Delta E \quad \text{with} \quad \Delta E = \sum_{n=0}^{\infty} \left\langle \Phi_0(N) \left| H_{\text{int}} \left( \frac{1}{E_0 - H_0} H_{\text{int}} \right)^n \right| \Phi_0(N) \right\rangle_c, \quad (3.22)$$

for the ground state  $E$ . The Hamiltonian  $H_{\text{int}}$  from equation (3.13) is treated as a perturbation to the Hamiltonian  $H_0$ . In our case, the energy of the unperturbed ground state is  $E_0 = 0$ . The ground state of  $H_0$  will be denoted as  $|\Phi_0(N)\rangle$ . It contains  $N$  particles in the condensed state as no interactions are present. The index  $c$  at the

expectation value stands for *connected*. Only those expectation values contribute to the ground state energy, which we cannot split into a product of two or more ground state expectation values. Goldstone's linked cluster expansion is equivalent to the standard perturbation theory in quantum mechanics.

In leading order, the ground state energy,

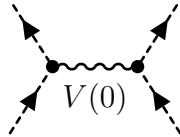
$$\begin{aligned} E^{(0)} &= \langle \Phi_0(N) | H_{\text{int}} | \Phi_0(N) \rangle = \frac{V(0)}{2\Omega} \langle \Phi_0(N) | a_0^\dagger a_0^\dagger a_0 a_0 | \Phi_0(N) \rangle \\ &= \frac{V(0)}{2\Omega} N(N-1) \approx \frac{V(0)N^2}{2\Omega} = E_{\text{mf}}, \end{aligned} \quad (3.23)$$

is the mean-field expression (3.15) from Bogoliubov's theory. Its energy stems from the interaction of two condensate particles. The second order term,

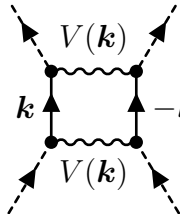
$$\begin{aligned} E^{(1)} &= - \left\langle \Phi_0(N) \left| H_{\text{int}} \frac{1}{H_0} H_{\text{int}} \right| \Phi_0(N) \right\rangle_c \\ &= - \frac{V(\mathbf{k})^2 N^2}{2\Omega^2} \sum_{\mathbf{k}} \frac{m}{\hbar^2 \mathbf{k}^2}, \end{aligned} \quad (3.24)$$

describes the excitation of two particles after the interaction of two condensate particles. The excited particles then propagate, which is described by  $1/H_0$ . During another interaction, both particles become part of the condensate again.

We will now introduce a graphical representation of the occurring terms that will make it easier to handle higher orders of the perturbation series. In addition, it will yield an intuitive explanation for the divergence. A more detailed explanation of the diagram technique is given in chapter 5 of this work, entirely dedicated to the diagrammatic treatment of weakly interacting Bose gases. For now, it is sufficient to link physical processes to diagrams. It will help us to understand which processes contribute to the ground state energy. Condensate particles are visualized by dashed lines, while we draw excited particles as solid lines. Interactions between particles are drawn with wavy lines. To obtain the energy, we sum over all inner momenta. With these rules, we can represent the mean-field contribution by

$$E_{\text{mf}} = \frac{V(0)N^2}{2\Omega} = \text{Diagram} \quad (3.25)$$


The second order term is

$$E^{(1)} = - \frac{V(\mathbf{k})^2 N^2}{2\Omega^2} \sum_{\mathbf{k}} \frac{m}{\hbar^2 \mathbf{k}^2} = \text{Diagram} \quad (3.26)$$




The third order contains three interaction lines. We find three distinct connected diagrams that contribute to the energy  $E^{(2)}$ ,

$$E^{(2)} = \text{Diagram 1} + \text{Diagram 2} + \text{Diagram 3} \quad (3.27)$$

The first diagram contains an interaction between excited particles. Thus, two different absolute values of momenta appear, namely  $k$  and  $k'$ . In the other two diagrams, two condensate particles are involved in every interaction. As the condensate particles carry no momentum, only a single pair of momenta  $(\mathbf{k}, -\mathbf{k})$  appears. Like Bogoliubov, Brueckner and Sawada argue that the interaction between excited particles can be neglected. Hence, only the last two terms in equation (3.27) contribute to the ground state energy. Under this approximation, they can evaluate the sum in Goldstone's linked cluster expansion (3.22) and obtain the ground state energy (3.14).

When comparing both approaches, we realize that Bogoliubov's transformation to a new pair of operators (3.9) corresponds to summing up all possible connected diagrams, which involve only a single pair of momenta  $(\mathbf{k}, -\mathbf{k})$ . Thus, we can represent the ground state energy (3.14) by

$$E = \text{Diagram 1} + \text{Diagram 2} + \text{Diagram 3} + \text{Diagram 4} + \dots \quad (3.28)$$

The problem of a diverging ground state energy arises when the potential  $V(\mathbf{k})$  is replaced by the pseudopotential (2.29)

$$\tilde{V}_{\text{pseudo}}(\mathbf{k}) = g_{3\text{D}} = \frac{4\pi\hbar^2 a_s}{m}.$$

In section 2.2 we saw that the pseudopotential matches the low-energy  $T$ -Matrix of the system

$$\langle \Phi_{\mathbf{k}'=0} | T(E_k) | \Phi_{\mathbf{k}=0} \rangle = \frac{4\pi\hbar^2 a_s}{m}.$$

The  $T$ -matrix contains the information of an infinite series of interactions

$$\langle \Phi_{\mathbf{k}'=0} | T(E_k) | \Phi_{\mathbf{k}=0} \rangle = \left\langle \Phi_{\mathbf{k}'=0} \left| \sum_{n=0}^{\infty} V (G_0(E_k) V)^n \right| \Phi_{\mathbf{k}=0} \right\rangle.$$

Using the diagrammatic description, we can represent the  $T$ -matrix by

$$(3.29)$$

Once we insert the pseudopotential into the ground state energy (3.28), the interactions are replaced by  $T$ -matrices. The energy becomes

$$E = \dots, \quad (3.30)$$

and the reason for the divergence gets clear. The second term in equation (3.30) contributes only diagrams that are already included by the first term, the mean field energy. Thus, an infinite amount of physical processes is taken into account too often, and the energy diverges.

To cure the divergence, we have to subtract the troublesome diagram

$$= -\frac{g_{3D}^2 N^2}{2\Omega^2} \sum_{\mathbf{k}} \frac{m}{\hbar^2 \mathbf{k}^2} \quad (3.31)$$

from the energy (3.14), to include the  $T$ -matrix properly. Note that the divergence occurs in a term proportional to  $n^2$ , which will be important for the field-theoretic approach in chapter 4.

### 3.6. Lee-Huang-Yang Correction

With the considerations of the previous section, we can finally give an expression for the ground state energy, including beyond-mean-field corrections

$$\begin{aligned} \frac{E}{\Omega} &= \frac{1}{2}g_{3\text{D}}n^2 + \frac{mg_{3\text{D}}^2n^2}{2\hbar^2} \int_{\mathbb{R}^3} \frac{d^3\mathbf{k}}{(2\pi)^3} \frac{1}{k^2} \\ &\quad - \frac{1}{2} \int_{\mathbb{R}^3} \frac{d^3\mathbf{k}}{(2\pi)^3} \left[ \varepsilon_0(\mathbf{k}) + ng_{3\text{D}} - \sqrt{\varepsilon_0(\mathbf{k})^2 + 2ng_{3\text{D}}\varepsilon_0(\mathbf{k})} \right]. \end{aligned} \quad (3.32)$$

The integral only depends on the absolute value  $|\mathbf{k}| = k$ . By the substitution

$$u = \sqrt{\frac{\hbar^2}{2mng_{3\text{D}}}}k, \quad (3.33)$$

the integral becomes dimensionless

$$\frac{E}{\Omega} = \frac{1}{2}g_{3\text{D}}n^2 - \frac{(ng_{3\text{D}})^{5/2}}{4\pi^2} \left( \frac{2m}{\hbar^2} \right)^{3/2} \int_0^\infty du u^2 \left( u^2 + 1 - \frac{1}{2u^2} - \sqrt{u^4 + 2u^2} \right).$$

The remaining integral has the value  $-8\sqrt{2}/15$ , so the final energy is

$$\begin{aligned} \frac{E}{\Omega} &= \frac{1}{2}g_{3\text{D}}n^2 + \frac{8}{15\pi^2} \left( \frac{m}{\hbar^2} \right)^{3/2} (ng_{3\text{D}})^{5/2} \\ &= \frac{2\pi\hbar^2 a_s}{m} n^2 \left( 1 + \frac{128}{15\sqrt{\pi}} (na_s^3) \right). \end{aligned} \quad (3.34)$$

The correction to the mean-field expression was first calculated by Lee, Huang and Yang [30, 31] and is called Lee-Huang-Yang (LHY) correction. The expansion parameter of the weakly interacting Bose gas is given by the gas parameter  $na_s^3$ . We can obtain the gas parameter by dimensional considerations as well. The density of the gas characterized a length scale, and thus a wave vector

$$k_n \sim n^{1/3}.$$

The gas is weakly interacting, so the interaction energy is much smaller than the kinetic energy,

$$\frac{\hbar^2 k_n^2}{m} \sim \frac{\hbar^2}{m} n^{2/3} \gg ng_{3\text{D}}.$$

Inserting the coupling constant  $g_{3\text{D}}$  from equation (2.32) then gives

$$na_s^3 \ll 1. \quad (3.35)$$

For low densities, the gas is weakly interacting.

A peculiarity of the LHY correction is its sign. From standard quantum mechanical perturbation theory, we would expect that the second order correction to the ground state always decreases the energy. The LHY correction increases the energy. The reason for this unusual behavior can be found in the use of the pseudopotential. Using the  $T$ -matrix in the mean-field expression already includes contributions that usually appear in higher order terms. Thus, the mean-field energy is lower than one would expect from a standard perturbation expansion. The higher orders that already lowered the mean-field energy have to be subtracted from the beyond-mean-field terms. Hence, the beyond-mean-field contributions are increased, and they become positive.

In the next section, we apply the Bogoliubov theory to the same system but in one dimension.

### 3.7. Bogoliubov Theory in One Dimension

We will end this chapter with the consideration of Bogoliubov's theory in one spatial dimension. Like in the previous section, we consider a Bose gas with repulsive interactions described by a delta-potential

$$\tilde{V}(z) = g_{1D}\delta(z). \quad (3.36)$$

The exact solution for this system was found by Lieb and Liniger in 1963 [32, 33]. Here, we restrict ourselves to the weakly interacting case and search for a perturbative solution for the ground state energy. Analog to the three-dimensional system, the one-dimensional density  $n_{1D} = N/L$ , where  $L$  is the size of the system, characterizes a wave vector

$$k_{n_{1D}} \sim n_{1D}.$$

The system is weakly interacting, so the kinetic energy is much larger than the interaction energy

$$\frac{\hbar^2 k_{n_{1D}}^2}{m} \sim \frac{\hbar^2}{m} n_{1D}^2 \gg n_{1D} g_{1D}.$$

By inserting the coupling constant obtained from scattering theory (2.44), we obtain

$$\frac{1}{n_{1D}|a_s^{1D}|} \ll 1. \quad (3.37)$$

In contrast to the three-dimensional case, the one-dimensional Bose gas is weakly interacting for high densities.

The same considerations as in the three-dimensional case yield an expression for the ground state energy

$$E = \frac{V(0)N^2}{2L} - \frac{1}{2} \sum'_{k_z} \left[ \varepsilon_0(k_z) + \frac{NV(k_z)}{L} - \sqrt{\varepsilon_0(k_z)^2 + \frac{2NV(k_z)}{L} \varepsilon_0(k_z)} \right], \quad (3.38)$$

where  $V(k_z)$  is the Fourier transform of the potential (3.36). In the thermodynamic limit  $L \rightarrow \infty$ , the one-dimensional energy density becomes

$$\frac{E}{L} = \frac{1}{2} g_{1D} n_{1D}^2 - \frac{1}{2} \int_{\mathbb{R}} \frac{dk_z}{2\pi} \left[ \varepsilon_0(k_z) + n_{1D} g_{1D} - \sqrt{\varepsilon_0(k_z)^2 + 2n_{1D} g_{1D} \varepsilon_0(k_z)} \right]. \quad (3.39)$$

The integral in equation (3.38) converges, in contrast to the three-dimensional case. To understand this difference, we have to recall chapter 2 of this work. For the three-dimensional system the divergence occurred once we inserted the pseudopotential. The pseudopotential matched the exact low-energy  $T$ -matrix of the system. Hence, every interaction was replaced by an infinite sum of interactions, and physical processes were taken into account too often. The delta-potential in one dimension does not match the low-energy  $T$ -matrix. Thus, the interactions are not replaced by an infinite series of interactions, and no physical process is taken into account too often. The energy converges without subtracting any terms.

With the substitution

$$u = \sqrt{\frac{\hbar^2}{2mn_{1D}g_{1D}}} k_z, \quad (3.40)$$

the energy density (3.39) becomes

$$\begin{aligned} \frac{E}{L} &= \frac{1}{2} g_{1D} n_{1D}^2 - \frac{(n_{1D} g_{1D})^{3/2}}{4\pi} \left( \frac{2m}{\hbar^2} \right)^{1/2} \int_0^\infty du \left[ u^2 + 1 - \sqrt{u^4 + 2u^2} \right], \\ &= \frac{1}{2} g_{1D} n_{1D}^2 - \frac{2}{3\pi} \left( \frac{m}{\hbar^2} \right)^{1/2} (n_{1D} g_{1D})^{3/2}. \end{aligned} \quad (3.41)$$

The beyond-mean-field correction is of lower order in the density than the mean-field expression. The sign of the beyond-mean-field corrections is negative, in contrast to the LHY correction. The one-dimensional delta-potential does not match the  $T$ -matrix, and hence a negative correction is expected from perturbation theory.

In this chapter, we have seen that Bogoliubov's approach allows us to treat weakly interacting Bose gases under simple assumptions. However, we also pointed out that it must be used with care, especially when combining Bogoliubov transformations with scattering properties. Otherwise, divergences in the description can occur. To obtain a finite energy and include the  $T$ -matrix properly, we had to cure the divergence manually by subtracting a troublesome diagram. The next chapter will introduce a field-theoretic approach to the weakly interacting Bose gas. The diagrammatic approach will allow us to treat the inclusion of the  $T$ -matrix consistently without the need to subtract any diagram manually.



## 4. Field-Theoretic Approach

In the previous chapter 3, we introduced Bogoliubov's approach to the weakly interacting Bose gas. Despite its simplicity, we have seen that the Bogoliubov theory has to be used with care, to prevent divergences in the description.

A different way to treat weakly interacting Bose gases is to use methods from quantum field theory. Field-theoretic methods were first applied to a Bose gas at temperature  $T = 0$  by Beliaev in 1958 [24, 25] and by Hugenholtz and Pines in 1959 [16]. While Beliaev was able to reproduce the LHY correction, the approach of Hugenholtz and Pines allowed them to go beyond the LHY correction and calculate the next order in perturbation theory. Besides, Hugenholtz and Pines were able to connect the chemical potential to the proper self-energies. The connection between the chemical potential and the proper self-energies is known as the Hugenholtz-Pines theorem.

In this chapter, we will introduce the method used by Hugenholtz and Pines. The approach will allow us to treat the divergences occurring in Bogoliubov theory consistently and without the need to manually regularize the theory by subtracting terms. Although the approach might seem more involved than the Bogoliubov theory, its consistency will allow us to treat the dimensional crossover from a three-dimensional Bose gas to a quasi-one-dimensional Bose gas in chapter 5.

We will introduce the field-theoretic methods briefly when they are needed. For a detailed description of the methods used in this chapter, the reader is either referred to standard books of many-body physics, e.g., [26, 27, 34], or to books on quantum field theory, e.g., [35, 36]. We will follow the procedure discussed in [34].

### 4.1. The Hamiltonian

The following section lays the foundation to apply methods from quantum field theory to a system of weakly interacting bosons. We have already introduced the Hamiltonian of the system during Bogoliubov's approach in section 3.1. By rewriting the Hamiltonian with the field operators

$$\Psi(\mathbf{r}) = \sum_{\mathbf{k}} \frac{1}{\sqrt{\Omega}} e^{i\mathbf{k} \cdot \mathbf{r}} a_{\mathbf{k}} \quad \text{and} \quad \Psi^\dagger(\mathbf{r}) = \sum_{\mathbf{k}} \frac{1}{\sqrt{\Omega}} e^{-i\mathbf{k} \cdot \mathbf{r}} a_{\mathbf{k}}^\dagger, \quad (4.1)$$

it takes the form

$$\begin{aligned} H &= H_0 + H_{\text{int}} \\ &= -\frac{\hbar^2}{2m} \int_{\mathbb{R}^3} d^3\mathbf{r} \Psi^\dagger(\mathbf{r}) \nabla^2 \Psi(\mathbf{r}) + \frac{1}{2} \int_{\mathbb{R}^3} \int_{\mathbb{R}^3} d^3\mathbf{r} d^3\mathbf{r}' \Psi^\dagger(\mathbf{r}) \Psi^\dagger(\mathbf{r}') \tilde{V}(\mathbf{r} - \mathbf{r}') \Psi(\mathbf{r}') \Psi(\mathbf{r}). \end{aligned} \quad (4.2)$$

The task is to find the ground state of the system that contains a fixed number of  $N$  bosons. As already argued in section 3.2, the number of condensate particles is large, and we can replace the creation and annihilation operators of the condensate mode by the number  $\sqrt{N_0}$ , where  $N_0$  is the number of condensate particles. By applying the Bogoliubov prescription to the field operators (4.1), they split into two parts

$$\Psi(\mathbf{r}) \rightarrow \sqrt{n_0} + \sum'_{\mathbf{k}} \frac{1}{\sqrt{\Omega}} e^{i\mathbf{k} \cdot \mathbf{r}} a_{\mathbf{k}} = \sqrt{n_0} + \psi(\mathbf{r}). \quad (4.3)$$

The primed sum in equation (4.3) indicates the absence of the mode  $\mathbf{k} = 0$ . The new field operators  $\psi(\mathbf{r})$  do not describe condensate particles. The condensate particles are described by their density  $n_0 = N_0/\Omega$ . Under the Bogoliubov prescription, the Hamiltonian  $H(n_0)$  becomes a function of the density  $n_0$ , and the interaction part splits into eight terms

$$H_{\text{int}}(n_0) = \sum_{i=1}^8 H_i(n_0), \quad (4.4)$$

where

$$\begin{aligned} H_1 &= \frac{1}{2} n_0^2 \int_{\mathbb{R}^3} \int_{\mathbb{R}^3} d^3\mathbf{r} d^3\mathbf{r}' \tilde{V}(\mathbf{r} - \mathbf{r}') = \frac{1}{2} n_0^2 V(\mathbf{k} = 0), \\ H_2 &= \frac{1}{2} n_0 \int_{\mathbb{R}^3} \int_{\mathbb{R}^3} d^3\mathbf{r} d^3\mathbf{r}' \tilde{V}(\mathbf{r} - \mathbf{r}') \psi(\mathbf{r}') \psi(\mathbf{r}), \\ H_3 &= \frac{1}{2} n_0 \int_{\mathbb{R}^3} \int_{\mathbb{R}^3} d^3\mathbf{r} d^3\mathbf{r}' \psi^\dagger(\mathbf{r}) \psi^\dagger(\mathbf{r}') \tilde{V}(\mathbf{r} - \mathbf{r}'), \\ H_4 &= n_0 \int_{\mathbb{R}^3} \int_{\mathbb{R}^3} d^3\mathbf{r} d^3\mathbf{r}' \psi^\dagger(\mathbf{r}') \tilde{V}(\mathbf{r} - \mathbf{r}') \psi(\mathbf{r}), \\ H_5 &= n_0 \int_{\mathbb{R}^3} \int_{\mathbb{R}^3} d^3\mathbf{r} d^3\mathbf{r}' \psi^\dagger(\mathbf{r}) \tilde{V}(\mathbf{r} - \mathbf{r}') \psi(\mathbf{r}), \\ H_6 &= n_0^{1/2} \int_{\mathbb{R}^3} \int_{\mathbb{R}^3} d^3\mathbf{r} d^3\mathbf{r}' \psi^\dagger(\mathbf{r}) \psi^\dagger(\mathbf{r}') \tilde{V}(\mathbf{r} - \mathbf{r}') \psi(\mathbf{r}), \\ H_7 &= n_0^{1/2} \int_{\mathbb{R}^3} \int_{\mathbb{R}^3} d^3\mathbf{r} d^3\mathbf{r}' \psi^\dagger(\mathbf{r}) \tilde{V}(\mathbf{r} - \mathbf{r}') \psi(\mathbf{r}') \psi(\mathbf{r}), \\ H_8 &= \frac{1}{2} \int_{\mathbb{R}^3} \int_{\mathbb{R}^3} d^3\mathbf{r} d^3\mathbf{r}' \psi^\dagger(\mathbf{r}) \psi^\dagger(\mathbf{r}') \tilde{V}(\mathbf{r} - \mathbf{r}') \psi(\mathbf{r}') \psi(\mathbf{r}). \end{aligned} \quad (4.5)$$



Due to the Bogoliubov prescription, the Hamiltonian  $H(n_0)$  does not conserve the total number of particles  $N$ ,

$$\left[ H_0 + H_{\text{int}}(n_0), \hat{N} \right] \neq 0.$$

Thus, we have to impose the additional condition

$$N = N_0 + \sum'_{\mathbf{k}} \langle \Phi_{\text{int}}(n_0) | a_{\mathbf{k}}^\dagger a_{\mathbf{k}} | \Phi_{\text{int}}(n_0) \rangle \quad (4.6)$$

to the ground state  $|\Phi_{\text{int}}(n_0)\rangle$  of the interacting system. As we are interested in the ground state of the system, the energy is minimal,

$$\frac{dE}{dN_0} = 0. \quad (4.7)$$

In Bogoliubov's approach in section 3.2, we replaced the number of condensate particles by

$$N_0 = N - \sum'_{\mathbf{k}} a_{\mathbf{k}}^\dagger a_{\mathbf{k}},$$

and hence recovered particle conservation. To treat the non-conservation of particles consistently, we will take a different route in the diagrammatic approach. In the following, we will use the grand canonical Hamiltonian

$$H'(n_0, \mu) = H(n_0) - \mu \hat{N}' \quad (4.8)$$

for the description of the system. The chemical potential  $\mu$  can be seen as a Lagrange multiplier of the condition (4.6). The ground state  $E$  of the Hamiltonian  $H(n_0)$  with the condition (4.6) is the same as the ground state  $E'$  of the Hamiltonian  $H'$ , without any further constraints. Thus, the ground state and the energy  $E$  are functions of  $n_0$  and  $\mu$ . The correct chemical potential that fulfills the considerations above is

$$\mu = \frac{dE}{dN}. \quad (4.9)$$

To show this, we first consider the derivative

$$\frac{\partial E}{\partial \mu} = \frac{\partial}{\partial \mu} (E' + \mu N') = \left\langle \Phi_{\text{int}}(n_0, \mu) \left| \frac{\partial H'}{\partial \mu} \right| \Phi_{\text{int}}(n_0, \mu) \right\rangle + N' + \mu \frac{\partial N'}{\partial \mu} = \mu \frac{\partial N'}{\partial \mu}, \quad (4.10)$$

where we have used the Hellmann-Feynman-theorem for the derivative of the expectation value. Next, we evaluate the derivative of the energy  $E$  with respect to the number of

particles  $N$  by using (4.7),

$$\begin{aligned} \frac{dE(N_0, \mu)}{dN} &= \left( \frac{\partial E}{\partial \mu} \right) \left( \frac{\partial \mu}{\partial N} \right)_{N_0} = \left( \frac{\partial E}{\partial \mu} \right) / \left( \frac{\partial}{\partial \mu} (N' + N_0) \right)_{N_0} \\ &= \left( \frac{\partial E}{\partial \mu} \right) / \left( \frac{\partial N'}{\partial \mu} \right)_{N_0}. \end{aligned} \quad (4.11)$$

Inserting (4.10) into the previous result (4.11) yields the desired result (4.9). Thus, the Bogoliubov prescription does not alter the thermodynamic relation between the energy and the chemical potential.

All calculations are performed with the grand canonical Hamiltonian  $H'$  and depend on the chemical potential  $\mu$ . To obtain an expression of the energy that only depends on the number of particles  $N$ , we will use the relation (4.9) at the end.

## 4.2. The Green's Function

For a field-theoretic description, we introduce the two-point Green's function

$$iG(x, y) = \langle \Phi_{\text{int}} | \mathcal{T} [\Psi(x) \Psi^\dagger(y)] | \Phi_{\text{int}} \rangle. \quad (4.12)$$

Note that  $x$  and  $y$  are four-vectors and the operators  $\Psi(x)$  and  $\Psi^\dagger(y)$  are given in the Heisenberg picture. The time-ordering operator is denoted by  $\mathcal{T}$ . When applying the Bogoliubov prescription, the Green's function (4.12) decomposes into two parts,

$$iG(x, y) = n_0 + iG'(x, y),$$

where we have introduced the new Green's function

$$iG'(x, y) = \langle \Phi_{\text{int}} | \mathcal{T} [\psi(x) \psi^\dagger(y)] | \Phi_{\text{int}} \rangle. \quad (4.13)$$

In its momentum representation, the Green's function  $G'$  reads

$$iG'(\mathbf{k}, t_2 - t_1) = \langle \Phi_{\text{int}} | \mathcal{T} [a_{\mathbf{k}}(t_1) a_{\mathbf{k}}^\dagger(t_2)] | \Phi_{\text{int}} \rangle. \quad (4.14)$$

It only depends on a single momentum  $\mathbf{k}$ , as the system is invariant under translations. The energy of the system is conserved, so only the difference  $t_2 - t_1$  appears in the Green's function. Keep in mind that there are no condensate operators in the Green's function  $G'(x, y)$ .

The remaining task is to connect the physical observables to the Green's function  $G'(x, y)$ . Using the Green's function (4.14), we can express the number of particles by

$$N = \langle \Phi_{\text{int}} | \hat{N} | \Phi_{\text{int}} \rangle = N_0 + \lim_{\eta \rightarrow 0^+} \sum_{\mathbf{k}}' iG'(\mathbf{k}, \eta) = N_0 + \Omega \int_{\mathbb{R}^4} \frac{d^4 k}{(2\pi)^4} iG'(k) e^{ik_0 \eta}. \quad (4.15)$$

The limit  $\eta \rightarrow 0^+$  will be implicit in the following. Note that the argument  $k$  is not the absolute value of  $\mathbf{k}$  but a four-vector with the zero-component  $k_0$ . The connection of the ground state energy to the Green's function  $G'$  is given by

$$E = \frac{1}{2}\mu N + \frac{\Omega}{2} \int_{\mathbb{R}^4} \frac{d^4k}{(2\pi)^4} \left( \hbar k_0 + \frac{\hbar^2 \mathbf{k}^2}{2m} \right) iG'(k) e^{ik_0\eta}. \quad (4.16)$$

The derivation of this result can be found in the appendix B. It is important to realize that equation (4.16) is a differential equation, as the chemical potential is the derivative of the energy with respect to the total number of particles.

### 4.3. Perturbation Theory

In the previous section 4.2, we have introduced the Green's function  $G'(x, y)$  and pointed out its connection to the number of particles and the energy. Now we need to find a way to calculate the Green's function.

The grand canonical Hamiltonian can be split into two parts,

$$H' = H'_0 + H'_{\text{int}}. \quad (4.17)$$

The Hamiltonian  $H'_0$  contains

$$H'_0 = H_0 - \mu N' + H_1, \quad (4.18)$$

and we can state its ground state directly

$$|\Phi_0\rangle = |N_{\mathbf{k}=0}, 0, \dots\rangle. \quad (4.19)$$

The Hamiltonian  $H'_{\text{int}}$  contains the interactions that involve excited particles,

$$H'_{\text{int}} = \sum_{i=2}^8 H_i. \quad (4.20)$$

Remember that  $H'_{\text{int}}$  does not contain any condensate operators. Hence, any annihilation operator within  $H'_{\text{int}}$  annihilates the state  $|\Phi_0\rangle$ .

Under these considerations, we come to the following conclusion. The ground state  $|\Phi_0\rangle$  of  $H'_0$  can be seen as the non-interacting vacuum of a quantum field theory. The Hamiltonian  $H'_{\text{int}}$  is a perturbation to this ground state. Thus, the standard methods from quantum field theory become applicable to the system and yield an expression for the Green's function

$$iG'(x, y) = \sum_{m=0}^{\infty} \left( \frac{-i}{\hbar} \right)^m \frac{1}{m!} \int_{\mathbb{R}} dt_1 \cdots \int_{\mathbb{R}} dt_m \langle \Phi_0 | \mathcal{T} \left[ H'_{\text{int}}(t_1) \cdots H'_{\text{int}}(t_m) \psi_{\text{I}}(x) \psi_{\text{I}}^\dagger(y) \right] | \Phi_0 \rangle_c. \quad (4.21)$$

The index  $c$  on the expectation value indicates that only connected diagrams contribute to the Green's function. The operators  $\psi_{\text{I}}(x)$  and  $\psi_{\text{I}}^{\dagger}(x)$  are the field operators in the interaction picture,

$$\psi_{\text{I}}(x) = \sum_{\mathbf{k}}' \frac{1}{\sqrt{\Omega}} \exp(i\mathbf{k} \cdot \mathbf{x} - i(\varepsilon_0(\mathbf{k}) - \mu)t_x/\hbar) a_{\mathbf{k}}. \quad (4.22)$$

In 0th-order, the Green's function reads

$$\begin{aligned} iG^{(0)}(x, y) &= \langle \Phi_0 | \mathcal{T} [\psi_{\text{I}}(x) \psi_{\text{I}}^{\dagger}(y)] | \Phi_0 \rangle \\ &= \begin{cases} 0 & , \text{ for } t_x < t_y \\ \frac{1}{\Omega} \sum_{\mathbf{k}}' \exp(i\mathbf{k} \cdot (\mathbf{x} - \mathbf{y}) - \frac{i}{\hbar} (\varepsilon_0(\mathbf{k}) - \mu) (t_x - t_y)) & , \text{ for } t_x > t_y. \end{cases} \end{aligned} \quad (4.23)$$

The Green's function  $G^{(0)}$  is that of a free Bose gas. As the Green's function vanishes for  $t_x < t_y$ , only propagations forward in time are allowed. In momentum space, the 0th-order becomes

$$G^{(0)}(k) = \frac{1}{k_0 - (\varepsilon_0(\mathbf{k}) - \mu)/\hbar + i\eta} = \text{---} \xrightarrow{k} \text{---}, \quad (4.24)$$

where we have introduced a graphical representation for the propagator.

The next contribution to the Green's function is

$$G^{(1)}(x, y) = -\frac{1}{\hbar} \int_{\mathbb{R}} dt_1 \langle \Phi_0 | \mathcal{T} [H'_{\text{int}}(t_1) \psi_{\text{I}}(x) \psi_{\text{I}}^{\dagger}(y)] | \Phi_0 \rangle_c. \quad (4.25)$$

We will discuss its contributions exemplarily, to obtain the general rules for constructing the relevant diagrams. The interactions described by  $H_2$ ,  $H_3$ ,  $H_6$  and  $H_7$  do not contribute to the expectation value, as they alter the number of particles. The remaining terms to consider are  $H_4$ ,  $H_5$  and  $H_8$ .

We will start with the contribution of  $H_4$ . By introducing

$$U(x_1 - x_2) = \tilde{V}(\mathbf{x}_1 - \mathbf{x}_2) \delta(t_1 - t_2), \quad (4.26)$$

the contribution of  $H_4$  is written as

$$-\frac{n_0}{\hbar} \int_{\mathbb{R}^4} \int_{\mathbb{R}^4} d^4x_1 d^4x_2 U(x_1 - x_2) \langle \Phi_0 | \mathcal{T} [\psi_{\text{I}}^{\dagger}(x_2) \psi_{\text{I}}(x_1) \psi_{\text{I}}(x) \psi_{\text{I}}^{\dagger}(y)] | \Phi_0 \rangle_c. \quad (4.27)$$

Making use of Wick's theorem allows us to express the expectation value in terms of the Green's function  $G^{(0)}(x, y)$ ,

$$\frac{n_0}{\hbar} \int_{\mathbb{R}^4} \int_{\mathbb{R}^4} d^4x_1 d^4x_2 U(x_1 - x_2) G^{(0)}(x, x_2) G^{(0)}(x_1, y). \quad (4.28)$$

In momentum space, we obtain a shorter form,

$$\frac{n_0}{\hbar} G'^{(0)}(k) V(\mathbf{k}) G'^{(0)}(k). \quad (4.29)$$

We draw each interaction as a wavy line,

$$V(\mathbf{k}) = \text{~~~~~}, \quad (4.30)$$

$\mathbf{k}$

and each factor  $\sqrt{n_0}$  by a dashed line,

$$\sqrt{n_0} = \text{-----} \rightarrow . \quad (4.31)$$

Hence, we can represent the contribution of  $H_4$  by

$$\frac{n_0}{\hbar} G'^{(0)}(k) V(\mathbf{k}) G'^{(0)}(k) = \begin{array}{c} \text{-----} \rightarrow \\ \text{-----} \rightarrow \\ \text{~~~~~} \\ \text{-----} \rightarrow \\ \text{-----} \rightarrow \end{array} . \quad (4.32)$$

$\mathbf{k}$

We calculate the contribution of  $H_5$  in complete analogy to  $H_4$  and obtain

$$\frac{n_0}{\hbar} G'^{(0)}(k) V(0) G'^{(0)}(k) = \begin{array}{c} \text{-----} \rightarrow \\ \text{-----} \rightarrow \\ \text{~~~~~} \\ \text{-----} \rightarrow \\ \text{-----} \rightarrow \end{array} . \quad (4.33)$$

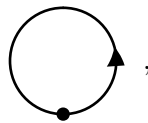
0

The contribution of the remaining interaction  $H_8$  is

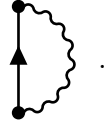
$$-\frac{1}{\hbar} \int_{\mathbb{R}^4} \int_{\mathbb{R}^4} d^4x_1 d^4x_2 U(x_1 - x_2) \langle \Phi_0 | \mathcal{T} \left[ \psi_1^\dagger(x_1) \psi_1^\dagger(x_2) \psi_1(x_2) \psi_1(x_1) \psi_1(x) \psi_1^\dagger(y) \right] | \Phi_0 \rangle_c . \quad (4.34)$$

The contribution of  $H_8$  vanishes, as can be seen by the use of Wick's theorem. To obtain a connected contribution from (4.34), we have to contract two field operators of the interaction Hamiltonian  $H_8$ . They are already normal-ordered and evaluated at the same time, so the expectation value vanishes.

We come to the general conclusion that diagrams, which include the contraction of field operators from the same Hamiltonian vanish. In terms of diagrams, no particle line can close itself



and no interaction line can start and end at the same particle line,



For the first order Green's function, we finally obtain

$$G^{(1)}(k) = \frac{n_0}{\hbar} G^{(0)}(k) [V(\mathbf{k}) + V(0)] G^{(0)}(k) = \text{diagram 1} + \text{diagram 2} \quad (4.35)$$

The diagram shows two terms. The first term is a diagram with two external dashed lines with arrows, each labeled with momentum  $k$ . They are connected by a wavy interaction line labeled with momentum  $\mathbf{k}$ . The second term is a similar diagram, but the wavy interaction line is labeled with momentum  $0$ .

After the consideration of the first order Green's function, we can conclude general rules for the contribution of diagrams in momentum space. Every distinct diagram of  $m$ -th order has to be counted once. The factors  $1/2$  that appear in the interactions  $H_1$ ,  $H_2$ ,  $H_3$  and  $H_8$  cancel, as they are symmetric under the exchange of their integration variables. An  $m$ -th order diagram carries the prefactor

$$\left(\frac{i}{\hbar}\right)^m (-i)^{\tilde{c}} (2\pi)^{4(\tilde{c}-m)}, \quad (4.36)$$

where  $\tilde{c}$  denotes the number of condensate factors  $n_0$ . Two field operators were replaced for each condensate factor  $n_0$ , and hence one less Green's function  $G^{(0)}$  is introduced. The factor  $1/m!$  in equation (4.21) cancels, as the integration can be relabeled  $m!$  times. Only propagations forward in time are allowed and loops are forbidden. In addition, interaction lines are not allowed to start and end at the same particle line.

With these rules, the contributions to the Green's function can be calculated. In the following, we will represent the full Green's function  $G'(k)$  by

$$G'(k) = \text{diagram} \quad (4.37)$$

The diagram shows a thick double-line arrow pointing to the right, representing the full Green's function.

## 4.4. Dyson Equations in Presence of a Condensate

The Dyson equations allow us to sum over a whole class of diagrams. As the Hamiltonian  $H'_{\text{int}}$  does not conserve the number of particles, the form of the Dyson equations is more complicated than for fermionic systems. Excited particles can become part of

the condensate and vice versa. To treat these processes consistently, we introduce the anomalous Green's functions

$$G'_{12}(x, y) = -i \langle \Phi_{\text{int}} | \mathcal{T} [\psi(x)\psi(y)] | \Phi_{\text{int}} \rangle, \quad (4.38)$$

$$G'_{21}(x, y) = -i \langle \Phi_{\text{int}} | \mathcal{T} [\psi^\dagger(x)\psi^\dagger(y)] | \Phi_{\text{int}} \rangle. \quad (4.39)$$

In momentum space, we will represent them as

$$G'_{12}(k) = \begin{array}{c} \text{---} \leftarrow \text{---} \text{---} \rightarrow \text{---} \\ \text{---} \end{array} \quad G'_{21}(k) = \begin{array}{c} \text{---} \rightarrow \text{---} \text{---} \leftarrow \text{---} \\ \text{---} \end{array}. \quad (4.40)$$

The non-conservation of particles also affects the proper self-energies. Instead of a single self-energy  $\Sigma_{11}$ , two additional self-energies  $\Sigma_{12}$  and  $\Sigma_{21}$  are needed to describe the condensate properly. We will represent them as

$$\begin{array}{ccc} \begin{array}{c} \uparrow k \\ \text{---} \circ \Sigma_{11} \text{---} \\ \uparrow k \end{array} & \begin{array}{c} \text{---} \circ \Sigma_{12} \text{---} \\ \uparrow k \quad \text{---} \text{---} \\ \downarrow k \quad \text{---} \text{---} \end{array} & \begin{array}{c} \text{---} \circ \Sigma_{21} \text{---} \\ \downarrow k \quad \text{---} \text{---} \\ \uparrow k \quad \text{---} \text{---} \end{array} \end{array}. \quad (4.41)$$

With the representations introduced above, we can write the Dyson equations in presence of a condensate as

$$\begin{array}{c} \text{---} \uparrow k \\ \text{---} \end{array} = \begin{array}{c} \uparrow k \\ \text{---} \end{array} + \begin{array}{c} \uparrow k \\ \text{---} \circ \Sigma_{11} \text{---} \\ \uparrow k \end{array} + \begin{array}{c} \text{---} \circ \Sigma_{12} \text{---} \\ \uparrow k \quad \text{---} \text{---} \\ \downarrow k \quad \text{---} \text{---} \end{array} \quad (4.42)$$

$$\begin{array}{c} \text{---} \uparrow k \\ \text{---} \downarrow -k \end{array} = \begin{array}{c} \text{---} \circ \Sigma_{12} \text{---} \\ \uparrow k \quad \text{---} \text{---} \\ \downarrow k \quad \text{---} \text{---} \end{array} + \begin{array}{c} \text{---} \circ \Sigma_{11} \text{---} \\ \uparrow k \quad \text{---} \text{---} \\ \downarrow -k \quad \text{---} \text{---} \end{array} \quad (4.43)$$

$$\begin{array}{c} \text{---} \downarrow -k \\ \text{---} \uparrow k \end{array} = \begin{array}{c} \text{---} \circ \Sigma_{21} \text{---} \\ \downarrow -k \quad \text{---} \text{---} \\ \uparrow k \quad \text{---} \text{---} \end{array} + \begin{array}{c} \text{---} \circ \Sigma_{11} \text{---} \\ \downarrow -k \quad \text{---} \text{---} \\ \uparrow k \quad \text{---} \text{---} \end{array}. \quad (4.44)$$

The system of linear equations (4.44) yields an expression for  $G'(k)$  that depends on the self-energies

$$G'(k) = \frac{k_0 + (\varepsilon_0(\mathbf{k}) - \mu) / \hbar + S(k) - A(k)}{[k_0 - A(k)]^2 - [(\varepsilon_0(\mathbf{k}) - \mu) / \hbar + S(p)]^2 + \Sigma_{12}(k)\Sigma_{21}(k)}, \quad (4.45)$$

where we have introduced

$$S(k) = \frac{1}{2} [\Sigma_{11}(k) + \Sigma_{11}(-k)] \quad \text{and} \quad A(k) = \frac{1}{2} [\Sigma_{11}(k) - \Sigma_{11}(-k)]. \quad (4.46)$$

The remaining task is to determine the self-energies, to complete the Green's function. For the chemical potential, we make use of a connection found by Hugenholtz and Pines [16]. In their paper, Hugenholtz and Pines were able to connect the proper self-energies to the chemical potential

$$\mu = \hbar\Sigma_{11}(0) - \hbar\Sigma_{12}(0). \quad (4.47)$$

This relation is known as the Hugenholtz-Pines theorem. It is correct in all orders of perturbation theory. We will skip its derivation here and refer the reader to [26, 37], where the proof is explained in detail.

## 4.5. Lowest-Order Contribution

In lowest order, the self-energies vanish

$$\Sigma_{11}(k) = \Sigma_{12}(k) = \Sigma_{21}(k) = 0, \quad (4.48)$$

and the Green's function is simply given by the free Green's function,

$$G^{(0)}(k) = \frac{1}{k_0 - (\varepsilon_0(\mathbf{k}) - \mu) / \hbar + i\eta},$$

from equation (4.23). We can now use the lowest-order Green's function  $G^{(0)}(k)$  to calculate the lowest order of the ground state energy. The connection between the Green's function  $G'(k)$  and the ground state energy was pointed out in section 4.2. By inserting the Green's function (4.23) into the differential equation for the ground state energy (4.16), we obtain

$$\begin{aligned} E - \frac{1}{2}N\mu &= \frac{\Omega}{2} \int_{\mathbb{R}^4} \frac{d^4k}{(2\pi)^4} [\hbar k_0 + \varepsilon_0(\mathbf{k})] iG^{(0)}(k) e^{ik_0\eta} \\ &= \frac{i\Omega}{2} \int_{\mathbb{R}^4} \frac{d^4k}{(2\pi)^4} [\hbar k_0 + \varepsilon_0(\mathbf{k})] (k_0 - (\varepsilon_0(\mathbf{k}) - \mu) / \hbar + i\eta)^{-1} e^{ik_0\eta} \\ &= 0. \end{aligned} \quad (4.49)$$



In the last line, we performed the  $k_0$ -integration by closing the contour of the integration in the upper half-plane. Thus, there are no poles enclosed by the contour and the integral vanishes. In lowest order, the ground state energy and the chemical potential are connected by

$$E = \frac{1}{2}\mu N. \quad (4.50)$$

Using the Hugenholtz-Pines theorem leads to a vanishing chemical potential, and hence a vanishing ground state energy. This is no surprise, as there are no interactions present. To obtain a non-zero ground state energy, we need to consider higher orders in the self-energies.

In the first non-vanishing order, the proper self-energies are given by

$$\Sigma_{11}(k) = \frac{n_0}{\hbar} [V(0) + V(\mathbf{k})] = \begin{array}{c} \text{---} \bullet \text{---} \text{---} \bullet \text{---} \\ \text{---} \bullet \text{---} \text{---} \bullet \text{---} \\ \text{---} \bullet \text{---} \text{---} \bullet \text{---} \end{array} + \begin{array}{c} \text{---} \bullet \text{---} \text{---} \bullet \text{---} \\ \text{---} \bullet \text{---} \text{---} \bullet \text{---} \\ \text{---} \bullet \text{---} \text{---} \bullet \text{---} \end{array} \quad (4.51)$$

$$\Sigma_{12}(k) = \frac{n_0}{\hbar} V(\mathbf{k}) = \begin{array}{c} \text{---} \bullet \text{---} \text{---} \bullet \text{---} \\ \text{---} \bullet \text{---} \text{---} \bullet \text{---} \\ \text{---} \bullet \text{---} \text{---} \bullet \text{---} \end{array} \quad (4.52)$$

$$\Sigma_{21}(k) = \frac{n_0}{\hbar} V(\mathbf{k}) = \begin{array}{c} \text{---} \bullet \text{---} \text{---} \bullet \text{---} \\ \text{---} \bullet \text{---} \text{---} \bullet \text{---} \\ \text{---} \bullet \text{---} \text{---} \bullet \text{---} \end{array} \quad (4.53)$$

Note that the particle and condensate lines are only drawn to illustrate the type of the interaction and are not part of the self-energies. By inserting the proper self-energies (4.53) to the Hugenholtz-Pines theorem (4.47), we arrive at an expression for the chemical potential,

$$\mu = n_0 V(0). \quad (4.54)$$

Hence, the lowest-order ground state energy (4.50) becomes

$$E = \frac{1}{2}\mu N = \frac{1}{2}n_0 V(0)N. \quad (4.55)$$

Under the assumption that the density of the condensate is approximately the same as the full density, we recover the mean-field energy from the Bogoliubov theory (3.15),

$$E_{\text{mf}} = \frac{V(0)N^2}{2\Omega} = \frac{g_{3\text{D}}N^2}{2\Omega}.$$

The validity of the assumption will be investigated in the course of the next section, dedicated to beyond-mean-field corrections. For the potential  $V(\mathbf{k})$ , we chose the pseudopotential (3.16), with the same argumentation as in the previous chapter 3.

## 4.6. Beyond-Mean-Field Corrections

We can now use the proper self-energies (4.53) and the chemical potential (4.54) to calculate the next order of the Green's function (4.45),

$$G'(k) = \frac{k_0 + [\varepsilon_0(\mathbf{k}) + n_0V(\mathbf{k})]/\hbar}{k_0^2 - [\varepsilon_0(\mathbf{k})^2 + 2n_0V(\mathbf{k})\varepsilon_0(\mathbf{k})]/\hbar^2} = \frac{k_0 + [\varepsilon_0(\mathbf{k}) + n_0V(\mathbf{k})]/\hbar}{k_0^2 - E_{\mathbf{k}}^2/\hbar^2}. \quad (4.56)$$

A partial fraction decomposition then yields the final result for the Green's function

$$G'(\mathbf{k}) = \frac{u_{\mathbf{k}}^2}{k_0 - E_{\mathbf{k}}/\hbar + i\eta} - \frac{v_{\mathbf{k}}^2}{k_0 + E_{\mathbf{k}}/\hbar - i\eta} \quad (4.57)$$

$$\text{with } u_{\mathbf{k}}^2 = \frac{1}{2} \left[ \frac{\varepsilon_0(\mathbf{k}) + n_0V(\mathbf{k})}{E_{\mathbf{k}}} + 1 \right] \quad (4.58)$$

$$v_{\mathbf{k}}^2 = \frac{1}{2} \left[ \frac{\varepsilon_0(\mathbf{k}) + n_0V(\mathbf{k})}{E_{\mathbf{k}}} - 1 \right] \quad (4.59)$$

$$\text{and } E_{\mathbf{k}}^2 = \varepsilon_0(\mathbf{k})^2 + 2\varepsilon_0(\mathbf{k})n_0V(\mathbf{k}). \quad (4.60)$$

The quantities  $u_{\mathbf{k}}$  and  $v_{\mathbf{k}}$  match the amplitudes of the Bogoliubov transformation in section 3.3. The poles of the Green's function (4.57) correspond to the low-energy excitations of the system and agree with the excitation spectrum obtained by the Bogoliubov theory (3.12).

Before calculating the energy, we first consider the total number of particles in the system. Inserting the Green's function (4.57) into equation (4.15) yields

$$\begin{aligned} n - n_0 &= \int_{\mathbb{R}^4} \frac{d^4k}{(2\pi)^4} iG'(k)e^{ik_0\eta} \\ &= \int_{\mathbb{R}^4} \frac{d^4k}{(2\pi)^4} i \left( \frac{u_{\mathbf{k}}^2}{k_0 - E_{\mathbf{k}}/\hbar + i\eta} - \frac{v_{\mathbf{k}}^2}{k_0 + E_{\mathbf{k}}/\hbar - i\eta} \right) e^{ik_0\eta} \\ &= \int_{\mathbb{R}^3} \frac{d^3\mathbf{k}}{(2\pi)^3} v_{\mathbf{k}}^2 = \frac{1}{2} \int_{\mathbb{R}^3} \frac{d^3\mathbf{k}}{(2\pi)^3} \left[ \frac{\varepsilon_0(\mathbf{k}) + n_0V(\mathbf{k})}{\sqrt{\varepsilon_0(\mathbf{k})^2 + 2\varepsilon_0(\mathbf{k})n_0V(\mathbf{k})}} - 1 \right]. \end{aligned} \quad (4.61)$$

The integration over  $k_0$  was carried out by closing the integral in the upper half-plane. We insert the pseudopotential (3.16) and substitute

$$u = \sqrt{\frac{\hbar^2}{2mng_{3D}}|\mathbf{k}|}, \quad (4.62)$$

so we arrive at

$$\begin{aligned} n - n_0 &= \left( \frac{2mn_0g_{3D}}{\hbar^2} \right)^{3/2} \frac{1}{(2\pi)^2} \int_0^\infty du u^2 \left[ \frac{u^2 + 1}{\sqrt{u^4 + 2u^2}} - 1 \right] \\ &= \frac{8}{3\sqrt{\pi}} (n_0a_s)^{3/2} \approx \frac{8}{3\sqrt{\pi}} (na_s)^{3/2}. \end{aligned}$$

Thus, the fractional depletion of the condensate becomes

$$\frac{n - n_0}{n} = \frac{8}{3} \left( \frac{na_s^3}{\pi} \right)^{1/2} \ll 1, \quad \text{for } na_s^3 \ll 1. \quad (4.63)$$

The depletion of the weakly interacting Bose gas is very low, and we will replace  $n_0$  by  $n$  in the following.

Like in the previous section, we can use the Green's function to calculate the ground state energy. By inserting the Green's function (4.57) into equation (4.16), we obtain a differential equation for the ground state energy,

$$\begin{aligned} E - \frac{1}{2}N \frac{dE}{dN} &= \frac{\Omega}{2} \int_{\mathbb{R}^4} \frac{d^4k}{(2\pi)^4} [\hbar k_0 + \varepsilon_0(\mathbf{k})] iG'(k) e^{ik_0\eta} \\ &= \frac{i\Omega}{2} \int_{\mathbb{R}^4} \frac{d^4k}{(2\pi)^4} [\hbar k_0 + \varepsilon_0(\mathbf{k})] \left( \frac{u_{\mathbf{k}}^2}{k_0 - E_{\mathbf{k}}/\hbar + i\eta} - \frac{v_{\mathbf{k}}^2}{k_0 + E_{\mathbf{k}}/\hbar - i\eta} \right) e^{ik_0\eta}. \end{aligned} \quad (4.64)$$

The integration over  $k_0$  is performed by closing the contour of the integration in the upper half-plane, and we divide by the quantization volume  $\Omega$ . We obtain a differential equation for the energy density  $\varepsilon = E/\Omega$ ,

$$\begin{aligned} \varepsilon - \frac{n}{2} \frac{d\varepsilon}{dn} &= \frac{1}{2} \int_{\mathbb{R}^3} \frac{d^3\mathbf{k}}{(2\pi)^3} [\varepsilon_0(\mathbf{k}) - E_{\mathbf{k}}] v_{\mathbf{k}}^2 \\ &= \frac{1}{4} \int_{\mathbb{R}^3} \frac{d^3\mathbf{k}}{(2\pi)^3} \left[ \frac{2\varepsilon_0(\mathbf{k})^2 + 3\varepsilon_0(\mathbf{k})nV(\mathbf{k})}{\sqrt{\varepsilon_0(\mathbf{k})^2 + 2\varepsilon_0(\mathbf{k})nV(\mathbf{k})}} - 2\varepsilon_0(\mathbf{k}) - nV(\mathbf{k}) \right] \\ &\equiv f(n). \end{aligned} \quad (4.65)$$

The form of the differential equation (4.65) allows determining the energy density except for contributions of order  $n^2$ . Contributions of order  $n^2$  remain undetermined, which can be seen by inserting  $n^2$  for  $\varepsilon$  on the left-hand side of equation (4.65). This is not a problem, as we already calculated the correct contribution of order  $n^2$  in the previous section 4.5,

$$\varepsilon_{\text{mf}}(n) = \frac{n^2 g_{3\text{D}}}{2}.$$

Hence, the general solution to the differential equation (4.65) can be written as

$$\varepsilon(n) = \varepsilon_{\text{mf}}(n) - n^2 \int_{n_c}^n dn' \frac{2f(n')}{n'^3}. \quad (4.66)$$

We must determine the constant  $n_c$  by an additional constraint, which is needed as the energy density is the solution of a first-order linear differential equation. The constraint

we impose is the following. For extremely weak interactions, the mean-field energy has to provide the dominant solution, as it is the leading order of the perturbation theory. The three-dimensional Bose gas is weakly interacting if it is dilute. Thus, the contribution of the beyond-mean-field energy has to vanish faster than  $n^2$ . We can achieve this by setting  $n_c = 0$ , so the integral itself vanishes for  $n \rightarrow 0$ . Under these considerations, we can perform the integration over  $n'$ ,

$$\begin{aligned}
 \varepsilon(n) &= \varepsilon_{\text{mf}}(n) - \frac{n^2}{2} \int_0^n dn' \int_{\mathbb{R}^3} \frac{d^3\mathbf{k}}{(2\pi)^3} \frac{1}{n'^3} \left[ \frac{2\varepsilon_0(\mathbf{k})^2 + 3\varepsilon_0(\mathbf{k})n'g_{3\text{D}}}{\sqrt{\varepsilon_0(\mathbf{k})^2 + 2\varepsilon_0(\mathbf{k})n'g_{3\text{D}}}} - 2\varepsilon_0(\mathbf{k}) - n'g_{3\text{D}} \right] \\
 &= \varepsilon_{\text{mf}}(n) - \frac{n^2}{2} \int_{\mathbb{R}^3} \frac{d^3\mathbf{k}}{(2\pi)^3} \frac{\varepsilon_0(\mathbf{k}) + n'g_{3\text{D}} - \sqrt{\varepsilon_0(\mathbf{k})^2 + 2\varepsilon_0(\mathbf{k})n'g_{3\text{D}}}}{n'^2} \Bigg|_0^n \\
 &= \varepsilon_{\text{mf}}(n) - \frac{1}{2} \int_{\mathbb{R}^3} \frac{d^3\mathbf{k}}{(2\pi)^3} \left[ \varepsilon_0(\mathbf{k}) + ng_{3\text{D}} - \frac{n^2 g_{3\text{D}}^2}{2\varepsilon_0(\mathbf{k})} - \sqrt{\varepsilon_0(\mathbf{k})^2 + 2ng_{3\text{D}}\varepsilon_0(\mathbf{k})} \right], \tag{4.67}
 \end{aligned}$$

and obtain the same finite integral as in Bogoliubov theory (3.32) after the subtraction of the troublesome diagram. Hence, we arrive at the same ground state energy,

$$\varepsilon = \frac{1}{2}g_{3\text{D}}n^2 + \frac{8}{15\pi^2} \left( \frac{m}{\hbar^2} \right)^{3/2} (ng_{3\text{D}})^{5/2},$$

without any divergences appearing at all. Note that the diagrammatic approach contains the same mistake as the Bogoliubov theory. Combining the Dyson equations with the  $T$ -matrix takes into account the same diagrams too often. Thus, the approach of Hugenholtz and Pines contains the divergence as well. The advantage of the diagrammatic approach lies in the differential equation and its clear illustration of the processes that are taken into account. As the differential equation provides an additional freedom, the divergence is cured automatically by imposing the correct constraint. This only works, as the divergence is of order  $n^2$ .

### 4.6.1. Dipolar Interaction

In this section, we want to make a short remark on the dipolar interaction. As already mentioned in the introduction of this work, the beyond-mean-field corrections play a crucial role for dipolar Bose gases. The beyond-mean-field correction of a dipolar Bose gas was first obtained by Lima and Pelster [23, 38]. In their work, they used the Bogoliubov theory to include the dipolar interaction. Like for a short-range potential, they obtain a divergent ground state energy. To treat this problem, Lima and Pelster subtract the divergent expression by hand and obtain an expression for the ground state energy, including beyond-mean-field corrections.

In the following, we will treat the dipolar interaction within the approach of Hugenholtz and Pines. With the same arguments as in the previous section, no divergences

appear, and we obtain the same ground state energy as Lima and Pelster. Note that the dipolar interaction is treated very briefly here, as the main focus of this work is the treatment of confined systems. For a more elaborate discussion of the dipolar interaction, the reader is referred to [39].

For the dipolar interaction, the pseudopotential can be written as [40, 41]

$$V(\mathbf{k}) = g_{3\text{D}} [1 + \varepsilon_{\text{dd}} (3 \cos^2(\theta) - 1)] \equiv g_{3\text{D}} d(\theta), \quad \text{with} \quad \varepsilon_{\text{dd}} = \frac{\mu_0 m_{\text{d}}^2}{3g_{3\text{D}}}. \quad (4.68)$$

The magnetic permeability is denoted by  $\mu_0$  and the magnetic dipole moment is given by  $m_{\text{d}}$ . The pseudopotential does not depend on the absolute value of  $\mathbf{k}$  but only on the angle  $\theta$  between  $\mathbf{k}$  and the direction of polarization. For  $\mathbf{k} = 0$ , the potential  $V(\mathbf{k})$  reduces to

$$V(0) = g_{3\text{D}}. \quad (4.69)$$

The considerations of the previous section remain unaltered, and so we can express the ground state energy by equation (4.65),

$$\varepsilon - \frac{n}{2} \frac{d\varepsilon}{dn} = \frac{1}{4} \int_{\mathbb{R}^3} \frac{d^3\mathbf{k}}{(2\pi)^3} \left[ \frac{2\varepsilon_0(\mathbf{k})^2 + 3\varepsilon_0(\mathbf{k})nV(\mathbf{k})}{\sqrt{\varepsilon_0(\mathbf{k})^2 + 2\varepsilon_0(\mathbf{k})nV(\mathbf{k})}} - 2\varepsilon_0(\mathbf{k}) - nV(\mathbf{k}) \right].$$

Instead of solving the differential equation first and then performing the integration over  $\mathbf{k}$ , we chose to take the opposite route this time. We start by evaluating the integral over  $\mathbf{k}$ . In spherical coordinates, the integral becomes

$$\frac{1}{4} \int_0^\infty dk \int_0^\pi d\theta \frac{k^2 \sin(\theta)}{(2\pi)^2} \left[ \frac{2\varepsilon_0(\mathbf{k})^2 + 3\varepsilon_0(\mathbf{k})ng_{3\text{D}}d(\theta)}{\sqrt{\varepsilon_0(\mathbf{k})^2 + 2\varepsilon_0(\mathbf{k})ng_{3\text{D}}d(\theta)}} - 2\varepsilon_0(\mathbf{k}) - ng_{3\text{D}}d(\theta) \right], \quad (4.70)$$

where we have set the direction of the polarization along  $k_z$ . As the potential  $V(\mathbf{k})$  does not depend on the absolute value of  $\mathbf{k}$ , we perform the radial integration analogous to the previous section. Therefore we substitute

$$k = \sqrt{\frac{2mng_{3\text{D}}}{\hbar^2}}u, \quad (4.71)$$

and we obtain

$$\frac{1}{16\pi^2} \left( \frac{2m}{\hbar^2} \right)^{3/2} (ng_{3\text{D}})^{5/2} \int_0^\infty du \int_0^\pi d\theta u^2 \sin(\theta) \left[ \frac{2u^4 + 3u^2d(\theta)}{\sqrt{u^4 + 2u^2d(\theta)}} - 2u^2 - d(\theta) \right]. \quad (4.72)$$

The integration over  $u$  yields

$$\begin{aligned}
\varepsilon - \frac{n}{2} \frac{d\varepsilon}{dn} &= \frac{1}{16\pi^2} \left( \frac{2m}{\hbar^2} \right)^{3/2} (ng_{3D})^{5/2} \int_0^\pi d\theta \sin(\theta) \left[ -\frac{4\sqrt{2}}{15} d(\theta)^{5/2} \right] \\
&= -\frac{64\sqrt{\pi}}{15} \frac{\hbar^2}{m} (na_s)^{5/2} \frac{1}{2} \int_0^\pi d\theta \sin(\theta) (1 + \varepsilon_{dd}(3\cos(\theta) - 1))^{5/2} \\
&= -\frac{64\sqrt{\pi}}{15} \frac{\hbar^2}{m} (na_s)^{5/2} \mathcal{Q}_5(\varepsilon_{dd}) \\
&= f(n),
\end{aligned} \tag{4.73}$$

where we have introduced the function

$$\mathcal{Q}_5(\varepsilon_{dd}) = \frac{1}{2} \int_0^\pi d\theta \sin(\theta) (1 + \varepsilon_{dd}(3\cos(\theta) - 1))^{5/2}. \tag{4.74}$$

The general solution to the differential equation (4.73) is the same as in the previous section (4.66),

$$\begin{aligned}
\varepsilon(n) &= \frac{V(0)n^2}{2} - n^2 \int_{n_c}^n dn' \frac{2f(n')}{n'^3} \\
&= \frac{2\pi\hbar^2 a_s}{m} n^2 + \frac{128\sqrt{\pi}}{15} \frac{\hbar^2 a_s^{5/2}}{m} \mathcal{Q}_5(\varepsilon_{dd}) n^2 \int_0^n dn' n'^{-1/2} \\
&= \frac{2\pi\hbar^2 a_s}{m} n^2 + \frac{256\sqrt{\pi}}{15} \frac{\hbar^2}{m} (na_s)^{5/2} \mathcal{Q}_5(\varepsilon_{dd}).
\end{aligned} \tag{4.75}$$

Note that we have set the constant  $n_c = 0$ , using the same argumentation as in the previous section. Our solution agrees with the expression from Lima and Pelster and has the advantage that no divergence appears. Again we want to emphasize that the approach of Hugenholtz and Pines allows for a consistent treatment of weakly interacting Bose gases, even with dipolar interactions.

The application of the diagrammatic approach to the one-dimensional Bose gas is briefly covered in the next section.

## 4.7. Diagrammatic Approach in One Dimension

The considerations of the previous sections of this chapter remain mostly valid for the treatment of the one-dimensional weakly interacting Bose gas. The differential equation for the ground state energy takes the same form as in the three-dimensional case,

$$\begin{aligned}
\varepsilon_{1D} - \frac{n_{1D}}{2} \frac{d\varepsilon_{1D}}{dn_{1D}} &= \frac{1}{4} \int_{\mathbb{R}} \frac{dk_z}{2\pi} \left[ \frac{2\varepsilon_0(k_z)^2 + 3\varepsilon_0(k_z)n_{1D}g_{1D}}{\sqrt{\varepsilon_0(k_z)^2 + 2\varepsilon_0(k_z)n_{1D}g_{1D}}} - 2\varepsilon_0(k_z) - n_{1D}g_{1D} \right] \\
&\equiv f^{1D}(n_{1D}).
\end{aligned} \tag{4.76}$$

Like in three dimensions, the general solution can be given by

$$\varepsilon_{1\text{D}}(n_{1\text{D}}) = \varepsilon_{\text{mf}}^{1\text{D}}(n_{1\text{D}}) - n^2 \int_{n_{1\text{D}}^c}^{n_{1\text{D}}} dn' \frac{2f^{1\text{D}}(n')}{n'^3}, \quad (4.77)$$

and we need to impose a constraint to determine the constant  $n_{1\text{D}}^c$ . To obtain the constraint, we follow the same reasoning as in the three-dimensional case. In contrast to the three-dimensional system, the one-dimensional Bose gas is weakly interacting for high densities, as discussed in section 3.7. Thus, we have to ensure that the corrections to the mean-field energy vanish faster than  $n_{1\text{D}}^2$  for high densities, which we can ensure by setting  $n_{1\text{D}}^c = \infty$ . By performing the integration over the density, we obtain

$$\begin{aligned} \varepsilon_{1\text{D}} &= \varepsilon_{\text{mf}}^{1\text{D}} - \frac{n_{1\text{D}}^2}{2} \int_{\infty}^{n_{1\text{D}}} dn' \int_{\mathbb{R}} \frac{dk_z}{(2\pi)} \frac{1}{n'^3} \left[ \frac{2\varepsilon_0(k_z)^2 + 3\varepsilon_0(k_z)n'g_{1\text{D}}}{\sqrt{\varepsilon_0(k_z)^2 + 2\varepsilon_0(k_z)n'g_{1\text{D}}}} - 2\varepsilon_0(k_z) - n'g_{1\text{D}} \right] \\ &= \varepsilon_{\text{mf}}^{1\text{D}} - \frac{n_{1\text{D}}^2}{2} \int_{\mathbb{R}^3} \frac{dk_z}{(2\pi)} \left. \frac{\varepsilon_0(\mathbf{k}) + n'g_{1\text{D}} - \sqrt{\varepsilon_0(k_z)^2 + 2\varepsilon_0(k_z)n'g_{1\text{D}}}}{n'^2} \right|_{\infty}^{n_{1\text{D}}} \\ &= \varepsilon_{\text{mf}}^{1\text{D}} - \frac{1}{2} \int_{\mathbb{R}} \frac{dk_z}{(2\pi)} \left[ \varepsilon_0(k_z) + n_{1\text{D}}g_{1\text{D}} - \sqrt{\varepsilon_0(k_z)^2 + 2n_{1\text{D}}g_{1\text{D}}\varepsilon_0(k_z)} \right]. \end{aligned} \quad (4.78)$$

The last expression agrees with the result obtained by the Bogoliubov theory from equation (3.38), and we arrive at the same ground state energy,

$$\varepsilon_{1\text{D}} = \frac{1}{2}g_{1\text{D}}n_{1\text{D}}^2 - \frac{2}{3\pi} \left( \frac{m}{\hbar^2} \right)^{1/2} (n_{1\text{D}}g_{1\text{D}})^{3/2}.$$

In this chapter, we have seen that the diagrammatic treatment of the weakly interacting Bose gas allows us to understand the underlying processes on a fundamental level. The theory does not come across divergences, as we have encountered them during the Bogoliubov theory. This is due to the differential equation, the ground state energy has to fulfill. A further physical constraint is needed to solve the differential equation. With the correct choice of the constraint, the divergence is cured automatically. Thus, we have a powerful tool to treat the weakly interacting Bose gas consistently, without the need to subtract terms manually.

In the next chapter, we will consider the dimensional crossover from a three-dimensional to a quasi-one-dimensional system, where we will greatly profit from the consistency of the diagrammatic approach.





# 5. Confined Systems

In the previous chapters, we discussed approaches to three- and one-dimensional systems in the thermodynamic limit. In experiments, however, the particles are often confined in a trap, and finite size effects play a role. In a recent paper of Edler *et al.* [42], the authors considered a system of dipolar bosons in a harmonic confinement. With the use of the approach of Hugenholtz and Pines, discussed in the previous chapter, they obtained the behavior of the quasi-one-dimensional system. Due to the complexity of the system, Edler *et al.* had to rely on the numerical evaluation of parts of the theory.

The following chapter is dedicated to the description of confined systems. In particular, we consider a system elongated in one direction, but tightly confined in the transverse directions. In contrast to Edler *et al.*, the system is confined by periodic boundary conditions, and we will not include the dipolar interaction. These simplifications will allow us to obtain the quasi-one-dimensional limit analytically. We will show that in the quasi-one-dimensional limit, the finite-size effects appear naturally, and we can describe a crossover between the three- and one-dimensional behavior of the system.

## 5.1. The Limiting Cases

In the following, we will consider a box of length  $L$  in the  $z$ -direction and height and width  $l_{\perp}$  in  $x$ - and  $y$ -direction. The box is elongated along the  $z$ -direction,

$$L \gg 1, \quad (5.1)$$

and tightly confined in the transverse directions,

$$\frac{l_{\perp}}{L} \ll 1. \quad (5.2)$$

The density of particles is given by

$$n = \frac{N}{l_{\perp}^2 L}. \quad (5.3)$$

We impose periodic boundary conditions. Therefore, the allowed wave vectors are

$$\mathbf{k} = \begin{pmatrix} k_x \\ k_y \\ k_z \end{pmatrix} \quad \text{with} \quad k_z \in \mathbb{R}, \quad k_x = \frac{2\pi}{l_{\perp}} i \quad k_y = \frac{2\pi}{l_{\perp}} j \quad \text{and} \quad i, j \in \mathbb{Z}. \quad (5.4)$$

Note that we will treat  $k_z$  as a continuous variable, as the box is elongated along the  $z$ -direction.

The scattering processes between the particles are treated in three dimensions, which is valid as long as the three-dimensional scattering length  $a_s$  is much smaller than the transverse confinement,

$$\frac{a_s}{l_\perp} \ll 1. \quad (5.5)$$

If the chemical potential  $\mu$  is much larger than the energy to excite transverse modes,

$$\frac{\hbar^2}{ml_\perp^2} \ll \mu = ng_{3D} \quad \Leftrightarrow \quad \kappa \equiv \frac{Na_s}{L} \gg 1, \quad (5.6)$$

scattering events can excite particles, and we can treat the system three-dimensionally. Here, we have introduced the crossover parameter  $\kappa$ . The ground state energy, in this case, is the three-dimensional expression from equation (3.34),

$$\frac{E_{3D}}{l_\perp^2 L} = \frac{1}{2}g_{3D}n^2 + \frac{8}{15\pi^2} \left(\frac{m}{\hbar^2}\right)^{3/2} (ng_{3D})^{5/2}.$$

We can express the energy in terms of the crossover parameter  $\kappa$  and obtain

$$E_{3D} = \frac{2\pi\hbar^2}{m} \frac{L}{l_\perp^2 a_s} \kappa^2 \left(1 + \frac{128}{15\sqrt{\pi}} \frac{a_s}{l_\perp} \kappa^{1/2}\right). \quad (5.7)$$

Note that the beyond-mean-field correction is of order  $a_s/l_\perp$ . We need to keep in mind that the expression (5.7) is only valid if the interactions are weak. For a three-dimensional system, this means

$$na_s^3 \ll 1 \quad \Leftrightarrow \quad \kappa \ll \frac{l_\perp^2}{a_s^2}. \quad (5.8)$$

Thus, the three-dimensional description is correct for  $1 \ll \kappa \ll l_\perp^2/a_s^2$ .

Next, we want to consider the quasi-one-dimensional regime. If the chemical potential  $\mu$  is much smaller than the energy to excite transverse modes,

$$\frac{\hbar^2}{ml_\perp^2} \gg \mu = ng_{3D} \quad \Leftrightarrow \quad \kappa \ll 1, \quad (5.9)$$

scattering events cannot excite the particles to transverse modes. In the absence of transverse excitations, we obtain a quasi-one-dimensional system with energy

$$\frac{E_{\text{pbc}}}{L} = \frac{1}{2}g_{\text{pbc}}n_{1D}^2 - \frac{2}{3\pi} \left(\frac{m}{\hbar^2}\right)^{1/2} (n_{1D}g_{\text{pbc}})^{3/2}.$$

The density  $n_{1D}$  is connected to the full density  $n$  by

$$n_{1D} = nl_{\perp}^2. \quad (5.10)$$

As discussed in chapter 2 of this work, the one-dimensional treatment of the problem holds if we use the correct coupling constant  $g_{\text{pbc}}$ . In section 2.4.2, we have determined the coupling constant to

$$g_{\text{pbc}} = \frac{4\pi\hbar^2 a_s}{m} \frac{1}{l_{\perp}^2} \left(1 - \frac{a_s}{l_{\perp}} C_{\text{pbc}}\right)^{-1} \approx \frac{g_{3D}}{l_{\perp}^2} \left(1 + \frac{a_s}{l_{\perp}} C_{\text{pbc}}\right).$$

The beyond-mean-field correction itself is of order  $a_s/l_{\perp}$ . Hence, we need to include orders  $a_s/l_{\perp}$  for the coupling constant  $g_{\text{pbc}}$  as well, but we will neglect all higher orders in the following. With the previous considerations, we can express the quasi-one-dimensional ground state energy  $E_{\text{pbc}}$  by

$$E_{\text{pbc}} = \frac{2\pi\hbar^2}{m} \frac{L}{l_{\perp}^2 a_s} \kappa^2 \left(1 + \frac{a_s}{l_{\perp}} C_{\text{pbc}} - \frac{8}{3\sqrt{\pi}} \frac{a_s}{l_{\perp}} \kappa^{-1/2}\right). \quad (5.11)$$

The confinement causes an additional term of order  $\kappa^2$ . The description of a crossover between the three-dimensional and quasi-one-dimensional behavior later in this chapter has to reproduce this confinement-induced shift.

Keep in mind, that the energy (5.11) is only valid in the weakly interacting regime. In section 3.7 we saw that the one-dimensional system is weakly interacting for

$$\frac{g_{1D}m}{n_{1D}\hbar^2} \ll 1.$$

Regarding the crossover parameter, this means

$$\kappa \gg \frac{a_s^2}{l_{\perp}^2}. \quad (5.12)$$

Taking into account the previous considerations, we can express the energy as a function of  $\kappa$

$$E = \frac{2\pi\hbar^2}{m} \frac{L}{l_{\perp}^2 a_s} \kappa^2 \left(1 + \begin{cases} \frac{a_s}{l_{\perp}} C_{\text{pbc}} - \frac{8}{3\sqrt{\pi}} \kappa^{-1/2}, & \text{for } \frac{a_s^2}{l_{\perp}^2} \ll \kappa \ll 1 \\ \frac{128}{15\sqrt{\pi}} \frac{a_s}{l_{\perp}} \kappa^{1/2}, & \text{for } 1 \ll \kappa \ll \frac{l_{\perp}^2}{a_s^2} \end{cases}\right). \quad (5.13)$$

The remaining task is to connect the limiting cases  $\kappa \ll 1$  and  $\kappa \gg 1$  consistently.

## 5.2. Description of the Crossover

In the previous chapter 4, we saw that the ground state energy has to fulfill a differential equation,

$$E - \frac{n}{2} \frac{dE}{dn} = f(n).$$

For the confined system, the function  $f(n)$  is given in analogy to equation (4.65),

$$f(n) = \frac{L}{4} \sum_{k_x, k_y} \int_{\mathbb{R}} \frac{dk_z}{2\pi} \left[ \frac{2\varepsilon_0(\mathbf{k})^2 + 3\varepsilon_0(\mathbf{k})ng_{3D}}{\sqrt{\varepsilon_0(\mathbf{k})^2 + 2\varepsilon_0(\mathbf{k})ng_{3D}}} - 2\varepsilon_0(\mathbf{k}) - ng_{3D} \right]. \quad (5.14)$$

The parameter  $\kappa$  describes the crossover. Hence, we need to express the differential equation in terms of  $\kappa$ . With the definitions of the previous section 5.1, we obtain

$$E(\kappa) - \frac{\kappa}{2} \frac{dE}{d\kappa} = f(\kappa), \quad (5.15)$$

where the function  $f(\kappa)$  is given by

$$\begin{aligned} f(\kappa) &= \frac{L}{4} \sum_{k_x, k_y} \int_{\mathbb{R}} \frac{dk_z}{2\pi} \left[ \frac{2\varepsilon_0(\mathbf{k})^2 + 3\varepsilon_0(\mathbf{k}) \frac{4\pi\hbar^2}{ml_{\perp}^2} \kappa}{\sqrt{\varepsilon_0(\mathbf{k})^2 + 2\varepsilon_0(\mathbf{k}) \frac{4\pi\hbar^2}{ml_{\perp}^2} \kappa}} - 2\varepsilon_0(\mathbf{k}) - \frac{4\pi\hbar^2}{ml_{\perp}^2} \kappa \right] \\ &= \frac{\hbar^2 L \sqrt{\pi}}{l_{\perp}^3 m} \sqrt{\pi} \kappa \sum_{i,j} \int_{\mathbb{R}} du \left[ \frac{2\tilde{\varepsilon}_0(i, j, u, \kappa)^2 + 3\tilde{\varepsilon}_0(i, j, u, \kappa)}{\sqrt{\tilde{\varepsilon}_0(i, j, u, \kappa)^2 + 2\tilde{\varepsilon}_0(i, j, u, \kappa)}} - 2\tilde{\varepsilon}_0(i, j, u, \kappa) - 1 \right] \\ &\equiv \frac{\hbar^2 L \sqrt{\pi}}{l_{\perp}^3 m} \tilde{f}(\kappa). \end{aligned} \quad (5.16)$$

In the second line, we have replaced the integration over  $k_z$  by an integration over  $u = l_{\perp} k_z / 2\pi$ , so the dimensionless function  $\tilde{\varepsilon}_0$  is

$$\tilde{\varepsilon}_0(i, j, u, \kappa) = \frac{\pi}{2\kappa} (i^2 + j^2 + u^2). \quad (5.17)$$

In the limiting cases, we can give the functions  $f(\kappa)$  and  $\tilde{f}(\kappa)$  explicitly. For a three-

dimensional system,  $f_{3\text{D}}$  reads

$$\begin{aligned}
 f_{3\text{D}} &= \frac{l_{\perp}^2 L}{4} \int_{\mathbb{R}^3} \frac{d^3 \mathbf{k}}{(2\pi)^3} \left[ \frac{2\varepsilon_0(\mathbf{k})^2 + 3\varepsilon_0(\mathbf{k})ng_{3\text{D}}}{\sqrt{\varepsilon_0(\mathbf{k})^2 + 2\varepsilon_0(\mathbf{k})ng_{3\text{D}}}} - 2\varepsilon_0(\mathbf{k}) - ng_{3\text{D}} \right] \\
 &= -\frac{2}{15\pi^2} l_{\perp}^2 L \left( \frac{m}{\hbar^2} \right)^{3/2} (ng_{3\text{D}})^{3/2} \\
 &= \frac{\hbar^2 L \sqrt{\pi}}{l_{\perp}^3 m} \left( -\frac{64}{15} \kappa^{5/2} \right) = \frac{\hbar^2 L \sqrt{\pi}}{l_{\perp}^3 m} \tilde{f}_{3\text{D}}(\kappa).
 \end{aligned} \tag{5.18}$$

In a one-dimensional description, we obtain

$$f_{1\text{D}} = \frac{L}{4} \int_{\mathbb{R}} \frac{dk_z}{2\pi} \left[ \frac{2\varepsilon_0(k_z)^2 + 3\varepsilon_0(k_z)n_{1\text{D}}g_{1\text{D}}}{\sqrt{\varepsilon_0(k_z)^2 + 2\varepsilon_0(k_z)n_{1\text{D}}g_{1\text{D}}}} - 2\varepsilon_0(k_z) - n_{1\text{D}}g_{1\text{D}} \right] \tag{5.19}$$

$$= -\frac{L}{6\pi} \left( \frac{m}{\hbar^2} \right)^{1/2} (n_{1\text{D}}g_{1\text{D}})^{3/2} \tag{5.20}$$

$$= \frac{\hbar^2 L \sqrt{\pi}}{l_{\perp}^3 m} \left( -\frac{4}{3} \kappa^{3/2} \right) = \frac{\hbar^2 L \sqrt{\pi}}{l_{\perp}^3 m} \tilde{f}_{1\text{D}}(\kappa). \tag{5.21}$$

To illustrate that the function  $\tilde{f}(\kappa)$  from equation (5.16), indeed, reproduces the limiting cases correctly, we have plotted the expressions  $-\tilde{f}(\kappa)/\kappa^3$ ,  $-\tilde{f}_{1\text{D}}(\kappa)/\kappa^3$  and  $-\tilde{f}_{3\text{D}}(\kappa)/\kappa^3$  in figure 5.1 on a double logarithmic scale. As expected,  $\tilde{f}(\kappa)$  connects the limiting cases smoothly.

Analogous to the considerations in the previous chapter, we can give the general solution of the differential equation (5.15) as

$$E(\kappa) = \frac{2\pi\hbar^2}{m} \frac{L}{l_{\perp}^2 a_s} \kappa^2 - \kappa^2 \int_{\kappa_c}^{\kappa} d\kappa' \frac{2f(\kappa')}{\kappa'^3} \tag{5.22}$$

$$= \frac{2\pi\hbar^2}{m} \frac{L}{l_{\perp}^2 a_s} \kappa^2 \left( 1 - \frac{a_s}{l_{\perp} \sqrt{\pi}} \int_{\kappa_c}^{\kappa} d\kappa' \frac{\tilde{f}(\kappa')}{\kappa'^3} \right). \tag{5.23}$$

The question that arises is how to choose the constant  $\kappa_c$ , to describe the system correctly. For a consistent treatment, we chose a different route than in the previous chapter. Instead of thinking about the constant  $k_c$ , we fix the lower bound of the integration to an arbitrary value  $\kappa^*$  and introduce a constant  $A(\kappa^*)$  to obtain the correct physical behavior,

$$E(\kappa) = \frac{2\pi\hbar^2}{m} \frac{L}{l_{\perp}^2 a_s} \kappa^2 \left( 1 + A(\kappa^*) - \frac{a_s}{l_{\perp} \sqrt{\pi}} \int_{\kappa^*}^{\kappa} d\kappa' \frac{\tilde{f}(\kappa')}{\kappa'^3} \right). \tag{5.24}$$

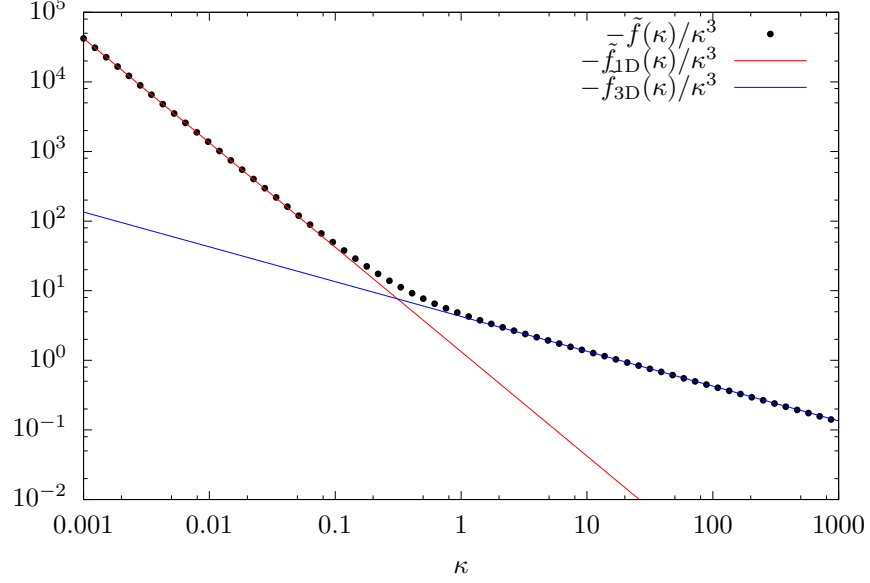


Figure 5.1.: Dimensionless function  $\tilde{f}(\kappa)/\kappa^3$  (black dots) compared to the limiting cases  $\tilde{f}_{1D}(\kappa)/\kappa^3$  (red line) and  $\tilde{f}_{3D}(\kappa)/\kappa^3$  (blue line) on a double logarithmic scale. For the evaluation of  $\tilde{f}(\kappa)$ , 2000 transverse modes were taken into account for both transverse directions. The function  $\tilde{f}(\kappa)$  connects the limiting cases smoothly and agrees with our expectations.

We will determine the constant  $A(\kappa^*)$  so that the solution (5.24) provides the correct result for the three-dimensional case. For  $\kappa \gg 1$ , we can write equation (5.24) as

$$\begin{aligned}
 E(\kappa) = \frac{2\pi\hbar^2}{m} \frac{L}{l_{\perp}^2 a_s} \kappa^2 \left( 1 - \frac{a_s}{\sqrt{\pi} l_{\perp}} \int_0^{\kappa} d\kappa' \frac{\tilde{f}_{3D}(\kappa')}{\kappa'^3} \right. \\
 \left. + \frac{a_s}{\sqrt{\pi} l_{\perp}} \int_0^{\kappa} d\kappa' \frac{\tilde{f}_{3D}(\kappa')}{\kappa'^3} + A_{3D}(\kappa^*) - \frac{a_s}{l_{\perp} \sqrt{\pi}} \int_{\kappa^*}^{\kappa} d\kappa' \frac{\tilde{f}(\kappa')}{\kappa'^3} \right). \quad (5.25)
 \end{aligned}$$

The first line leads to the correct ground state energy (5.7). Thus, we have to choose

$$A_{3D}(\kappa^*) = \frac{a_s}{\sqrt{\pi} l_{\perp}} \left( \int_{\kappa^*}^{\kappa_{\infty}} d\kappa' \frac{\tilde{f}(\kappa')}{\kappa'^3} - \int_0^{\kappa_{\infty}} d\kappa' \frac{\tilde{f}_{3D}(\kappa')}{\kappa'^3} \right), \quad (5.26)$$

to make the second line vanish. Remember,  $A_{3D}(\kappa^*)$  does not depend on  $\kappa$ . As  $\tilde{f}(\kappa)$  matches  $\tilde{f}_{3D}(\kappa)$  for large values of  $\kappa$ ,  $A_{3D}(\kappa^*)$  does not depend on the newly introduced quantity  $\kappa_{\infty}$  as long as it is large enough. Hence, we are interested in the limit  $\kappa_{\infty} \rightarrow \infty$ .

Note that we can fix the constant  $A(\kappa^*)$  to the quasi-one-dimensional case as well, but we must keep in mind to include the confinement-induced shift. Fixing the constant to

the three-dimensional case will provide the confinement-induced shift automatically, as we will see in the following.

With the previous considerations, we ensured that equation (5.24) describes the three-dimensional system correctly. Next, we need to check if the energy (5.24) reproduces the correct results in the quasi-one-dimensional regime. In the limit  $\kappa \ll 1$ , we can write the energy (5.24) as

$$\begin{aligned}
E(\kappa) &= \frac{2\pi\hbar^2}{m} \frac{L}{l_{\perp}^2 a_s} \kappa^2 \left( 1 - \frac{a_s}{\sqrt{\pi} l_{\perp}} \int_{\infty}^{\kappa} d\kappa' \frac{\tilde{f}_{1D}(\kappa')}{\kappa'^3} \right. \\
&\quad \left. + \frac{a_s}{\sqrt{\pi} l_{\perp}} \int_{\infty}^{\kappa} d\kappa' \frac{\tilde{f}_{1D}(\kappa')}{\kappa'^3} + A_{3D}(\kappa^*) - \frac{a_s}{l_{\perp} \sqrt{\pi}} \int_{\kappa^*}^{\kappa} d\kappa' \frac{\tilde{f}(\kappa')}{\kappa'^3} \right) \\
&\stackrel{\kappa \ll 1}{=} \frac{2\pi\hbar^2}{m} \frac{L}{l_{\perp}^2 a_s} \kappa^2 \left( 1 + A_{3D}(\kappa^*) - A_{1D}(\kappa^*) - \frac{a_s}{\sqrt{\pi} l_{\perp}} \int_{\infty}^{\kappa} d\kappa' \frac{\tilde{f}_{1D}(\kappa')}{\kappa'^3} \right) \\
&= \frac{2\pi\hbar^2}{m} \frac{L}{l_{\perp}^2 a_s} \kappa^2 \left( 1 + A_{3D}(\kappa^*) - A_{1D}(\kappa^*) - \frac{8}{3\sqrt{\pi}} \frac{a_s}{l_{\perp}} \kappa^{-1/2} \right), \tag{5.27}
\end{aligned}$$

where we have introduced

$$A_{1D}(\kappa^*) = \frac{a_s}{\sqrt{\pi} l_{\perp}} \left( \int_{\kappa^*}^{\kappa_0} d\kappa' \frac{\tilde{f}(\kappa')}{\kappa'^3} - \int_{\infty}^{\kappa_0} d\kappa' \frac{\tilde{f}_{1D}(\kappa')}{\kappa'^3} \right). \tag{5.28}$$

The constant  $A_{1D}(\kappa^*)$  does not depend on the newly introduced quantity  $\kappa_0$  as long as  $\kappa_0$  is small enough. Thus, we will consider the limit  $\kappa_0 \rightarrow 0$  in the following.

In the quasi-one-dimensional regime  $\kappa \ll 1$ , we see a shift to the mean-field expression appearing. If our approach is consistent, this shift has to match the confinement-induced shift from equation (5.11),

$$A_{3D}(\kappa^*) - A_{1D}(\kappa^*) = \frac{a_s}{l_{\perp}} C_{\text{pbc}}. \tag{5.29}$$

In the next section, we will calculate the shift explicitly.

### 5.3. Confinement-Induced Shift

In the previous section, we obtained a shift to the mean-field energy of the form

$$A_{3D} - A_{1D} = \frac{a_s}{\sqrt{\pi} l_{\perp}} \left( \int_{\kappa_0}^{\kappa_{\infty}} d\kappa' \frac{\tilde{f}(\kappa')}{\kappa'^3} - \int_0^{\kappa_{\infty}} d\kappa' \frac{\tilde{f}_{3D}(\kappa')}{\kappa'^3} - \int_{\kappa_0}^{\infty} d\kappa' \frac{\tilde{f}_{1D}(\kappa')}{\kappa'^3} \right). \tag{5.30}$$

With the definitions (5.18) and (5.21) of the functions  $\tilde{f}_{3\text{D}}$  and  $\tilde{f}_{1\text{D}}$ , we can evaluate the last two integrals immediately,

$$A_{3\text{D}} - A_{1\text{D}} = \frac{a_s}{\sqrt{\pi}l_{\perp}} \left( \int_{\kappa_0}^{\kappa_{\infty}} d\kappa' \frac{\tilde{f}(\kappa')}{\kappa'^3} + \frac{128}{15}\kappa_{\infty}^{1/2} + \frac{8}{3}\kappa_0^{-1/2} \right). \quad (5.31)$$

Next, we consider the first integral of the shift,

$$\int_{\kappa_0}^{\kappa_{\infty}} d\kappa' \frac{\tilde{f}(\kappa')}{\kappa'^3} = \frac{ml_{\perp}^3}{4\sqrt{\pi}\hbar^2} \sum_{k_x, k_y} \int_{\mathbb{R}} \frac{dk_z}{2\pi} \int_{\kappa_0}^{\kappa_{\infty}} d\kappa' \frac{1}{\kappa'^3} \left[ \frac{2\varepsilon_0(\mathbf{k})^2 + 3\varepsilon_0(\mathbf{k})\tilde{g}\kappa}{\sqrt{\varepsilon_0(\mathbf{k})^2 + 2\varepsilon_0(\mathbf{k})\tilde{g}\kappa}} - 2\varepsilon_0(\mathbf{k}) - \tilde{g}\kappa \right]. \quad (5.32)$$

We have introduced the constant

$$\tilde{g} = \frac{4\pi\hbar^2}{ml_{\perp}^2} \quad (5.33)$$

for a shorter notation. The integration over  $\kappa'$  can be performed analogously to the integration over  $n'$  in equation (4.67), and we obtain

$$\begin{aligned} \int_{\kappa_0}^{\kappa_{\infty}} d\kappa' \frac{\tilde{f}(\kappa')}{\kappa'^3} &= \frac{ml_{\perp}^3}{4\hbar^2} \frac{1}{\sqrt{\pi}} \sum_{k_x, k_y} \int_{\mathbb{R}} \frac{dk_z}{2\pi} \left[ \frac{\varepsilon_0(\mathbf{k}) + \tilde{g}\kappa_{\infty} - \sqrt{\varepsilon_0(\mathbf{k})^2 + 2\varepsilon_0(\mathbf{k})\tilde{g}\kappa_{\infty}}}{\kappa_{\infty}^2} \right] \\ &\quad - \frac{ml_{\perp}^3}{4\hbar^2} \frac{1}{\sqrt{\pi}} \sum_{k_x, k_y} \int_{\mathbb{R}} \frac{dk_z}{2\pi} \left[ \frac{\varepsilon_0(\mathbf{k}) + \tilde{g}\kappa_0 - \sqrt{\varepsilon_0(\mathbf{k})^2 + 2\varepsilon_0(\mathbf{k})\tilde{g}\kappa_0}}{\kappa_0^2} \right]. \end{aligned} \quad (5.34)$$

Keep in mind that we are interested in the limits  $\kappa_0 \rightarrow 0$  and  $\kappa_{\infty} \rightarrow \infty$ . Let us start with the first term of the right-hand side of equation (5.34). As  $\kappa_{\infty}$  is very large, we can replace the sum over the transverse modes by an integration, analogously to the procedure for  $f(\kappa)$  in the region  $\kappa \gg 1$ . Hence, we obtain

$$\begin{aligned} &\frac{ml_{\perp}^3}{4\hbar^2} \frac{1}{\sqrt{\pi}} \sum_{k_x, k_y} \int_{\mathbb{R}} \frac{dk_z}{2\pi} \left[ \frac{\varepsilon_0(\mathbf{k}) + \tilde{g}\kappa_{\infty} - \sqrt{\varepsilon_0(\mathbf{k})^2 + 2\varepsilon_0(\mathbf{k})\tilde{g}\kappa_{\infty}}}{\kappa_{\infty}^2} \right] \\ &= \frac{ml_{\perp}^5}{4\hbar^2\sqrt{\pi}\kappa_{\infty}^2} \int_{\mathbb{R}^3} \frac{d^3\mathbf{k}}{(2\pi)^3} \left[ \varepsilon_0(\mathbf{k}) + \tilde{g}\kappa_{\infty} - \sqrt{\varepsilon_0(\mathbf{k})^2 + 2\varepsilon_0(\mathbf{k})\tilde{g}\kappa_{\infty}} \right]. \end{aligned} \quad (5.35)$$

The remaining integral is the same as the beyond-mean-field term from Bogoliubov theory (3.20), before the troublesome diagram was subtracted. Thus, the integral diverges. To extract the divergence, we proceed with adding and subtracting the divergent term



of the integral,

$$\begin{aligned}
& \frac{ml_{\perp}^5}{4\hbar^2\sqrt{\pi}} \frac{1}{\kappa_{\infty}^2} \int_{\mathbb{R}^3} \frac{d^3\mathbf{k}}{(2\pi)^3} \left[ \varepsilon_0(\mathbf{k}) + \tilde{g}\kappa_{\infty} - \sqrt{\varepsilon_0(\mathbf{k})^2 + 2\varepsilon_0(\mathbf{k})\tilde{g}\kappa_{\infty}} \right] \\
&= \frac{ml_{\perp}^5}{4\hbar^2\sqrt{\pi}} \frac{1}{\kappa_{\infty}^2} \int_{\mathbb{R}^3} \frac{d^3\mathbf{k}}{(2\pi)^3} \left[ \varepsilon_0(\mathbf{k}) + \tilde{g}\kappa_{\infty} - \sqrt{\varepsilon_0(\mathbf{k})^2 + 2\varepsilon_0(\mathbf{k})\tilde{g}\kappa_{\infty}} - \frac{\tilde{g}^2\kappa_{\infty}^2}{2\varepsilon_0(\mathbf{k})} + \frac{\tilde{g}^2\kappa_{\infty}^2}{2\varepsilon_0(\mathbf{k})} \right] \\
&= -\frac{128}{15}\kappa_{\infty}^{1/2} + 4\pi^{3/2}l_{\perp} \int_{\mathbb{R}^3} \frac{d^3\mathbf{k}}{(2\pi)^3} \frac{1}{\mathbf{k}^2}.
\end{aligned} \tag{5.36}$$

We can evaluate a part of the integral in analogy to equation (3.32). Note that the first term of equation (5.36) exactly cancels the second term appearing in the shift (5.31).

Next, we consider the second term in equation (5.34),

$$-\frac{ml_{\perp}^3}{4\hbar^2} \frac{1}{\sqrt{\pi}} \sum_{k_x, k_y} \int_{\mathbb{R}} \frac{dk_z}{2\pi} \left[ \frac{\varepsilon_0(\mathbf{k}) + \tilde{g}\kappa_0 - \sqrt{\varepsilon_0(\mathbf{k})^2 + 2\varepsilon_0(\mathbf{k})\tilde{g}\kappa_0}}{\kappa_0^2} \right].$$

We split off the term  $k_x = k_y = 0$  to ensure the numerator does not vanish when taking the limit  $\kappa_0 \rightarrow 0$ ,

$$\begin{aligned}
& -\frac{ml_{\perp}^3}{4\hbar^2} \frac{1}{\sqrt{\pi}} \left[ \sum'_{k_x, k_y} \int_{\mathbb{R}} \frac{dk_z}{2\pi} \left[ \frac{\varepsilon_0(\mathbf{k}) + \tilde{g}\kappa_0 - \sqrt{\varepsilon_0(\mathbf{k})^2 + 2\varepsilon_0(\mathbf{k})\tilde{g}\kappa_0}}{\kappa_0^2} \right] \right. \\
& \quad \left. + \int_{\mathbb{R}} \frac{dk_z}{2\pi} \left[ \frac{\varepsilon_0(k_z) + \tilde{g}\kappa_0 - \sqrt{\varepsilon_0(k_z)^2 + 2\varepsilon_0(k_z)\tilde{g}\kappa_0}}{\kappa_0^2} \right] \right].
\end{aligned} \tag{5.37}$$

For the first term, we take the limit  $\kappa_0 \rightarrow 0$  and the integral of the second term is evaluated in analogy to equation (3.39). A short calculation yields

$$-4\pi^{3/2} \frac{1}{l_{\perp}} \sum'_{k_x, k_y} \int_{\mathbb{R}} \frac{dk_z}{2\pi} \frac{1}{\mathbf{k}^2} - \frac{8}{3}\kappa_0^{-1/2}. \tag{5.38}$$

We can now insert both terms (5.36) and (5.38) into the shift (5.31) and obtain

$$A_{3D} - A_{1D} = 4\pi a_s \left( \int_{\mathbb{R}} \frac{d^3\mathbf{k}}{(2\pi)^3} \frac{1}{\mathbf{k}^2} - \frac{1}{l_{\perp}^2} \sum'_{k_x, k_y} \int_{\mathbb{R}} \frac{dk_z}{2\pi} \frac{1}{\mathbf{k}^2} \right). \tag{5.39}$$

The same expression already appeared in section 2.4.2, during the calculation of the coupling constant  $g_{\text{pbc}}$ . If we compare equations (2.63) and (2.66) to the shift (5.39), we immediately arrive at

$$A_{3D} - A_{1D} = \frac{a_s}{l_{\perp}} C_{\text{pbc}},$$

which is what we wanted to show. Thus, the ground state energy (5.27) reads

$$E(\kappa) \stackrel{\kappa \ll 1}{\cong} \frac{2\pi\hbar^2}{m} \frac{L}{l_\perp^2 a_s} \kappa^2 \left( 1 + \frac{a_s}{l_\perp} C_{\text{pbc}} - \frac{8}{3\sqrt{\pi}} \frac{a_s}{l_\perp} \kappa^{-1/2} \right), \quad (5.40)$$

which agrees with the quasi-one-dimensional description given by equation (5.11).

We have seen that the ground state energy (5.24) reproduces the correct behavior in the three- and quasi-one-dimensional case. The confinement-induced shift appears naturally in the description. In the next section, we illustrate the crossover behavior.

## 5.4. Crossover Behavior

In the last section of this chapter, we will briefly illustrate the behavior of the ground state energy

$$E(\kappa) = \frac{2\pi\hbar^2}{m} \frac{L}{l_\perp^2 a_s} \kappa^2 \left( 1 + A_{3D}(\kappa^*) - \frac{a_s}{l_\perp \sqrt{\pi}} \int_{\kappa^*}^{\kappa} d\kappa' \frac{\tilde{f}(\kappa')}{\kappa'^3} \right).$$

For illustrative reasons, we introduce the dimensionless energies

$$\tilde{E}(\kappa) = \kappa^2 \left( 1 + A_{3D}(\kappa^*) - \frac{a_s}{l_\perp \sqrt{\pi}} \int_{\kappa^*}^{\kappa} d\kappa' \frac{\tilde{f}(\kappa')}{\kappa'^3} \right), \quad (5.41)$$

$$\tilde{E}_{\text{pbc}} = \kappa^2 \left( 1 + \frac{a_s}{l_\perp} C_{\text{pbc}} - \frac{8}{3\sqrt{\pi}} \frac{a_s}{l_\perp} \kappa^{-1/2} \right), \quad (5.42)$$

$$\tilde{E}_{3D} = \kappa^2 \left( 1 + \frac{128}{15\sqrt{\pi}} \frac{a_s}{l_\perp} \kappa^{1/2} \right), \quad (5.43)$$

and the dimensionless beyond-mean-field corrections

$$\Delta \tilde{E}(\kappa) = \kappa^2 \left( \frac{l_\perp}{a_s} A_{3D}(\kappa^*) - \frac{1}{\sqrt{\pi}} \int_{\kappa^*}^{\kappa} d\kappa' \frac{\tilde{f}(\kappa')}{\kappa'^3} \right), \quad (5.44)$$

$$\Delta \tilde{E}_{\text{pbc}}(\kappa) = \kappa^2 \left( C_{\text{pbc}} - \frac{8}{3\sqrt{\pi}} \kappa^{-1/2} \right), \quad (5.45)$$

$$\Delta \tilde{E}_{3D}(\kappa) = \kappa^2 \left( \frac{128}{15\sqrt{\pi}} \kappa^{1/2} \right). \quad (5.46)$$

Figure 5.2a) illustrates the crossover behavior by comparing the numerically obtained data of  $\Delta \tilde{E}(\kappa)/\kappa^2$  with the limiting cases for  $\kappa \ll 1$  and  $\kappa \gg 1$ . For the numerical

evaluation of  $\tilde{E}(\kappa)$ , 2000 modes in each transverse directions were taken into account. For the ratio  $a_s/l_\perp$ , we chose  $a_s/l_\perp = 1/1000$ . The numerical data agrees with the limiting cases and connects them smoothly.

In figure 5.2b), we compare the numerical data for  $\Delta\tilde{E}(\kappa)$  with the limiting cases  $\Delta\tilde{E}_{\text{pbc}}(\kappa)$  and  $\Delta\tilde{E}_{\text{3D}}(\kappa)$ . If  $\kappa$  is small, the energy correction is negative, as one would expect from a one-dimensional system. The transverse degrees of freedom play a minor role. Increasing  $\kappa$  first decreases the energy correction. By increasing  $\kappa$ , the transverse modes gain in importance, and the energy correction reaches a maximal negative value at  $\kappa \approx 0.07$ . Afterwards, increasing  $\kappa$  increases the energy correction as well. For  $\kappa \approx 0.12$  the beyond-mean-field correction vanishes entirely. As expected from a three-dimensional system, the energy correction is positive for larger values of  $\kappa$ .

The diagrammatic approach, discussed in chapter 4, allowed us to treat the confined system consistently. By restricting the considerations to periodic boundary conditions, we were able to give analytic expressions for the quasi-one-dimensional and three-dimensional limit. We were able to connect both regions smoothly and saw that in the crossover, the confinement-induced shift appears naturally.

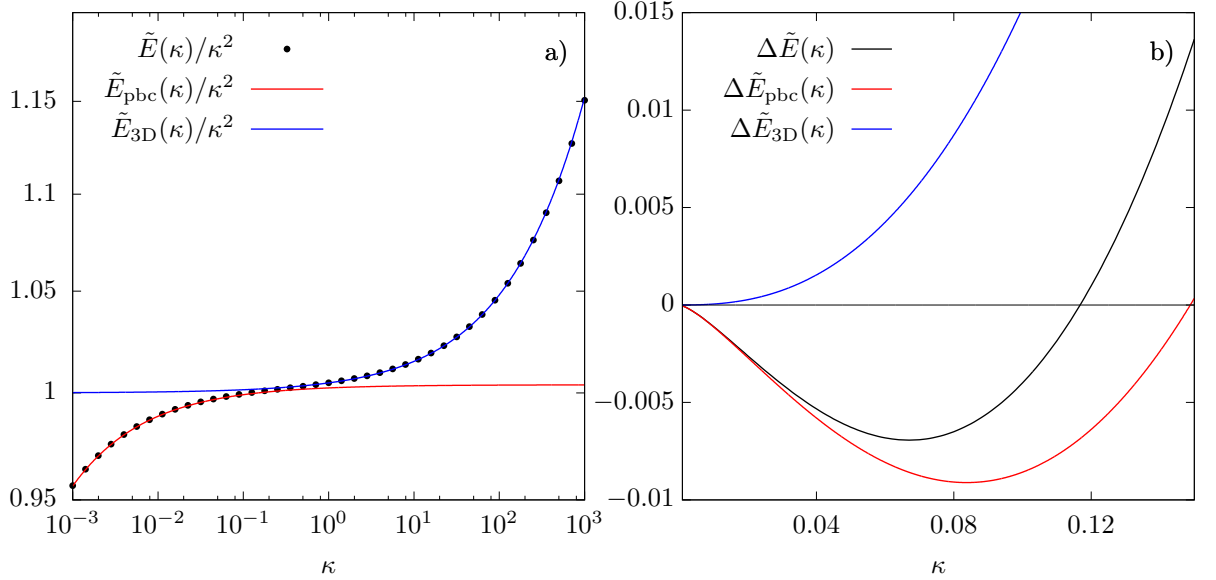


Figure 5.2.: a) Behavior of the dimensionless ground state energy  $\tilde{E}(\kappa)/\kappa^2$  as a function of  $\kappa$  on a double logarithmic scale. The exact ground state energy  $\tilde{E}(\kappa)/\kappa^2$  (black dots) is compared to the three-dimensional ground state energy  $\tilde{E}_{\text{3D}}(\kappa)/\kappa^2$  (blue line) and the quasi-one-dimensional ground state energy  $\tilde{E}_{\text{pbc}}(\kappa)/\kappa^2$  (red line). The exact ground state energy matches the limiting cases perfectly and describes a smooth crossover. For the numerical evaluation, 2000 transverse modes in each direction were taken into account, and we set  $a_s/l_\perp = 1/1000$ . b) Dimensionless beyond-mean-field correction  $\Delta\tilde{E}(\kappa)$  of the ground state energy as a function of  $\kappa$ . We compare the exact energy correction (black line) to the quasi-one-dimensional (red line) and three-dimensional (blue line) energy correction for small values of  $\kappa$ . The exact energy correction is negative for small values of  $\kappa$  but becomes positive for larger values, as more and more transverse modes become important. The correction vanishes entirely for  $\kappa \approx 0.12$ . For the numerical evaluation, 2000 transverse modes in each direction were taken into account.

## 6. Conclusion

With the rising interest in beyond-mean-field corrections in both experimental and theoretical physics, the goal of this work was to understand the underlying mechanisms on a fundamental level.

Before treating many-body systems, the interaction processes between only two particles were discussed in detail in the first part of this work. In the low-energy regime, the scattering processes are completely characterized by the scattering length of the potential. Thus, the actual form of the potential is of minor interest, and we can model the interaction by a pseudopotential. In three dimensions, however, the pseudopotential matches the exact  $T$ -matrix of the system, which one has to keep in mind when using it in a theoretical description. In one dimension, the delta-potential does not match the  $T$ -matrix but the low-energy scattering processes are universal as well. The understanding of scattering processes in one and three dimensions allowed us to treat the scattering problem in confined systems. We were able to calculate the coupling constant of a quasi-one-dimensional system, confined in periodic boundary conditions.

With the knowledge we gained from scattering theory, we were able to understand the concepts behind the Bogoliubov theory. Bogoliubov's theory allows obtaining an expression for the ground state energy of a weakly interacting Bose gas under simple assumptions. However, the inclusion of scattering properties can lead to divergences and must be treated with care. We saw that the Bogoliubov transformations effectively sums up an entire class of interaction diagrams, and hence can get in conflict with the pseudopotential.

The main focus of this work was on the field-theoretic treatment of the weakly interacting Bose gas. In the approach of Hugenholtz and Pines, the ground state energy has to fulfill a first order differential equation. For its solution, an additional constraint is needed. The correct constraint allowed for a consistent treatment of the weakly interacting Bose gas. Within the field-theoretic approach, we could include the dipolar interaction as well. In contrast to the approach of Lima and Pelster [23, 38], who relied on the Bogoliubov theory, we were able to calculate the beyond mean-field correction of the dipolar Bose gas, without coming across any divergence at all.

Having understood the principles of the field-theoretic treatment, we were able to discuss the dimensional crossover in a system confined with periodic boundary conditions. A similar, but more complicated system was already discussed by Edler *et al.* [42], who considered dipolar bosons in a harmonic confinement. The complexity of the system forced the authors to rely on numerical results for the chemical potential. For periodic boundary conditions, however, we showed that the quasi-one- and three-dimensional

limit can be obtained analytically. Using the results from scattering theory, we saw that the confinement-induced shift automatically appears in the quasi-one-dimensional limit.

Lastly, we want to give a short outlook on interesting aspects that are still open for considerations. Although weakly interacting dipolar bosons in a harmonic confinement have already been treated by Edler *et al.*, the treatment of the same system using contact interactions is still open. The simpler nature of the interaction compared to the dipolar interaction might allow to give analytic results and thus lead to a deeper understanding of the crossover. In this work, we focused on weakly interacting Bose gases in one and three dimensions. Hence, the application of the field-theoretic approach of Hugenholtz and Pines to a two-dimensional system seems natural. This could allow for a consistent treatment of dipolar Bose gases in two dimensions. In addition, the dimensional crossover from three to two dimensions should work in the same manner as the crossover from three to one dimension, discussed in this work.

# A. Scattering Theory

## A.1. Born Series in Three Dimensions

We want to determine the scattering amplitude  $f(\mathbf{k}, \mathbf{k}')$  for the potential

$$V_\Lambda(\mathbf{r})\psi(\mathbf{r}) = g_\Lambda h_\Lambda^*(\mathbf{r}) \int_{\mathbb{R}^3} d^3\mathbf{u} h_\Lambda(\mathbf{u})\psi(\mathbf{u}).$$

As a reminder, the scattering amplitude is given by

$$f(\mathbf{k}, \mathbf{k}') = -\frac{m}{4\pi\hbar^2} \int_{\mathbb{R}^3} d^3\mathbf{r}' e^{-i\mathbf{k}' \cdot \mathbf{r}'} V(\mathbf{r}') \Psi_{\mathbf{k}}(\mathbf{r}'),$$

and the wave function  $\Psi_{\mathbf{k}}(\mathbf{r})$  fulfills the Lippmann-Schwinger equation

$$\Psi_{\mathbf{k}}(\mathbf{r}) = e^{i\mathbf{k} \cdot \mathbf{r}} + \int_{\mathbb{R}^3} d^3\mathbf{r}' G_0^+(\mathbf{r}, \mathbf{r}', E_{\mathbf{k}}) V(\mathbf{r}') \Psi_{\mathbf{k}}(\mathbf{r}').$$

For a shorter notation, we introduce

$$G_{\mathbf{k}}(\mathbf{r} - \mathbf{r}') = G_0^+(\mathbf{r}, \mathbf{r}', E_{\mathbf{k}}).$$

By calculating the first few Born approximations, the form of the entire Born series becomes clear.

The first Born approximation yields

$$\begin{aligned} & -\frac{m}{4\pi\hbar^2} \int_{\mathbb{R}^3} d^3\mathbf{r} e^{-i\mathbf{k}' \cdot \mathbf{r}} V_\Lambda(\mathbf{r}) e^{i\mathbf{k} \cdot \mathbf{r}} \\ &= -\frac{m}{4\pi\hbar^2} \int_{\mathbb{R}^3} d^3\mathbf{r} e^{-i\mathbf{k}' \cdot \mathbf{r}} g_\Lambda h_\Lambda^*(\mathbf{r}) \int_{\mathbb{R}^3} d^3\mathbf{u} h_\Lambda(\mathbf{u}) e^{i\mathbf{k} \cdot \mathbf{u}} \\ &= -\frac{mg_\Lambda}{4\pi\hbar^2} \left( \int_{\mathbb{R}^3} d^3\mathbf{r} e^{-i\mathbf{k}' \cdot \mathbf{r}} h_\Lambda^*(\mathbf{r}) \right) \left( \int_{\mathbb{R}^3} d^3\mathbf{u} e^{-i\mathbf{k} \cdot \mathbf{u}} h_\Lambda(\mathbf{u}) \right)^* \\ &= -\frac{mg_\Lambda}{4\pi\hbar^2} \tilde{h}_\Lambda^*(\mathbf{k}') \tilde{h}_\Lambda(\mathbf{k}), \end{aligned}$$

where  $\tilde{h}_\Lambda(\mathbf{k})$  is the Fourier transform of the function  $h_\Lambda(\mathbf{r})$ . The second term in the series expansion becomes

$$\begin{aligned} & -\frac{m}{4\pi\hbar^2} \int_{\mathbb{R}^3} \int_{\mathbb{R}^3} d^3\mathbf{r} d^3\mathbf{r}' e^{-i\mathbf{k}' \cdot \mathbf{r}'} V(\mathbf{r}) G_{\mathbf{k}}(\mathbf{r} - \mathbf{r}') V(\mathbf{r}') e^{i\mathbf{k} \cdot \mathbf{r}} \\ &= -\frac{mg_\Lambda^2}{4\pi\hbar^2} \tilde{h}_\Lambda^*(\mathbf{k}') \left[ \int_{\mathbb{R}^3} \int_{\mathbb{R}^3} d^3\mathbf{u} d^3\mathbf{r}' h_\Lambda(\mathbf{u}) G_{\mathbf{k}}(\mathbf{u} - \mathbf{r}') h_\Lambda^*(\mathbf{r}') \right] \tilde{h}_\Lambda(\mathbf{k}). \end{aligned}$$

The third term of the series is the last we will give explicitly,

$$\begin{aligned} & -\frac{m}{4\pi\hbar^2} \int_{\mathbb{R}^3} d^3\mathbf{r} \int_{\mathbb{R}^3} d^3\mathbf{r}' \int_{\mathbb{R}^3} d^3\mathbf{r}'' e^{-i\mathbf{k}' \cdot \mathbf{r}} V(\mathbf{r}) G_{\mathbf{k}}(\mathbf{r} - \mathbf{r}') V(\mathbf{r}') G_{\mathbf{k}}(\mathbf{r}' - \mathbf{r}'') V(\mathbf{r}'') e^{i\mathbf{k} \cdot \mathbf{r}''} \\ & = -\frac{mg_{\Lambda}^3}{4\pi\hbar^2} \tilde{h}_{\Lambda}^*(\mathbf{k}') \left[ \int_{\mathbb{R}^3} d^3\mathbf{u} \int_{\mathbb{R}^3} d^3\mathbf{u}' h_{\Lambda}(\mathbf{u}) G_{\mathbf{k}}(\mathbf{u} - \mathbf{u}') h_{\Lambda}^*(\mathbf{u}') \right]^2 \tilde{h}_{\Lambda}(\mathbf{k}), \end{aligned}$$

as the structure of the series becomes clear now. The entire Born series of the potential can be written as

$$\begin{aligned} f(\mathbf{k}, \mathbf{k}') & = -\frac{mg_{\Lambda}}{4\pi\hbar^2} \tilde{h}_{\Lambda}^*(\mathbf{k}') \tilde{h}_{\Lambda}(\mathbf{k}) \sum_{n=0}^{\infty} \left[ g_{\Lambda} \int_{\mathbb{R}^3} d^3\mathbf{u} \int_{\mathbb{R}^3} d^3\mathbf{u}' h_{\Lambda}(\mathbf{u}) G_{\mathbf{k}}(\mathbf{u} - \mathbf{u}') h_{\Lambda}^*(\mathbf{u}') \right]^n \\ & = -\frac{mg_{\Lambda}}{4\pi\hbar^2} \tilde{h}_{\Lambda}^*(\mathbf{k}') \tilde{h}_{\Lambda}(\mathbf{k}) \sum_{n=0}^{\infty} \left[ \frac{mg_{\Lambda}}{\hbar^2} \int_{\mathbb{R}^3} \frac{d^3\mathbf{p}}{(2\pi)^3} \frac{\tilde{h}_{\Lambda}(-\mathbf{p}) \tilde{h}_{\Lambda}^*(\mathbf{p})}{k^2 - p^2 + i\eta} \right]^n. \end{aligned}$$

Using the geometric series, the scattering amplitude finally becomes

$$\begin{aligned} f(\mathbf{k}, \mathbf{k}') & = -\frac{mg_{\Lambda}}{4\pi\hbar^2} \frac{\tilde{h}_{\Lambda}^*(\mathbf{k}') \tilde{h}_{\Lambda}(\mathbf{k})}{1 - \frac{mg_{\Lambda}}{\hbar^2} \int_{\mathbb{R}^3} \frac{d^3\mathbf{p}}{(2\pi)^3} \frac{\tilde{h}_{\Lambda}(-\mathbf{p}) \tilde{h}_{\Lambda}^*(\mathbf{p})}{k^2 - p^2 + i\eta}} \\ & = -\left( \frac{4\pi\hbar^2}{mg_{\Lambda} \tilde{h}_{\Lambda}^*(\mathbf{k}') \tilde{h}_{\Lambda}(\mathbf{k})} - \frac{4\pi}{\tilde{h}_{\Lambda}^*(\mathbf{k}') \tilde{h}_{\Lambda}(\mathbf{k})} \int_{\mathbb{R}^3} \frac{d^3\mathbf{p}}{(2\pi)^3} \frac{\tilde{h}_{\Lambda}(-\mathbf{p}) \tilde{h}_{\Lambda}^*(\mathbf{p})}{k^2 - p^2 + i\eta} \right)^{-1}. \end{aligned}$$

## A.2. Harmonic Confinement

We want to apply the approach that allowed us to treat scattering in periodic boundary conditions to a harmonic confinement and show that it reproduces Olshanii's result.

The particles can move freely along the  $z$ -axis, however, their motion in the  $x$ - $y$ -plane is influenced by an axial symmetric harmonic potential of frequency  $\omega_{\perp}$ . The background Hamiltonian consists of the kinetic energy along the  $z$ -direction and also the Hamiltonian of a two-dimensional harmonic oscillator,

$$H_0 = \frac{p_z^2}{m} + \frac{p_x^2 + p_y^2}{m} + \frac{m\omega_{\perp}^2(x^2 + y^2)}{4} \quad \text{with} \quad \omega_{\perp} = \frac{2\hbar}{ma_{\perp}^2}. \quad (\text{A.1})$$

The oscillator length  $a_{\perp}$  introduces a physical length scale. The eigenfunctions of  $H_0$  are characterized by the wave vector  $k_z$  of the longitudinal direction and the quantum numbers of the harmonic oscillator  $n \in \mathbb{N}_0$  and  $l \in [-n, -n+2, \dots, n-2, n]$  in the transverse directions,

$$H_0 |k_z, n, l\rangle = \left( \frac{\hbar^2 k_z^2}{m} + \hbar\omega_{\perp}(n+1) \right) |k_z, n, l\rangle = E_{k_z, n, l} |k_z, n, l\rangle. \quad (\text{A.2})$$



In coordinate representation, the states  $|k_z, n, l\rangle$  are expressed by

$$\langle \mathbf{r} | k_z, n, l \rangle = e^{ik_z z} + \Phi_{n,l}(\rho, \varphi), \quad (\text{A.3})$$

where  $\Phi_{n,l}(\rho, \varphi)$  are the eigenstates of the two-dimensional harmonic oscillator in polar coordinates.

The Green's function of the background Hamiltonian  $H_0$  can be written as

$$\begin{aligned} G_0^+(\mathbf{r}, \mathbf{r}', k_z, n, l) &= \left\langle \mathbf{r} \left| (E_{k_z, n, l}^+ - H_0)^{-1} \right| \mathbf{r}' \right\rangle \\ &= \frac{m}{\hbar^2} \int_{\mathbb{R}} \frac{dk'_z}{2\pi} \sum_{n', l'} \frac{e^{ik'_z(z-z')} \Phi_{n', l'}(\rho, \varphi) \Phi_{n', l'}^*(\rho', \varphi')}{k_z^2 - k'^2_z + \frac{2}{a_\perp^2}(n - n') + i\eta}, \end{aligned} \quad (\text{A.4})$$

and the Lippmann-Schwinger equation takes the form

$$\Psi_{k_z, n, l}(\mathbf{r}) = e^{ik_z z} \Phi_{n, l}(\rho, \varphi) + \int_{\mathbb{R}^3} d^3 \mathbf{r}' G_0^+(\mathbf{r}, \mathbf{r}', k_z, n, l) V(r') \Psi_{k_z, n, l}(\mathbf{r}'). \quad (\text{A.5})$$

Unless otherwise specified, the occurring sums run over all allowed values of  $n$  and  $l$ . We are interested in a particular case of the Lippmann-Schwinger equation. Assume that the particles are in the transverse ground state and kinetic energy of the particles along the  $z$ -axis is much smaller than the energy to excite a transverse mode,

$$\frac{\hbar^2 k_z^2}{m} \ll \hbar \omega_\perp. \quad (\text{A.6})$$

Thus, it is sufficient to consider only  $\Psi_{k_z, 0, 0}(\mathbf{r})$ . To treat the scattering processes in three dimensions, the scattering length  $a_s$  has to be much smaller than the confinement,

$$a_s \ll a_\perp. \quad (\text{A.7})$$

Under these assumptions, we must now find the quasi-one-dimensional scattering amplitude that describes the scattering processes along the  $z$ -axis. Analog to the three- and one-dimensional systems, we first consider the far-field behavior of the Green's function,

$$\begin{aligned} G_0^+(\mathbf{r}, \mathbf{r}', k_z, 0, 0) &= \frac{m}{\hbar^2} \int_{\mathbb{R}} \frac{dk'_z}{2\pi} \sum_{n, l} \frac{e^{ik'_z(z-z')} \Phi_{n, l}(\rho, \varphi) \Phi_{n, l}^*(\rho', \varphi')}{k_z^2 - k'^2_z - \frac{2}{a_\perp^2}n + i\eta} \\ &= -\frac{im}{2\hbar^2} \sum_{n, l} \frac{e^{i\sqrt{k_z^2 - 2n/a_\perp^2 + i\eta}|z-z'|}}{\sqrt{k_z^2 - 2n/a_\perp^2 + i\eta}} \Phi_{n, l}(\rho, \varphi) \Phi_{n, l}^*(\rho', \varphi') \\ &= -\frac{im}{2\hbar^2} \frac{e^{ik_z|z-z'|}}{k_z} \Phi_{0, 0}(\rho, \varphi) \Phi_{0, 0}^*(\rho', \varphi') \\ &\quad - \frac{m}{2\hbar^2} \sum_{n=1, l} \frac{e^{-\sqrt{2n/a_\perp^2 - k_z^2}|z-z'|}}{\sqrt{2n/a_\perp^2 - k_z^2}} \Phi_{n, l}(\rho, \varphi) \Phi_{n, l}^*(\rho', \varphi') \\ &\xrightarrow{z \rightarrow \infty} -\frac{im}{2\hbar^2} \frac{e^{ik_z(z-z')}}{k_z} \Phi_{0, 0}(\rho, \varphi) \Phi_{0, 0}^*(\rho', \varphi'). \end{aligned} \quad (\text{A.8})$$

As a first step, we evaluated the integration over  $k'_z$  with the residue theorem. Then, the contributions of  $n = l = 0$  were split off the sum. Finally, we took the far-field limit  $z \rightarrow \infty$ . The limit only holds if  $2n/a_\perp^2 > k_z^2$ , which is guaranteed by the condition (A.6). With the far-field behavior of the Green's function we can now consider the Lippmann-Schwinger equation,

$$\Psi_{k_z,0,0}(\mathbf{r}, \mathbf{r}') \xrightarrow{z \rightarrow \infty} (e^{ik_z z} + f_{\text{ho}}(k_z) e^{ik_z z}) \Phi_{0,0}(\rho, \varphi) \quad (\text{A.9})$$

where we have introduced the quasi-one-dimensional scattering amplitude

$$f_{\text{ho}}(k_z) = \frac{m}{2i\hbar^2 k_z} \int_{\mathbb{R}^3} d^3\mathbf{r} e^{-ik_z z} \Phi_{0,0}^*(\rho, \varphi) V(\mathbf{r}) \Psi_{k_z,0,0}(\mathbf{r}). \quad (\text{A.10})$$

The form of the scattering amplitude  $f_{\text{ho}}(k_z)$  is very similar to the scattering amplitude of a truly one-dimensional system (2.39). It describes the scattering processes in the quasi-one-dimensional system correctly as long as the potential  $V(\mathbf{r})$  possesses the same scattering length  $a_s$  as the actual interatomic potential. For the potential  $V_\Lambda$ , we have ensured this in the section 2.4.1. We evaluate the Born series analog to appendix A.1. Using the potential (2.45), the entire Born series of the scattering amplitude reads

$$f_{\text{ho}}(k_z) = \frac{m}{2i\hbar^2 k_z} g_\Lambda |H_\Lambda(k_z)|^2 \sum_{n=0}^{\infty} \left[ g_\Lambda \int_{\mathbb{R}^3} \int_{\mathbb{R}^3} d^3\mathbf{r} d^3\mathbf{r}' h_\Lambda(\mathbf{r}) G_{k_z}(\mathbf{r}, \mathbf{r}') h_\Lambda^*(\mathbf{r}') \right]^n. \quad (\text{A.11})$$

The function

$$H_\Lambda(k_z) = \int_{\mathbb{R}^3} d^3\mathbf{r} h_\Lambda(\mathbf{r}) \Phi_{0,0}(\rho, \varphi) e^{ik_z z} \quad (\text{A.12})$$

is the analog to the function  $\tilde{h}_\Lambda(\mathbf{r})$  for the given geometry. In addition, we have introduced the short notation

$$G_{k_z}(\mathbf{r}, \mathbf{r}') = G_0^+(\mathbf{r}, \mathbf{r}', k_z, 0, 0). \quad (\text{A.13})$$

As mentioned previously, the scattering amplitude  $f_{\text{ho}}$  describes the scattering processes in one dimension of the system. In a one-dimensional description, the problems of a delta-potential are absent, as we have seen in 2.3. Thus, we can now take the limit  $\Lambda \rightarrow 0$ . The function  $H_\Lambda$  becomes

$$\lim_{\Lambda \rightarrow 0} H_\Lambda(k_z) = \int_{\mathbb{R}^3} d^3\mathbf{r} e^{ik_z z} \Phi_{0,0}(\rho, \varphi) \delta(\mathbf{r}) = \Phi_{0,0}(0) = \frac{1}{\sqrt{\pi a_\perp^2}}. \quad (\text{A.14})$$

and the argument of the sum simplifies to

$$\begin{aligned} & \lim_{\Lambda \rightarrow 0} \int_{\mathbb{R}^3} \int_{\mathbb{R}^3} d^3\mathbf{r} d^3\mathbf{r}' h_\Lambda(\mathbf{r}) G_{k_z}(\mathbf{r}, \mathbf{r}') h_\Lambda^*(\mathbf{r}') \\ &= G_{k_z}(0) = \frac{m}{\hbar^2} \int_{\mathbb{R}} \frac{dk'_z}{2\pi} \sum_{n,l} \frac{|\Phi_{n,l}(0)|^2}{k_z^2 - k_z'^2 - 2n/a_\perp^2 + i\eta}. \end{aligned} \quad (\text{A.15})$$

With the use of the geometric series, we obtain the final result for the scattering amplitude

$$\begin{aligned}
f_{\text{ho}}(k_z) &= \left( \frac{2i\hbar^2 a_{\perp}^2 \pi k_z}{mg_0} - 2ia_{\perp}^2 \pi k_z \int_{\mathbb{R}} \frac{dk'_z}{2\pi} \sum_{n,l} \frac{|\Phi_{n,l}(0)|^2}{k_z^2 - k'^2_z - 2n/a_{\perp}^2 + i\eta} \right)^{-1} \\
&= - \left( 1 - ik_z \left( \frac{2\hbar^2 a_{\perp}^2 \pi}{mg_0} + 2a_{\perp}^2 \pi \int_{\mathbb{R}} \frac{dk'_z}{2\pi} \sum_{n=1,l} \frac{|\Phi_{n,l}(0)|^2}{k'^2_z + 2n/a_{\perp}^2 - i\eta} \right) + \mathcal{O}(k_z^3) \right)^{-1}.
\end{aligned} \tag{A.16}$$

In the last step, we separated the terms involving  $n = l = 0$  from the sum. For these terms, we were then able to perform the integration over  $k_z$ .

An one-dimensional treatment of this quasi-one-dimensional system by a potential  $V(z) = g_{\text{ho}}\delta(z)$  has to reproduce the scattering amplitude (A.16). Otherwise the scattering properties of the system are not taken into account properly. If we compare the scattering amplitude of the one-dimensional delta-potential (2.43) to the quasi-one-dimensional scattering amplitude (A.16), we obtain an equation for  $g_{\text{ho}}$ ,

$$\frac{2\hbar^2}{mg_{\text{ho}}} = \frac{2\hbar^2 a_{\perp}^2 \pi}{mg_0} + 2a_{\perp}^2 \pi \int_{\mathbb{R}} \frac{dk'_z}{2\pi} \sum_{n=1,l} \frac{|\Phi_{n,l}(0)|^2}{k'^2_z + 2n/a_{\perp}^2 - i\eta}. \tag{A.17}$$

After inserting  $g_{\Lambda=0}$  and short manipulations, we arrive at

$$g_{\text{ho}} = \frac{4\pi\hbar^2 a_s}{m} \frac{1}{\pi a_{\perp}^2} \left( 1 - 4\pi a_s \left( \int_{\mathbb{R}^3} \frac{d^3k}{(2\pi)^3} \frac{1}{k^2 - i\eta} - \int_{\mathbb{R}} \frac{dk'_z}{2\pi} \sum_{n=1,l} \frac{|\Phi_{n,l}(0)|^2}{k'^2_z + 2n/a_{\perp}^2 - i\eta} \right) \right)^{-1}. \tag{A.18}$$

The remaining task is now to evaluate the occurring sums and integrals in equation (A.18). Let us start with the expression involving the sum over the transverse modes

$$\int_{\mathbb{R}} \frac{dk'_z}{2\pi} \sum_{n=1,l} \frac{|\Phi_{n,l}(0)|^2}{k'^2_z + 2n/a_{\perp}^2 - i\eta}. \tag{A.19}$$

Here, the eigenfunctions of the harmonic oscillator are evaluated at the center of coordinates, where their absolute value can only take two distinct values

$$|\Phi_{n,l}(0)|^2 = \begin{cases} \frac{1}{\pi a_{\perp}^2} & \text{for } l = 0 \\ 0 & \text{for } l \neq 0. \end{cases} \tag{A.20}$$

Hence, the summation over  $l$  vanishes and the  $n$  takes only even values

$$\frac{1}{\pi a_{\perp}^2} \int_{\mathbb{R}} \frac{dk'_z}{2\pi} \sum_{n=2,4,\dots} \frac{1}{k'^2_z + 2n/a_{\perp}^2 - i\eta}.$$

Making use of the residue theorem, we evaluate the integral and introduce a new summation index  $s' = n/2$ ,

$$\int_{\mathbb{R}} \frac{dk'_z}{2\pi} \sum_{n=1, l} \frac{|\Phi_{n,l}(0)|^2}{k'^2_z + 2n/a^2_{\perp} - i\eta} = \frac{1}{4\pi a_{\perp}} \lim_{s \rightarrow \infty} \sum_{s'=1}^s \frac{1}{\sqrt{s'}}. \quad (\text{A.21})$$

The expression

$$\int_{\mathbb{R}^3} \frac{d^3k}{(2\pi)^3} \frac{1}{k^2 - i\eta}, \quad (\text{A.22})$$

must be treated with care. Both expressions (A.19) and (A.22) contained the functions  $h_{\Lambda}$ , which introduced the same high momentum cut off for both expressions simultaneously. Thus, to obtain the correct result after taking the limit  $\Lambda \rightarrow 0$ , we have to make sure to treat both terms equally. Introducing cylindrical coordinates and performing the integration over  $k_z$  yields

$$\int_{\mathbb{R}^3} \frac{d^3k}{(2\pi)^3} \frac{1}{k^2 - i\eta} = \frac{1}{4\pi} \int_0^{\infty} dk_{\rho}.$$

By substituting

$$\frac{\hbar^2 k_{\rho}^2}{m} = \hbar\omega_{\perp} n = \frac{4}{a_{\perp}^2} s', \quad (\text{A.23})$$

we ensure that we can take the same limit for both terms,

$$\int_{\mathbb{R}^3} \frac{d^3k}{(2\pi)^3} \frac{1}{k^2 - i\eta} = \frac{1}{4\pi a_{\perp}} \lim_{s \rightarrow \infty} \int_0^s ds' \frac{1}{\sqrt{s'}}. \quad (\text{A.24})$$

Plugging both terms (A.21) and (A.24) back into the expression for the coupling constant (A.18), we obtain our final result

$$g_{\text{ho}} = \frac{4\pi\hbar^2 a_s}{m} \frac{1}{\pi a_{\perp}^2} \left(1 - \frac{a_s}{a_{\perp}} C_{\text{ho}}\right)^{-1} \quad \text{with} \quad C_{\text{ho}} = \lim_{s \rightarrow \infty} \left( \int_0^s ds' \frac{1}{\sqrt{s'}} - \sum_0^s \frac{1}{\sqrt{s'}} \right), \quad (\text{A.25})$$

which is in exact agreement with Olshanii's result [22].

## B. Ground State Energy

We want to derive the connection between the Green's function

$$iG'(\mathbf{k}, t_2 - t_1) = \langle \Phi_{\text{int}} | \mathcal{T} [a_{\mathbf{k}}(t_1) a_{\mathbf{k}}^\dagger(t_2)] | \Phi_{\text{int}} \rangle$$

and the ground state energy  $E$ . The ground state energy consists of the kinetic energy  $E_{\text{kin}}$  of the particles the interaction energy  $E_{\text{int}}$ . Let us start with the connection between the kinetic energy and the Green's function. In the following  $\hat{T}$  will denote the kinetic energy operator. Following the same steps as for the number of particles  $N$  in equation (4.15), we obtain

$$E_{\text{kin}} = \langle \Phi_{\text{int}} | \hat{T} | \Phi_{\text{int}} \rangle = \Omega \int_{\mathbb{R}^4} \frac{d^4 k}{(2\pi)^4} \frac{\hbar^2 \mathbf{k}^2}{2m} iG'(k) e^{i\eta k_0}.$$

The evaluation of the interaction energy however is more involved. Consider the field operators in the Heisenberg picture

$$\psi(x) = e^{iH't/\hbar} \psi(\mathbf{x}) e^{-iH't/\hbar} = e^{iK't/\hbar} \psi(\mathbf{x}) e^{-iK't/\hbar},$$

where

$$K' = \hat{T} - \mu \hat{N}' + \sum_{j=2}^8 H_j.$$

The time evolution of the operators in the Heisenberg picture can then be written as

$$i\hbar \frac{\partial \psi(\mathbf{x})}{\partial t} = [\psi(x), K'] = \left[ \psi(x), \sum_{j=2}^8 H_j \right] + \left[ \psi(x), \int_{\mathbb{R}^3} d^3 \mathbf{x}' \psi^\dagger(x') (\hat{T} - \mu) \psi(x') \right]$$

Multiplying both sides by  $\psi(x)$  and integrating over  $\mathbf{x}$  then gives

$$\int_{\mathbb{R}^3} d^3 \mathbf{x} \psi^\dagger(x) \left( i\hbar \frac{\partial}{\partial t} - \hat{T} + \mu \right) \psi(x) = \int_{\mathbb{R}^3} d^3 \mathbf{x} \psi^\dagger(x) \left[ \psi(x), \sum_{j=2}^8 H_j \right]$$

The evaluation of commutator on the right side is lengthy but straightforward and yields

$$\int_{\mathbb{R}^3} d^3 \mathbf{x} \psi^\dagger(x) \left( i\hbar \frac{\partial}{\partial t} - \hat{T} + \mu \right) \psi(x) = 2H_3 + H_4 + H_5 + 2H_6 + H_7 + 2H_8.$$

The adjoint of the previous equation is

$$\int_{\mathbb{R}^3} d^3\mathbf{x} \left[ \left( -i\hbar \frac{\partial}{\partial t} - \hat{T} + \mu \right) \psi^\dagger(x) \right] \psi(x) = 2H_2 + H_4 + H_5 + H_6 + 2H_7 + 2H_8.$$

Adding both equations and dividing by two yields the expression

$$\begin{aligned} & \frac{1}{2} \int_{\mathbb{R}^3} d^3\mathbf{x} \left( i\hbar \frac{\partial}{\partial t} - \hat{T} + \mu \right) \psi(x) + \left[ \left( -i\hbar \frac{\partial}{\partial t} - \hat{T} + \mu \right) \psi^\dagger(x) \right] \psi(x) \\ &= H_2 + H_3 + H_4 + H + 5 + \frac{3}{2}(H_6 + H_7) + H_8 \\ &= H_{\text{int}} - n_0 \frac{\partial H_{\text{int}}}{\partial n_0}. \end{aligned}$$

Now, we can take the ground state expectation value and obtain after short manipulation

$$\begin{aligned} & 2 \langle \Phi_{\text{int}} | H_{\text{int}} | \Phi_{\text{int}} \rangle - n_0 \langle \Phi_{\text{int}} | \frac{\partial H_{\text{int}}}{\partial n_0} | \Phi_{\text{int}} \rangle \\ &= \int_{\mathbb{R}^3} d^3\mathbf{x} \lim_{\mathbf{x}' \rightarrow \mathbf{x}} \lim_{t' \rightarrow t^+} \frac{1}{2} \left[ i\hbar \frac{\partial}{\partial t} - \hat{T}(\mathbf{x}) + \mu - i\hbar \frac{\partial}{\partial t'} - \hat{T}(\mathbf{x}') + \mu \right] iG'(x, x'). \end{aligned}$$

Thus, we finally obtain the interaction energy

$$\begin{aligned} E_{\text{int}} &= \langle \Phi_{\text{int}} | H_{\text{int}} | \Phi_{\text{int}} \rangle \\ &= \frac{1}{2} \mu N + \frac{1}{4} \int_{\mathbb{R}^3} d^3\mathbf{x} \lim_{\mathbf{x}' \rightarrow \mathbf{x}} \lim_{t' \rightarrow t^+} \left[ i\hbar \left( \frac{\partial}{\partial t} - \frac{\partial}{\partial t'} \right) - \hat{T}(\mathbf{x}) - \hat{T}(\mathbf{x}') \right] iG'(x, x'), \end{aligned}$$

where we have used

$$\langle \Phi_{\text{int}} | \frac{\partial H_{\text{int}}}{\partial n_0} | \Phi_{\text{int}} \rangle = \mu \Omega.$$

Combining the kinetic energy and the interaction energy, we obtain an expression for the ground state energy

$$\begin{aligned} E &= E_{\text{kin}} + E_{\text{int}} \\ &= \frac{1}{2} \mu N + \frac{1}{4} \int_{\mathbb{R}^3} d^3\mathbf{x} \lim_{\mathbf{x}' \rightarrow \mathbf{x}} \lim_{t' \rightarrow t^+} \left[ i\hbar \left( \frac{\partial}{\partial t} - \frac{\partial}{\partial t'} \right) - 4\hat{T}(\mathbf{x}) - \hat{T}(\mathbf{x}) - \hat{T}(\mathbf{x}') \right] iG'(x, x') \\ &= \frac{1}{2} \mu N + \frac{1}{4} \int_{\mathbb{R}^3} d^3\mathbf{x} \lim_{t' \rightarrow t^+} \left[ i\hbar \left( \frac{\partial}{\partial t} - \frac{\partial}{\partial t'} \right) + 2\hat{T}(\mathbf{x}) \right] iG'(x, x') \\ &= \frac{1}{2} \mu N + \lim_{\eta \rightarrow 0^+} \frac{\Omega}{2} \int_{\mathbb{R}^4} \frac{d^4k}{(2\pi)^4} \left( \hbar k_0 + \frac{\hbar^2 \mathbf{k}^2}{2m} \right) iG'(k) e^{ik_0 \eta}. \end{aligned}$$

# Bibliography

- [1] Mike H Anderson, Jason R Ensher, Michael R Matthews, Carl E Wieman, Eric A Cornell, et al. Observation of bose-einstein condensation in a dilute atomic vapor. *science*, 269(5221):198–201, 1995.
- [2] C. C. Bradley, C. A. Sackett, J. J. Tollett, and R. G. Hulet. Evidence of bose-einstein condensation in an atomic gas with attractive interactions. *Phys. Rev. Lett.*, 75:1687–1690, Aug 1995.
- [3] K. B. Davis, M. O. Mewes, M. R. Andrews, N. J. van Druten, D. S. Durfee, D. M. Kurn, and W. Ketterle. Bose-einstein condensation in a gas of sodium atoms. *Phys. Rev. Lett.*, 75:3969–3973, Nov 1995.
- [4] Herman Feshbach. Unified theory of nuclear reactions. *Annals of Physics*, 5(4):357 – 390, 1958.
- [5] Cheng Chin, Rudolf Grimm, Paul Julienne, and Eite Tiesinga. Feshbach resonances in ultracold gases. *Rev. Mod. Phys.*, 82:1225–1286, Apr 2010.
- [6] Axel Griesmaier, Jörg Werner, Sven Hensler, Jürgen Stuhler, and Tilman Pfau. Bose-einstein condensation of chromium. *Phys. Rev. Lett.*, 94:160401, Apr 2005.
- [7] Holger Kadau, Matthias Schmitt, Matthias Wenzel, Clarissa Wink, Thomas Maier, Igor Ferrier-Barbut, and Tilman Pfau. Observing the rosenzweig instability of a quantum ferrofluid. *Nature*, 530(7589):194–197, February 2016.
- [8] S. Komineas and N. R. Cooper. Vortex lattices in bose-einstein condensates with dipolar interactions beyond the weak-interaction limit. *Phys. Rev. A*, 75:023623, Feb 2007.
- [9] Matthias Wenzel, Fabian Böttcher, Tim Langen, Igor Ferrier-Barbut, and Tilman Pfau. Striped states in a many-body system of tilted dipoles. *arXiv preprint arXiv:1706.09388*, 2017.
- [10] Igor Ferrier-Barbut, Holger Kadau, Matthias Schmitt, Matthias Wenzel, and Tilman Pfau. Observation of quantum droplets in a strongly dipolar bose gas. *Phys. Rev. Lett.*, 116:215301, May 2016.

- 
- [11] E. P. Gross. Structure of a quantized vortex in boson systems. *Il Nuovo Cimento (1955-1965)*, 20(3):454–477, May 1961.
- [12] LP Pitaevskii. Vortex lines in an imperfect bose gas. *Sov. Phys. JETP*, 13(2):451–454, 1961.
- [13] Raphael Lopes, Christoph Eigen, Nir Navon, David Clément, Robert P. Smith, and Zoran Hadzibabic. Quantum depletion of a homogeneous bose-einstein condensate. *Phys. Rev. Lett.*, 119:190404, Nov 2017.
- [14] Nir Navon, Swann Piatecki, Kenneth Günter, Benno Rem, Trong Canh Nguyen, Frédéric Chevy, Werner Krauth, and Christophe Salomon. Dynamics and thermodynamics of the low-temperature strongly interacting bose gas. *Phys. Rev. Lett.*, 107:135301, Sep 2011.
- [15] N Bogoliubov. On the theory of superfluidity. *J. Phys*, 11(1):23, 1947.
- [16] N. M. Hugenholtz and D. Pines. Ground-state energy and excitation spectrum of a system of interacting bosons. *Phys. Rev.*, 116:489–506, Nov 1959.
- [17] L.D. Landau and E.M. Lifshits. *Quantum Mechanics: Non-relativistic Theory*. Butterworth-Heinemann. Butterworth-Heinemann, 1977.
- [18] D.J. Griffiths. *Introduction to Quantum Mechanics*. Prentice Hall, 1995.
- [19] L.I. Schiff. *Quantum Mechanics*. International series in pure and applied physics. McGraw-Hill, 1955.
- [20] L. H. Thomas. The interaction between a neutron and a proton and the structure of  $h^3$ . *Phys. Rev.*, 47:903–909, Jun 1935.
- [21] K. Wódkiewicz. Fermi pseudopotential in arbitrary dimensions. *Phys. Rev. A*, 43:68–76, Jan 1991.
- [22] M. Olshanii. Atomic scattering in the presence of an external confinement and a gas of impenetrable bosons. *Phys. Rev. Lett.*, 81:938–941, Aug 1998.
- [23] A. R. P. Lima and A. Pelster. Beyond mean-field low-lying excitations of dipolar bose gases. *Phys. Rev. A*, 86:063609, Dec 2012.
- [24] ST Beliaev. Application of the methods of quantum field theory to a system of bosons. *SOVIET PHYSICS JETP-USSR*, 7(2):289–299, 1958.
- [25] ST Beliaev. Energy spectrum of a non-ideal bose gas. *Sov. Phys. JETP*, 34(2):299, 1958.



- [26] A.A. Abrikosov, L.P. Gorkov, I.E. Dzyaloshinski, and R.A. Silverman. *Methods of Quantum Field Theory in Statistical Physics*. Dover Books on Physics. Dover Publications, 2012.
- [27] Philippe Nozieres and David Pines. *Theory Of Quantum Liquids*. Hachette UK, 1999.
- [28] K. A. Brueckner and K. Sawada. Bose-einstein gas with repulsive interactions: General theory. *Phys. Rev.*, 106:1117–1127, Jun 1957.
- [29] Jeffrey Goldstone. Derivation of the brueckner many-body theory. In *Proceedings of the Royal Society of London A: Mathematical, Physical and Engineering Sciences*, volume 239, pages 267–279. The Royal Society, 1957.
- [30] T. D. Lee and C. N. Yang. Many-body problem in quantum mechanics and quantum statistical mechanics. *Phys. Rev.*, 105:1119–1120, Feb 1957.
- [31] T. D. Lee, Kerson Huang, and C. N. Yang. Eigenvalues and eigenfunctions of a bose system of hard spheres and its low-temperature properties. *Phys. Rev.*, 106:1135–1145, Jun 1957.
- [32] Elliott H. Lieb and Werner Liniger. Exact analysis of an interacting bose gas. i. the general solution and the ground state. *Phys. Rev.*, 130:1605–1616, May 1963.
- [33] Elliott H. Lieb. Exact analysis of an interacting bose gas. ii. the excitation spectrum. *Phys. Rev.*, 130:1616–1624, May 1963.
- [34] A.L. Fetter and J.D. Walecka. *Quantum Theory of Many-Particle Systems*. Dover Books on Physics. Dover Publications, 2012.
- [35] M.E. Peskin and D.V. Schroeder. *An Introduction To Quantum Field Theory, Student Economy Edition*. Frontiers in Physics. Avalon Publishing, 2015.
- [36] C. Itzykson and J.B. Zuber. *Quantum Field Theory*. Dover Books on Physics. Dover Publications, 2012.
- [37] W.H. Dickhoff and D. Van Neck. *Many-body Theory Exposed!: Propagator Description of Quantum Mechanics in Many-body Systems*. World Scientific, 2008.
- [38] Aristeu R. P. Lima and Axel Pelster. Quantum fluctuations in dipolar bose gases. *Phys. Rev. A*, 84:041604, Oct 2011.
- [39] T Lahaye, C Menotti, L Santos, M Lewenstein, and T Pfau. The physics of dipolar bosonic quantum gases. *Reports on Progress in Physics*, 72(12):126401, 2009.
- [40] S. Yi and L. You. Trapped atomic condensates with anisotropic interactions. *Phys. Rev. A*, 61:041604, Mar 2000.

- 
- [41] S. Yi and L. You. Trapped condensates of atoms with dipole interactions. *Phys. Rev. A*, 63:053607, Apr 2001.
- [42] D Edler, C Mishra, F Wächtler, R Nath, S Sinha, and L Santos. Quantum fluctuations in quasi-one-dimensional dipolar bose-einstein condensates. *Physical Review Letters*, 119(5):050403, 2017.

# Aknowledgement

After working for a year on my master thesis, the time has come to express my gratitude for the support I received throughout the entire time.

First of all, I want to thank Prof. Büchler for all the time he has invested in me. Our discussions were always thought-provoking and encouraged me to dive deeper into the topic. Under his supervision, I learned a lot from his physical intuition.

I want to thank Jan Kumlin and Krzysztof Jachymski for their support. Although I took up a lot of their time with many questions, both were always interested in the discussion of my problems and helped me to overcome them.

I would also like to thank Holger Cartarius, not just for being my secondary corrector and discussing my work with me, but also for long discussions throughout my entire physics studies.

Of course, I want to express my thanks to all members of the institute for interesting discussions of all kind. Especially with Kevin Kleinbeck I had both helpful and funny discussions.

I want to thank my friends Marcel Wagner, Sascha Polatkan and Andreas Ehrmann for helping me improve my master thesis and of course all my other friends, who helped me to escape the world of physics for a while.

Finally, I would like to send special thanks to my family and Desirée for their great support in all aspects of my life.